Class 1 PI3K Clinical Candidates and Recent Inhibitor Design Strategies - A Medicinal Chemistry Perspective

*Aimie E. Garces, Michael J. Stocks**

Centre for Biomolecular Sciences, University Park Nottingham, Nottingham, NG7 2RD, UK.

KEYWORDS

Phosphatidylinositol 3-kinase, PI3K inhibitor, kinase, cancer, asthma, structure-activity relationship, PK/PD studies.

ABSTRACT

Phosphatidylinositol 3-kinases (PI3Ks) are a family of lipid kinases that phosphorylate the 3-OH of the inositol ring of phosphoinositides and deregulation of this pathway has implications in many diseases. The search for novel PI3K inhibitors has been at the forefront of academic and industrial medicinal chemistry with over 600 medicinal chemistry-based publications and patents appearing to date, leading to 38 clinical candidates and the launch of 2 drugs, idelalisib in 2014 and copanlisib in 2017. This perspective will discuss medicinal chemistry design approaches to novel isoform-selective inhibitors through considering brief case histories of compounds that have progressed

either into clinical development or that have revealed new structural motifs in this highly competitive area of research.

INTRODUCTION

Phosphatidylinositol 3-kinases (PI3Ks) are a family of intracellular signal transducer enzymes possessing regulatory roles in critical cellular processes including cell growth, proliferation, differentiation, motility and intracellular trafficking. Specifically, these lipid kinases phosphorylate the 3-position hydroxyl group of the inositol ring of phosphatidylinositol.[1] Deregulation of the phosphoinositide 3-kinase (PI3K) pathway has been implicated in numerous pathologies such as: cancer, diabetes, thrombosis, rheumatoid arthritis, activated PI3K-delta syndrome (APDS) and asthma. The eight known family members are sub-divided into three classes, I, II, and III where class I PI3Ks have been the most extensively studied; the class I is further subdivided into IA (PI3Kα, β, and δ) and IB (PI3Kγ), based upon the types of regulatory subunits, with which the catalytic domains combine in the active heterodimeric forms. Class 1A PI3Ks mediate the signal transduction from receptor tyrosine kinases (RTKs), while PI3Kγ is principally activated by G protein-coupled receptors (GPCRs). PI3Kα and β are ubiquitously expressed whereas PI3Kδ and γ are present in the hematopoietic system, epithelial cells and the central nervous system (CNS). Genetic deregulation of PI3K activity (such as overexpression) has been implicated in cancer for all the class I PI3K isoforms. [2, 3, 4, 5, 6, 7] In addition, mounting evidence supports a role for inhibition of PI3Kα in diabetes, [8,9] PI3Kβ in thrombosis therapy, [10,11] PI3Kδ and PI3Kγ in both rheumatoid arthritis and asthma therapy [12, 13, 14] and PI3Kδ for APDS.[15–17,18,19] Further, increased PI3Kγ expression in fibroblasts and basal cells has been

implicated in idiopathic pulmonary fibrosis. [20] It should be noted though that apart from cancer therapy, none of the other indications have been clinically validated to date. [21]

Consequently, the selective inhibition of individual PI3K isoforms using small molecule ATP-competitive inhibitors has been well documented as a promising therapeutic strategy to treat these conditions. This increasing validation of the role of PI3K in several diseases has seen an expansion of research outputs from Pharmaceutical companies and academic groups alike. This perspective examines the published recent chemical literature, concentrating on case histories for the design of PI3K inhibitors that have entered into clinical development, as well as selected examples of structurally diverse compounds. However, we should comment on the huge amount of medicinal chemistry-based patent disclosures within this time frame, with a total of 418 chemical patents being published since 2012 alone. This clearly demonstrates the large medicinal chemistry effort being employed to discover new inhibitors of PI3Ks. The number of patent publications has been mirrored to a good degree by the number of medicinal chemistry publications (n = 192) that have been published within this corresponding time frame (Figure 1).

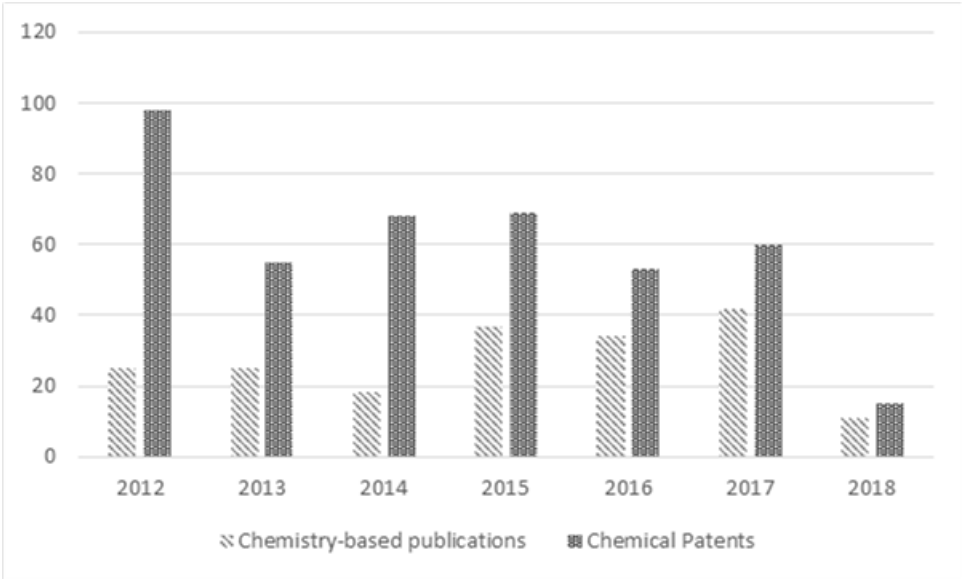

Figure 1. PI3K medicinal chemistry-based publications and PI3K chemical patents from 2012-2018 - source SciFinder

In order to understand mechanisms underlying the isoform selectivity of these inhibitors, ligand-bound X-ray structures on isoform- and pan-selective class I PI3K inhibitors have been extensively studied. These results have revealed selectivity, mainly towards PI3Kδ, can be achieved by exploiting the conformational flexibility and sequence diversity of active site residues that do not contact ATP.[22] In their pioneering work, Berndt *et al*. [23] suggested that inhibitors can be organized into three general classes through a consideration of their binding to the ATP active site, namely:

(a) inhibitors that adopt a "propeller-shaped" conformation when bound to the enzyme leading to the stabilization of a conformation that opens a hydrophobic "specificity" pocket in the active site that is not present in the apo-structure of the enzyme – these are mostly PI3Kδ selective inhibitors

(b) inhibitors that are essentially "flat" which are mostly pan-selective class I PI3K inhibitors that do not provoke such a conformational rearrangement

(c) inhibitors which have a "distorted propeller-shape" when bound to the enzyme but do not open the "specificity" pocket, again these are these are mostly PI3Kδ selective inhibitors

The ATP-binding pocket of the compounds discussed by Berndt *et al*. were shown to contact a core set of six residues in the ATP-binding pocket and, apart from the hinge residue Val827 in PI3Kδ, were invariant in all of the class I PI3K isoforms. Four regions within the ATP-binding pocket were shown to be important for inhibitor binding including: an "adenine" pocket (hinge); a "specificity" pocket; an "affinity" pocket and the hydrophobic region II located at the mouth of the active-site (Figure 2).

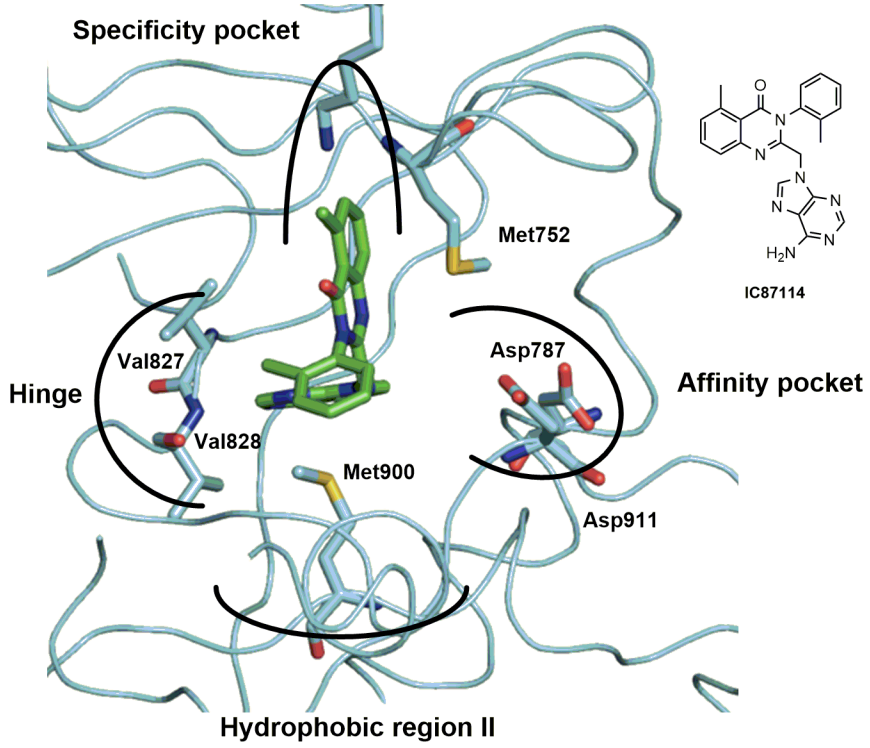

Figure 2. The ligand bound X-ray crystal structure of IC87114 in PI3Kδ showing the essential hinge binding interaction of Val828 and the specificity and affinity pockets as well as the hydrophobic region II (PDB 2X38) visualized in PyMOl.[24]

As well as searching for isoform-specific PI3K inhibitors, many groups have investigated dual inhibition design and these approaches will be discussed in this perspective.[25]

The major dual inhibitor approach is the search for compounds that inhibit both PI3Kα and the mammalian target of rapamycin (mTOR). The kinase mTOR is a member of the PIKK (phosphatidylinositol like kinase) family and is activated downstream of AKT leading to increased protein synthesis and growth. Analogs of rapamycin, which inhibit mTOR when complexed in part to rapamycin-insensitive companion of mammalian target of rapamycin (rictor, mTORC1 complex), have been approved for the treatment of advanced renal cell carcinoma, thus validating this target in humans.[26] However, a potential limitation of exclusive

mTORC1 inhibition by such analogs is that the mTOR kinase can also participate in the mTORC2 protein complex, leading to activation of the oncogene AKT and, in doing so, promote cell survival through other signaling mechanisms.[27] Therefore, to avoid this undesired feedback mechanism leading to potential resistance, ATP competitive mTOR kinase inhibitors that can inhibit both mTORC1 and mTORC2 have been pursued as alternatives to the rapamycin analogs.[28] Given the quantity of evidence implicating both PI3K and mTOR in cancer, various groups have developed compounds that inhibit both kinases.

This perspective will investigate the medicinal chemistry evolution of these inhibitor classes leading to clinical candidates (Table 1), as well as discussing new series of compounds grouped by chemical structure highlighting those that have progressed to deliver structurally diverse clinical candidates.

Table 1. PI3K inhibitors progressed to clinical evaluation and development status as of July 2018

Inhibitor[a]	Other names	Primary indication	Biological target	Trial phase[b]	Company
Alpelisib	BYL719	oncology	PI3Kα	III	Novartis
AMG319		oncology	PI3Kδ	II	Amgen
Apitolisib	GDC-0980	oncology	PI3K/mTOR	Not progressing	Genentech
AZD8186		oncology	PI3Kβ	I	AstraZeneca
BGT226	NVP-BGT226	oncology	PI3K/mTOR	Not progressing	Novartis
Bimiralisib	PQR309	oncology	PI3K/mTOR	I/II	PIQUR
Buparlisib	BKM120	oncology	Pan-PI3K	III	Novartis
CH5132799		oncology	PI3Kα	Not progressing	Chugai
Copanlisib	BAY 80-6946	oncology	Pan-PI3K	Approved	Bayer
CUDC-907	Fimepinostat	oncology	PI3Kα,β,δ/HDAC	II	Curacite

Inhibitor[a]	Other names	Primary indication	Biological target	Trial phase[b]	Company
Dactolisisb	BEZ235	oncology	PI3K/mTOR	Not progressing	Novartis
Duvelisib	IPI-145	oncology	PI3Kδ,γ	III	Verastem
GDC-0084		oncology	PI3K/mTOR	II	Genentech
Gedatolisib	PF-05212384; PKI-587	oncology	PI3K/mTOR	II	Pfizer
GSK2292767		COPD/Asthma	PI3Kδ	I	GlaxoSmithKline
GSK2636771		oncology	PI3Kβ	II	GlaxoSmithKline
Idelalisib		oncology	PI3Kδ	Approved	Gilead
IPI-549		oncology	PI3Kγ	I	Infinity
Leniolisib	CDZ173	primary immunodeficiency disease	PI3Kδ	III	Novartis
LY3023414		oncology	PI3K/mTOR	II	Lilly
Nemiralisib	GSK2269557	COPD/Asthma	PI3Kδ	II	GlaxoSmithKline
Omipalisib	GSK2126458	oncology	PI3K/mTOR	I/II	GlaxoSmithKline
PF-04691502		oncology	PI3K/mTOR	Not progressing	Pfizer
Pictilisib	GDC-0941	oncology	Pan-PI3K	II	Genentech
Pilaralisib	SAR245408; XL147	oncology	Pan-PI3K	II	Sanofi/Exelixis
RV-1729		COPD/Asthma	PI3Kδ/γ	I	RespiVert
Sapanisertib	MLN0128; TAK-228;, INK128	oncology	mTOR	II	Millenium
SAR260301		oncology	PI3Kβ	I	Sanofi
Serabelisib	MLN1117; INK1117; TAK-117	oncology	PI3Kα	II	Takeda
SF1126		oncology	Pan-PI3K (prodrug)	Not progressing	SignalRx
Sonolisib	PX-866	oncology	PI3Kα,γ,δ	II	Oncothyreon
Taselisib	GDC-0032	oncology	PI3Kα / PI3Kβ-sparing	III	Genentech

Inhibitor[a]	Other names	Primary indication	Biological target	Trial phase[b]	Company
Tenalisib	RP6530	oncology	PI3Kδ/γ	II	Rhizen-Pharmaceuticals
Umbralisib	TGR-1202	oncology	PI3Kδ	III	TG Therapeutics
Voxtalisib	SAR245409; XL-765	oncology	PI3K/mTOR	II	Exelixis/Sanofi
VS-5584	SB2343	oncology	PI3K/mTOR	Not progressing	Verastem
WX-037		oncology	Pan-PI3K	Not progressing	WILEX AG
ZSTK474		oncology	Pan-PI3K	Not progressing	Zenyaku

[a] For chemical structures see Supplementary material (Table ST1). [b] Source Fruman *et al.* [21], PubChem [29]

The propeller-shaped PI3Kδ-selective inhibitors

In 2006, a series of compounds were disclosed [8] describing a new class of PI3K compounds that existed in a "propeller-shaped" configuration. The class of compounds exemplified by **1** (PIK-39) was more potent (>50-fold) towards the PI3Kδ isoform relative to the other class 1 PI3Ks. This selectivity was attributed to the unusual overall shape of the molecules, as typical "flat kinase inhibitors" bound in the ATP-binding pocket with no significant difference in activity between the PI3K isoforms. It was considered, and demonstrated through X-ray crystallography [8] that the quinazolinone forces a key methionine (Met752 PI3Kδ numbering) that is conserved in all isoforms to move to accommodate the large quinazolinone group. This ligand-induced fit confers a conformational shift in the peptide backbone leading to a conformational change in the ATP-binding region, enhancing isoform selectivity in favor of the PI3Kδ isoform (Figure 3). This unique binding mode has been the source of inspiration for many groups

involved in the search for selective PI3Kδ inhibitors and a summary of key findings will be discussed here.

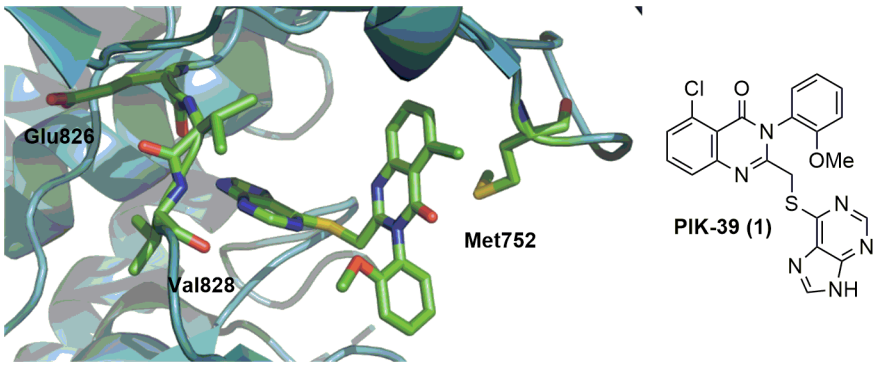

Figure 3. Crystal structure of **1** (PIK-39) in PI3Kδ demonstrating the propeller-shape conformation (PDB 2WXF) - visualized in PyMol.

Idelalisib (**2**) was the first-in-class selective inhibitor of PI3Kδ, which was approved by the FDA in 2014 for use with patients with chronic lymphocytic leukemia (CLL), focular lymphoma (FL) and small lymphocytic lymphoma (SLL). Idelalisib was initially discovered by Calistoga and was later advanced by Gilead and represented an important advance in the search for highly-selective PI3Kδ inhibitors.[30] The European Medicines Agency (EMA), at the request of the European Commission, is currently reviewing idelalisib following concerns over serious adverse events in ongoing trials, mostly due to infections. TGR-1202 (**3**) a selective PI3Kδ inhibitor, is currently undergoing Phase 2 Studies to assess the safety and efficacy in patients with CLL who are intolerant to prior Bruton Tyrosine Kinase (BTK) or PI3Kδ inhibitor therapy. Duvelisib (**4**), a dual inhibitor of phosphoinositide 3-kinase PI3Kδ and PI3Kγ was shown to be clinically active in advanced hematologic malignancies and US FDA approval is currently being sought in both FL and CLL. In addition, a structural analog tenalisib (**5**), a dual inhibitor of phosphoinositide 3-

kinase PI3Kδ and PI3Kγ recently obtained US FDA Fast Track Designations for treatment of relapsed/refractory peripheral T-cell lymphoma and relapsed refractory cutaneous T-cell lymphoma in addition to orphan-drug designations for treatment of peripheral and cutaneous T-cell lymphoma.

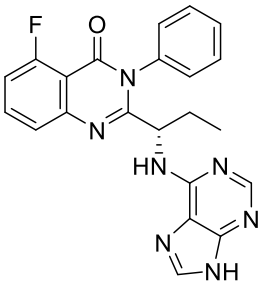

Idelalisib **(2)**

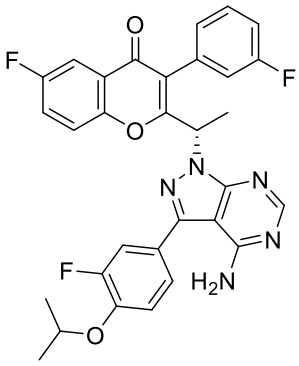

TGR-1202 **(3)**

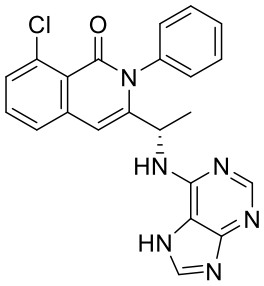

Duvelisib **(4)**

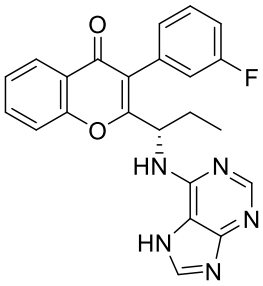

Tenalisib **(5)**

Unfortunately, to date there has been no journal publication detailing the discovery of idelalisib. However, the ligand-bound X-ray crystal structure (Figure 4) revealed the rationale for the observed high PI3Kδ selectivity. Idelalisib binds in a similar conformation to **1** in the ATP binding site of the P110 catalytic subunit of PI3Kδ, with the purine forming two hydrogen bonds with key hinge residues (Val828 and Glu826).[31]

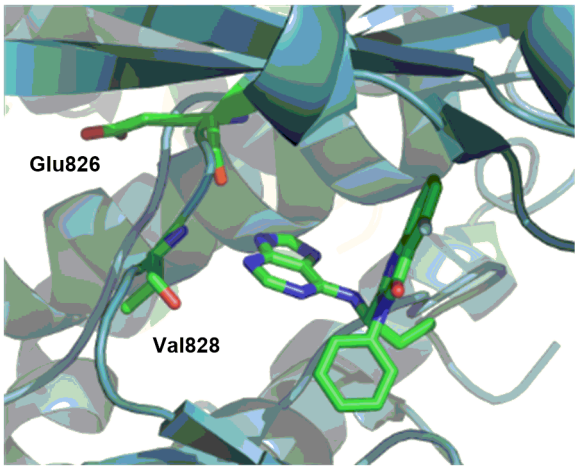

Figure 4. X-ray crystal structure of idelalisib bound to the ATP site of the P110 catalytic subunit of PI3Kδ showing the "propeller shape" adopted and the key hinge interactions with Val828 and Glu826 (PDB 4XEO) - visualized in PyMol.[7]

The fluorine containing quinazolinone ring assumes a perpendicular conformation to the hinge binder and is embedded in a specificity pocket between Trp760 and Met752 that is closed in the apo structure of the enzyme. The phenyl ring adopts a binding conformation perpendicular to the quinazolinone ring and protrudes into a hydrophobic region out of the ATP-binding pocket. The improved PI3Kδ selectivity of these "propeller shaped" compounds is proposed to be a consequence of the lower energy requirement for the creation of the specificity pocket in PI3Kδ relative to the other class 1 PI3K isoforms. The remainder of this section will concentrate on new medicinal chemistry disclosures based around the core structures of compounds **2**-**5** disclosed since 2012, highlighting key areas of SAR and learning from the original papers.

Scientists at Gilead Sciences investigated the replacement of the hinge binding purine ring present in idelalisb, which was a known primary site of metabolism.[32] The starting compound for their studies was **6**, as this had a combination of good activity (PI3Kδ IC_{50} = 1 nM) and good overall isoform selectivity (1200 α/δ; 290 β/δ; 55 γ/δ).[33]

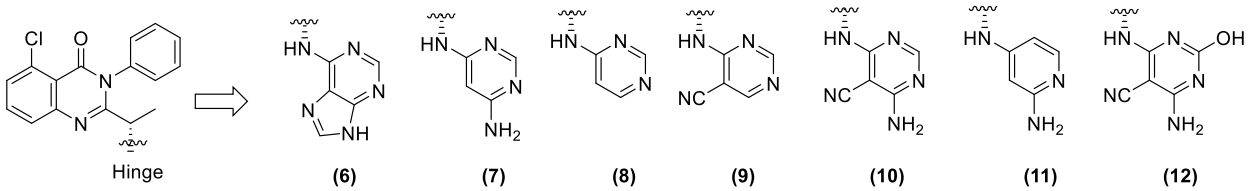

Scheme 1. Exploration of the hinge binding groups present in **2** (idelalisib)

In their initial design, the purine was replaced with a series of substituted heterocyclic rings, maintaining the N-3 pyrimidine nitrogen and the 4-amino moiety which were believed to be

essential for activity (Scheme 1). Unfortunately, the structural modification led to a 100-fold drop in potency **7** (PI3Kδ IC_{50} = 99 nM, selectivity >100 α/δ; β/δ; γ/δ). It was suggested that the loss in potency was due to the removal of the *N-7* nitrogen of the purine ring which participates in a water-mediated hydrogen bonding interaction. In addition, removal of the 4-amino group resulted in a large drop in potency **8** (PI3Kδ IC_{50} = 1700 nM). The potency and isoform selectivity was recovered through the introduction of a 5-cyano group **9** (PI3Kδ IC_{50} = 8 nM), **10** (PI3Kδ IC_{50} = 0.4 nM, selectivity 4600 α/δ; 200 β/δ; 680 γ/δ) however, conversion to the pyridine analogue led to a drop-off in activity **11** (PI3Kδ IC_{50} = 30 nM). Compound **10** was progressed to an *in vivo* metabolism study however, its clearance (1.1 L/h/kg) was 5-fold higher from its predicted clearance derived from *in vitro* microsomes, signifying the possibility of extra hepatic aldehyde oxidase (AO) metabolism. This was confirmed by the addition of the known AO inhibitor raloxifene in metabolism studies. In the presence of raloxifene there was very little turn over in human hepatocytes which was similar to that observed in human liver microsomes. In addition, metabolite identification demonstrated a major metabolite **12** (PI3Kδ IC_{50} = 1500 nM). Extensive structure activity relationship studies were initiated exploring modification of the pyrimidine ring to generate **13** (PI3Kδ IC_{50} = 0.1 nM, selectivity 2200 α/δ; 80 β/δ; 60 γ/δ, hHeps 0.21, 0.10 (+ raloxifene)). This was followed by derivatization of the phenyl ring and replacement of the 2-chloro substituent with a fluorine atom to give **14** (PI3Kδ IC_{50} = 2.2 nM, selectivity 1900 α/δ; 650 β/δ; 180 γ/δ, *h*Heps 0.34 L/h/kg).

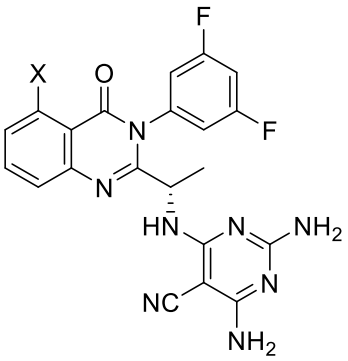

(13) X = Cl
(14) X = F

Compound **14** offered a favorable combination of biochemical potency, isoform selectivity and metabolic stability. Additionally, when tested in a whole blood basophil cellular assay, **14** inhibited PI3Kδ with an EC_{50} of 1 nM. In a KinomeScan screen against 395 non-mutant kinases **14** displayed a high degree of kinase selectivity. When administered *in vivo*, **14** demonstrated low to intermediate total clearance in both rat (0.74 L/h/kg) and dog (0.58 L/h/kg), high volumes of distribution and high oral bioavailability (rat F = 106 ± 24%) and (dog F = 100 ± 40%), suggesting a good profile for target coverage at predicted trough concentrations after twice-daily dosing. Additionally, in a rat whole blood assay, **14** inhibited *ex vivo* anti-IgD stimulation of B cells with EC_{50} and EC_{90} values of 11 and 100 nM respectively. Therefore, **14** was progressed to a rat collagen-induced arthritis (CIA) model. In this model, dosing of **14** to rats with established CIA showed a significant and dose-dependent reduction in ankle swelling. In addition, a pharmacokinetic/pharmacodynamic (PK/PD) correlation between plasma concentration and efficacy was established. Although **14** proved a good compound for *in vivo* concept testing, it was still predicted to require twice-daily dosing and so Gilead scientists explored further refinement to reduce clearance and improve half-life.[34] A correlation had been shown between a reduction of calculated lipophilicity (*c*LogP) and predicted clearance in *h*HEPS.[33] Replacement of the phenyl group present in **14** (cLogP = 3.0) with a pyridine ring gave **15** (*c*LogP = 1.6, PI3Kδ IC_{50} = 0.6 nM), a compound with lower predicted clearance and excellent isoform

selectivity (selectivity 1720 α/δ; 167 β/δ; 120 γ/δ, *h*Heps = 0.34 L/h/kg). When dosed in rats, **15** had a good overall PK profile (CL 1.5 ± 0.13 L/h.kg; V_{ss} 1.9 ± 0.3 L/kg; $t_{1/2}$ 2.5 ± 1.4 h; F 42%). However, it was demonstrated that the pyridine-containing compounds degraded rapidly at low pH due to ring opening of the quinazolinone ring, mediated through protonation of the pyridine nitrogen. A strategy to reduce the basicity of the N-1 quinazolinone nitrogen by substitution with small electron withdrawing groups in the 5- and 8-positions on the quinazolinone ring resulted in **16** (PI3Kδ IC_{50} = 0.4 nM, cpK_a 0.28), a compound with a reduced *N*-1 basicity compared to **15** (cpK_a 1.97). This change resulted in a 7-fold increase in chemical stability ($T_{1/2}$ = 19 h) when measured at 40°C, pH 2. Further SAR through changing the methyl substituent to a cyclopropyl group afforded **17,** which was selected as the pre-clinical development candidate as GS-9901 (PI3Kδ IC_{50} = 1 nM, selectivity 750 α/δ; 100 β/δ; 190 γ/δ, stability at 40°C, pH 2 $T_{1/2}$ = 20 h, rat PK CL 0.43 L/h.kg; V_{ss} 0.83 L/kg; F 57%).

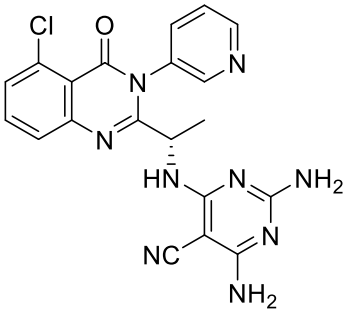

15

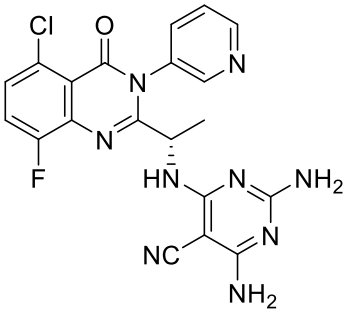

16

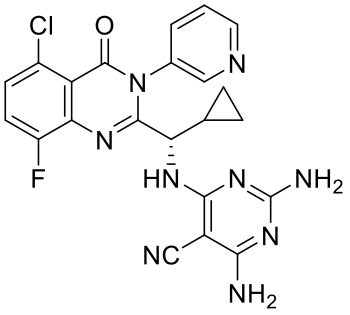

17

Further exploration to build PI3Kβ potency into the PI3Kδ-selective template was achieved through targeting the non-conserved PI3Kβ Asp856 in the hydrophobic region of class 1 PI3Ks. This was achieved through incorporating an H-bond donor moiety on the phenyl ring (Figure 5).[35]

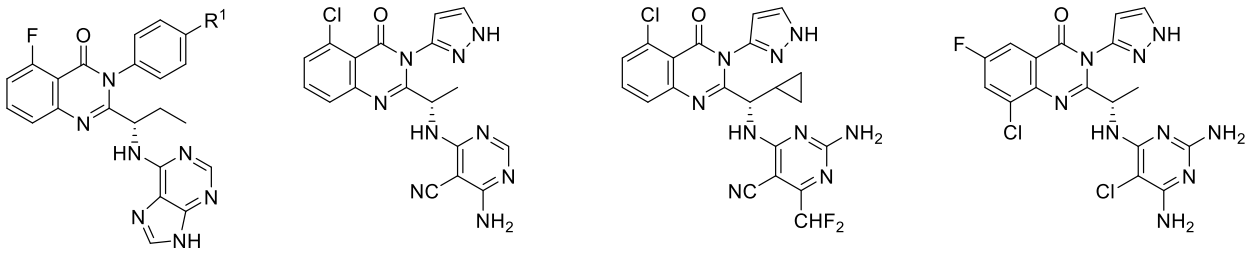

Figure 5. Building on PI3Kδ inhibitor idealisib to generate the PI3Kα/β inhibitor **21**

In their initial work they replaced the phenyl ring in idelalisib (**2**) with a 4-phenol group to give **18 (**PI3Kδ IC_{50} = 14 nM; PI3Kβ IC_{50} = 2.7 nM; PI3Kα IC_{50} = 1600 nM; PI3Kγ IC_{50} = 4300 nM). This change led to a large increase in PI3Kβ activity compared to **2** (PI3Kδ IC_{50} = 18 nM; PI3Kβ IC_{50} = 3700 nM; PI3Kα IC_{50} = 7500 nM; PI3Kγ IC_{50} = 2100 nM), demonstrating that the concept of targeting the non-conserved Asp856 present in PI3Kβ was correct, to increase PI3Kβ activity. Further SAR studies demonstrated that the phenol could be replaced with a pyrazol-3-yl group **19** (PI3Kδ IC_{50} = 0.6 nM; PI3Kβ IC_{50} = 2.5 nM; PI3Kα IC_{50} = 82 nM; PI3Kγ IC_{50}= 990 nM) with slightly improved physicochemical properties, although selectivity over PI3Kα was compromised. Unfortunately, the addition of the further H-bond donor groups dramatically decreased permeability **20** as well as decreasing metabolic stability. Further structural modifications afforded **21** (PI3Kδ IC_{50} = 5.3 nM; PI3Kβ IC_{50} = 7.8 nM; PI3Kα IC_{50} = 850 nM; PI3Kγ IC_{50} >10000 nM; Caco-2 (AB / BA) 5.7 / 21.7 10^6 cms^{-1}; rat PK CL 0.26 L/h.kg; V_{ss} 0.52 L/kg; F 66 ± 17%) as a potent and selective PI3Kβ/δ inhibitor with good pharmacokinetic properties that demonstrated efficacy in a PTEN-deficient LNCaP prostate carcinoma xenograft tumor model.

Scientists at Amgen were also inspired by the rationalization of the PI3Kδ/β isoform selectivity imposed by the induced fit of the propeller-shaped compounds. In 2012 they reported the discovery and *in vivo* evaluation of a series of dual PI3Kδ/β inhibitors for the treatment of inflammatory diseases. A series of constrained and highly-substituted 4-aminoquinolines (e.g. **22** - **25**) were prepared. After several rounds of SAR **22** (PI3Kδ IC_{50} = 30 nM; PI3Kβ IC_{50} = 58 nM; PI3Kα IC_{50} = 3960 nM; PI3Kγ IC_{50} = 2010 nM) became a promising lead. The addition of a pyridine ring led to a slight increase in activity and selectivity (PI3Kδ IC_{50} = 7 nM; PI3Kβ IC_{50} = 30 nM; PI3Kα IC_{50} = 1720 nM; PI3Kγ IC_{50} = 92 nM). Replacement of the hinge binding morpholine with other heterocycles could be achieved, although PI3Kδ/β isoform selectivity was reduced e.g. **24** (PI3Kδ IC_{50} = 3 nM; PI3Kβ IC_{50} = 18 nM; PI3Kα IC_{50} = 510 nM; PI3Kγ IC_{50} = 28 nM). The addition of a tetrahydropyran ring afforded a compound with enhanced water solubility, improved selectivity and good *in vivo* pharmacokinetics **25** (PI3Kδ IC_{50} = 11 nM; PI3Kβ IC_{50} = 44 nM; PI3Kα IC_{50} = 3250 nM; PI3Kγ IC_{50} = 509 nM, sol. (PBS) 146 mg/μL, rat PK CL 0.8 L/h/kg; V_{ss} 3.3 L/kg; F 65%). Compound **25** was found to be efficacious in several inflammation models including a keyhole limpet hemocyanin study and a collagen-induced arthritis model.[36]

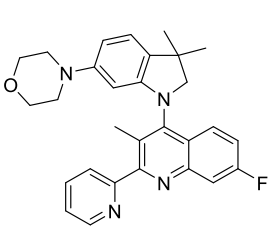

22

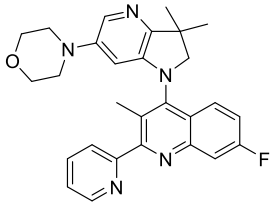

23

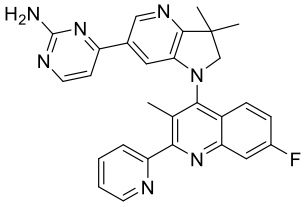

24

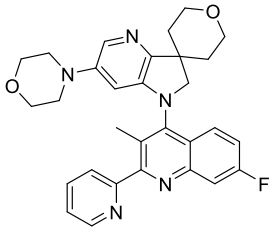

25

Further investigation of this class of compound initially explored the linker group between the quinoline bicycle and the purine hinge binder (Figure 6).[37]

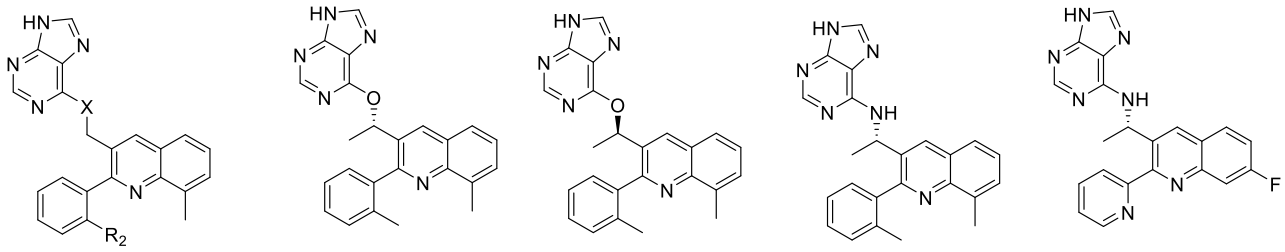

Figure 6. Discovery of the selective PI3Kδ inhibitor **33** (AMG319)

Although **26** (PI3Kδ IC_{50} = 0.24 μM) was a reasonable starting point, the thioether was highlighted as a potential metabolic liability and SAR exploration revealed that the ether linkage **27** (PI3Kδ IC_{50} = 0.017 μM) had higher enzymatic activity, whereas the methylene linker **29** was much less active (PI3Kδ IC_{50} = 3.6 μM). In addition, because of specific ligand-protein interactions, there was a demonstrable difference between the enantiomers **30** ((*S*)-enantiomer PI3Kδ IC_{50} = 7.1 nM) and **31** (PI3Kδ IC_{50} = 2.6 μM) due to a steric clash between the (*R*)-methyl and the protein. Importantly, the amino linker **28** (PI3Kδ IC_{50} = 0.041 μM) had a similar level of activity to **27** which was mirrored in the preference for the (*S*)-enantiomer **32** (PI3Kδ IC_{50} = 8 nM). Unsurprisingly, the compounds proved poorly soluble and had high microsomal instability displaying poor rat pharmacokinetics. Extensive SAR to optimize biological activity, isoform selectivity and CYP2D6 inhibition was achieved. Removal of the 8-methyl group and subsequent fluorination of the quinoline ring, in addition to substitution of the 2-aryl group with a 2-pyridyl group led to an increase in solubility and improvement in rat pharmacokinetics. The detailed SAR study eventually resulted in the identification of **33** (PI3Kδ IC_{50} = 18 nM; PI3Kβ IC_{50} = 2.7 μM; PI3Kα IC_{50} = 33 μM; PI3Kγ IC_{50} = 0.85 μM, sol. (PBS) 146 mg/μL, rat PK CL 0.34 L/h/kg; F 54%). Compound **33** had excellent activity in a whole blood assay (IC_{50} = 16 nM)

and selectivity over a large panel of kinases. In addition, **33** displayed a high level of *in vivo* efficacy as measured in two rodent disease models of inflammation and is currently being evaluated in phase 2 clinical trials for the treatment of human papillomavirus (HPV) and negative head and neck squamous cell carcinoma (HNSSCC).

In a series of papers and patent disclosures, Amgen scientists demonstrated that the core quinoline scaffold present in **22-33** could be exchanged for a wide range of heterocycles[38] in combination with exchanging the purine ring for other hinge binding motifs. The regioisomeric quinoline underwent extensive SAR studies exploring substitution at the quinoline 4-position, as typified by compound **34 (**PI3Kδ IC_{50} = 2.4 nM, rat PK CL = 0.057 L/h/kg; F 51%).[39] In an additional publication, [40] exploration of the quinoline with a novel 4-carboxamide group generated compounds as typified by **35 (**PI3Kδ IC_{50} = 2.9 nM; rat PK CL = 0.51 L/h/kg; F 70%) and **36 (**PI3Kδ IC_{50} = 4.6 nM; rat PK CL = 0.42 L/h/kg; F 29%), with very high selectivity over the Class-1 PI3K isoforms **35** (6068 α/δ; 979 β/δ; 1217 γ/δ), **36** (3082 α/δ; 478 β/δ; 700 γ/δ). **36** had selectivity against a panel of 442 protein kinases as well as excellent cellular potency in mouse B cells (pAKT IC_{50} = 0.7 nM and 0.8 nM respectively). Efficacy experiments in a key rat limpet hemocyanin model demonstrated that administration of **35** or **36** resulted in a strong dose-dependent reduction in IgG and IgM antibodies, making the compounds suitable for pre-clinical development.

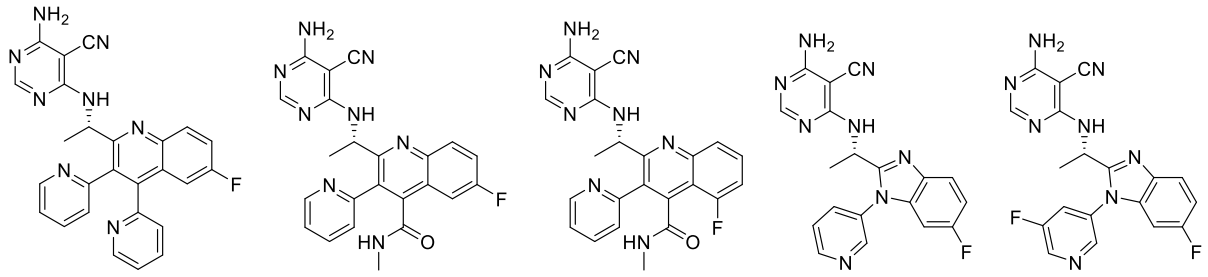

34 **35** AM-0687 **36** AM-1430 **37** (AM-8508) **38** (AM-9635)

In a final publication[38] the quinoline core was exchanged for a substituted benzimidazole, resulting in the disclosure of two further pre-clinical candidates with good pharmacokinetic properties: **37** (PI3Kδ IC_{50} = 16 nM; PI3Kβ IC_{50} = 1.78 μM; PI3Kα IC_{50} = 58.2 μM; PI3Kγ IC_{50} = 5.8 μM; mouse B cell (pAKT) IC_{50} = 4.6 nM; rat PK CL 0.93 L/h.kg; F 45%); and **38** (PI3Kδ IC_{50} = 19 nM; PI3Kβ IC_{50} = 2.33 μM; PI3Kα IC_{50} = 27.2 μM; PI3Kγ IC_{50} = 5.9 μM; mouse B cell (pAKT) IC_{50} = 4.2 nM; rat PK CL 0.99 L/h.kg; F 41%). The compounds inhibited B cell receptor (BCR)-mediated AKT phosphorylation (pAKT) in PI3Kδ-dependent *in vitro* cell based assays and were effective when administered *in vivo* at unbound concentrations consistent with their *in vitro* cell potency as a consequence of improved unbound drug concentration (0.36, 0.32 respectively fraction unbound (rat)) with lower unbound clearance. In addition, the compounds demonstrated efficacy in a rat Keyhole Limpet Hemocyanin, where the blockade of PI3Kδ activity led to effective inhibition of antigen-specific IgG and IgM formation after immunization with KLH.

Erra *et al.* reported on a series of selective PI3Kδ inhibitors based on a pyrrolotriazine scaffold (Scheme 2).[41] Moving the methyl group from the phenyl ring in **39 (**PI3Kδ IC_{50} = 130 nM) to the linker in **40 (**PI3Kδ IC_{50} = 75 nM) not only resulted in a slight increase in activity but also removed the potential for atropisomerism. Extensive SAR studies exploring the hinge binder,

linker and substitution on the pyrrolotriazine resulted in **41** (PI3Kδ IC_{50} = 2.6 nM; PI3Kβ IC_{50} = 94 μM; PI3Kα IC_{50} = 8.2 μM; PI3Kγ IC_{50} = 72 μM; M-CSF-induced AKT in THP-1 cells IC_{50} = 7.8 nM rat PK CL 1.4 mL/min/kg; V_z 1.2 L/kg ; F 98%) and entered clinical development as LAS191954 for the treatment of pemphigus.[41]

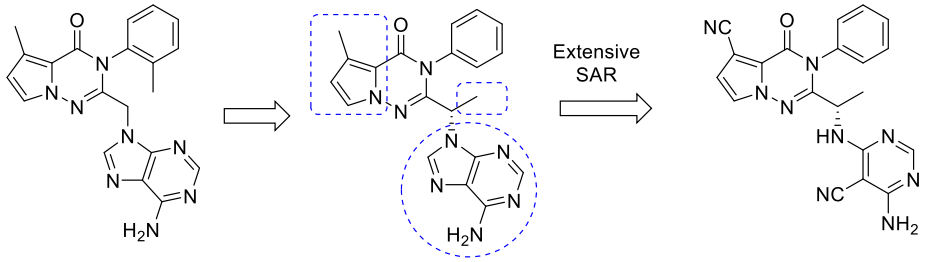

39 **40** **41** (LAS191954)

Scheme 2. Discovery of **41** (LAS191954) through an extensive SAR exploration

Wei *et al.* reported on the synthesis and evaluation of 5-alkynyl substituted quinazolin-4(3H)-ones as selective PI3Kδ inhibitors.[42] Interestingly, they also reported on a series of analogs where the hinge binder is linked to the quinazolin-4(3H)-one *via* a 4- or 5-membered ring. The optimal compounds had good potency e.g. **42** (PI3Kδ IC_{50} = 6.7 nM), **43** (PI3Kδ IC_{50} = 7.1 nM), demonstrating that the incorporation of the ring linking group was not detrimental to biological activity. In addition, the compounds had good selectivity over PI3Kα (133-fold) and good cellular activity of IC_{50} = 37.2 nM and 58.9 nM in a SU-DHL-6 cell line challenge.

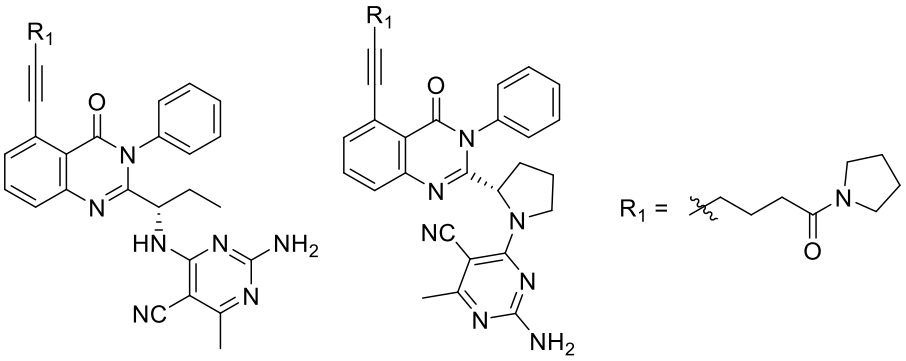

42 **43**

Evans *et al.* from Infinity Pharmaceuticals described the discovery of a series of selective PI3Kγ inhibitors for the treatment of immuno-oncology diseases.[43] Once again starting from the 8-Cl *iso*quinolone core, a series of hinge binding groups were explored resulting in the discovery of a substituted pyrazolo[1,5-a]pyrimidine as a new hinge binding motif. Interestingly, this change resulted in a PI3Kγ-selective inhibitor e.g. **44** (PI3Kδ IC_{50} = 400 nM; PI3Kγ IC_{50} = 40 nM). Further SAR of the C-8 alkynyl substitution in **45** (PI3Kδ IC_{50} = 700 nM; PI3Kγ IC_{50} = 14 nM) resulted in the discovery of **46** (PI3Kδ IC_{50} >8400 nM; PI3Kγ IC_{50} = 16 nM), a compound with very good mouse hepatocyte stability ($T_{1/2}$ = 6 hours) and selectivity over other lipid kinases. In addition, **46** demonstrated favorable pharmacokinetic properties (mouse PK CL 3.6 mL/min/kg; V_{ss} 10.8 L/kg; F 88%) and showed robust inhibition of PI3Kγ mediated neutrophil migration *in vivo* and is currently in phase 1 clinical trials in patients with advanced solid tumors as IPI-549 for a monotherapy or in combination with pembrolizumab (Scheme 3).

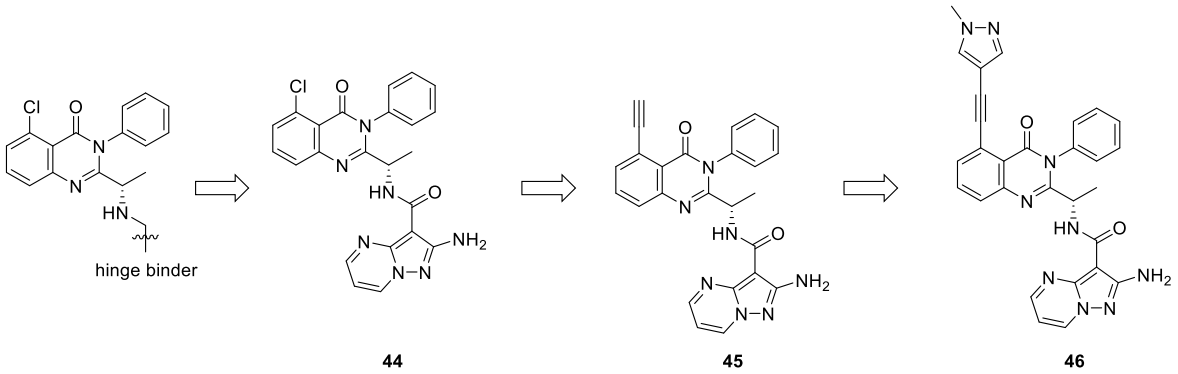

Scheme 3. Exploration of the hinge binding regions and introduction of a C-8 alkynyl substituent

In the search for further new hinge binding motifs Srinivas *et al.* used the Huisgen cycloaddition reaction to synthesize a range of 1,4-substituted 1*H*-12,3-triazolo-quinazolin-4(3*H*)-ones (Scheme 4).[44] The chemistry resulted in the identification of a series of weak PI3Kδ inhibitors e.g. **47** (PI3Kδ IC_{50} = 5 μM; PI3Kβ IC_{50} = 430 μM; PI3Kα IC_{50} = 250 μM; PI3Kγ IC_{50} = 1 μM).

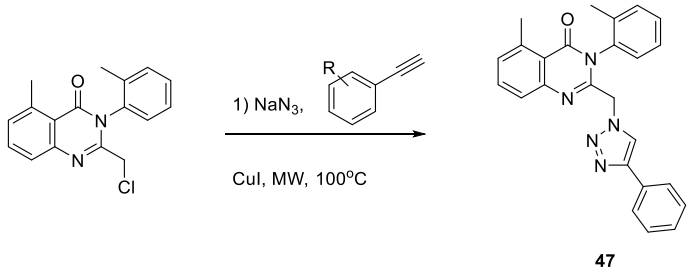

Scheme 4. Huisgen cycloaddition to generate a range of analogs such as **47**

Perry *et al.* disclosed the synthesis of soluble and cell-permeable PI3Kδ inhibitors for long-acting inhaled administration for the treatment of asthma (Figure 7).[45]

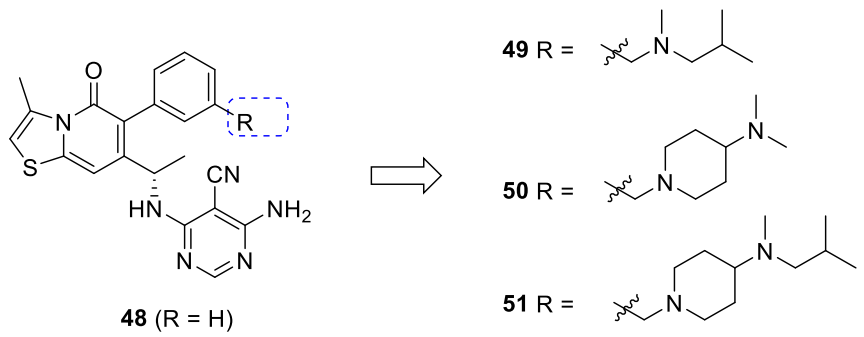

Figure 7. The incorporation of dibasic groups to improve lung tissue retention after delivery through inhalation

The novel thiazolidinpyridone core was substituted to give **48**, a potent and selective PI3Kδ inhibitor (PI3Kδ pIC_{50} = 9.4; PI3Kβ pIC_{50} = 7.3; PI3Kα pIC_{50} = 6.2 μM; PI3Kγ pIC_{50} = 7.9). Unfortunately, the compound had modest solubility and had no detectable level in lung tissue when dosed through inhalation (i.t.). An X-ray crystal structure of **48** in PI3Kδ revealed that substitution of the aryl group in the *meta*-position (group R) was favorable to position a potential solubilizing group into the exposed solvent. In light of this, a strategy was evolved to attach a (di)basic group to improve both the solubility and improve lung tissue retention. [46, 47] This resulted in **49** (PI3Kδ pIC_{50} = 9.3), however this compound was not retained in lung tissue for sufficient time to have a pharmacodynamic effect. The addition of a dibasic group e.g. **50** (PI3Kδ pIC_{50} = 9.3) and **51** (PI3Kδ pIC_{50} = 9.2) gave compounds with excellent solubility and lung pharmacokinetic half-lives of 23.2 and 9.9 hours respectively. However, dibasic compounds generally exhibit poor cell permeability resulting in a decrease in activity from the isolated enzyme activity. Perry *et al.* describe the basicity and lipophilicity requirements required to balance lung tissue retention and cell permeability and suggested the overall driver of cell permeability was lipophilicity and concluded if log D is greater than ~1.6 then a compound with

a good enzyme activity will most probably have good cell potency and this was reflected in the cell-based potency of pIC_{50} 8.0 and 8.9 respectively.

The flat PI3K inhibitors

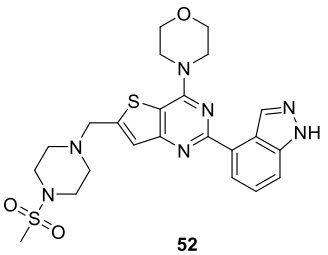

52

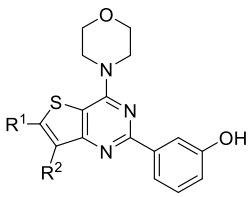

53 $R^1 = R^2 = H$
54 R^1 = Me, R^2 = H
55 R^1 = H, R^2 = Me

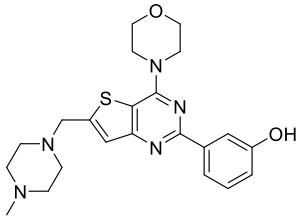

56

In 2008, Folkes *et al.* from Genentech disclosed the synthesis and biological evaluation of a series of thieno[3,2-d]pyrimidines that demonstrate potent inhibition of PI3Kα culminating in the discovery of the pan PI3K inhibitor pictilisib **52** (GDC-0941).[48] A crystal structure of **52** bound to PI3Kγ was obtained demonstrating a binding mode that many compounds in this perspective section share: the morpholine oxygen forms a pivotal hydrogen bond to the hinge region of the kinase *via* the amide of Val882 and the indazole moiety points towards the affinity pocket where the indazole nitrogen atoms make key interactions with the carboxyl group of Asp841 and the phenol oxygen of Tyr867.[23] In addition, the 4-methanesulfonyl-piperazin-1-ylmethyl group extends out to solvent where the piperazine ring packs against the side chain of Met804, and the sulfonyl group oxygen atoms are within hydrogen bond distance of the side chain of Lys802 and the amide nitrogen of Ala805 (Figure 8).

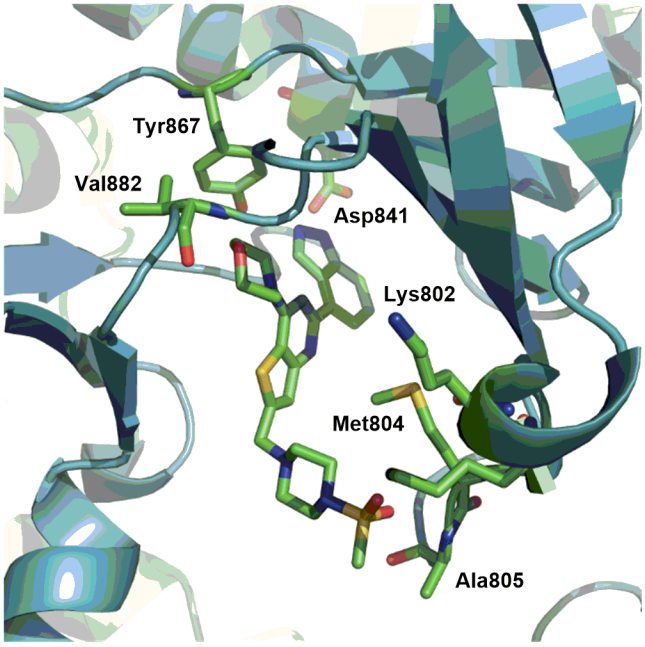

Figure 8. X-ray crystal structure of **52** (GDC-0941) in PI3Kγ (PDB 3DBS) visualized in PyMol.

In their discovery, Genentech scientists utilized the thienopyrimidine **53** previously identified by Hayakawa *et al*. [49] which was shown to be potent against PI3Kα and showed significant anti-proliferative activity *in vitro.* However, the PK profile of **53** was poor with a half-life of less than 10 min after inter-peritoneal administration in mice and, at the onset of the project, Genentech's scientists aim was to improve upon physicochemical properties, metabolic stability and potency of **53**.

Initially, the importance of the morpholine ring for P13K activity was shown when its substitution resulted in large reductions in potency, thus the morpholine group on all further derivatives was maintained.[50] Methyl substitutions at the 6- and 7- position on the thienopyrimidine ring was investigated showing that 6-Me substitution **54** (PI3Kα IC_{50} = 6 nM) was well tolerated but 7-Me substitution showed a decrease in activity **55** (PI3Kα IC_{50} = 21 nM).

Effort was focused on the 6-position to block metabolism at this position. From the large range of active substituents, the addition of tertiary amines offering the potential for salt formation to aid kinetic solubility dissolution rates as well as *in vivo* absorption and tumor exposure proved promising. Of these, the piperazine analogs, such as **56** (PI3Kα IC_{50} = 10 nM), displayed enhanced metabolic stability in human and mouse microsomes (85 - 90%). However, they exhibited low bioavailability in mouse and rat (F = 0-11%) mainly due to glucuronidation of the phenol. This metabolic liability led to the exploration of bioisostere replacements using hydrogen bond donating heterocyclic groups. Ultimately, these changes led to the discovery of **52** (IC_{50} PI3Kα = 0.003 μM, PI3Kβ = 0.033 μM, PI3Kδ = 0.003 μM, PI3Kγ = 0.075 μM, mTOR = 0.58 μM). Acceptable oral bioavailability was achieved in all species tested including mouse (77%), rat (30%), dog (71%), and monkey (20%).

Good levels of selectivity were observed for **52** when tested against members of PI3K classes II, III, and IV, including C2β (0.670 μM), Vps34 (>10 μM), DNA-PK (1.23 μM), and mTOR (0.58 μM). Additionally, **52** displayed outstanding selectivity for the PIK family kinases over a panel of 228 kinases in the Kinase Profiler panel from Millipore (formerly Upstate Biotechnologies). Only two kinases displayed greater than 50% inhibition at 1 μM. Flt3 displayed 59% inhibition and TrkA displayed 61% inhibition by **52** μM, (IC_{50} 2.85 μM). **52** showed minimal inhibition of six of the principal cytochrome P450 isoforms and, at a concentration of 25 μM there was negligible induction of CYP1A and CYP3A4. There was also no significant blockade of the *h*ERG channel (IC_{50} 64 μM) in the patch clamp assay. **52** was progressed to *in vivo* studies and it was found that **52** exhibited a strong inhibitory effect on the growth of human U87MG glioblastoma xenografts in athymic mice (tumor growth inhibition of

83%). **52** progressed to phase I and II clinical trials but further studies have been not progressed at this time.

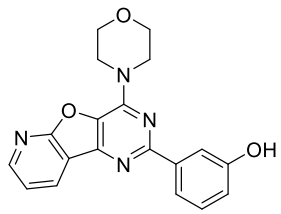

57

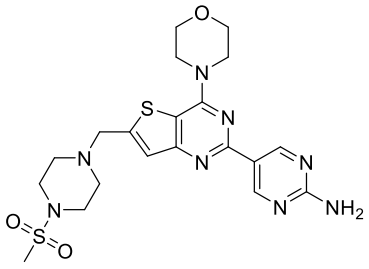

58

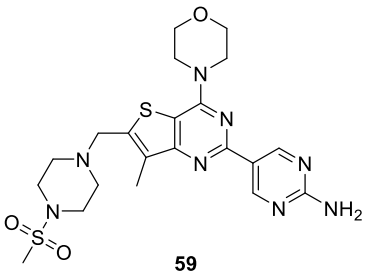

59

In 2009, with increasing evidence of clinical need for a dual mTOR/PI3K inhibitor, Genentech scientists set out to build mTOR activity into **52**. They used Piramed's PI-103 (**57**) as a tool compound as it contained the morpholino-pyrimidine core and was known to inhibit mTOR and the PI3Ks. They aimed to improve clearance of the compounds whilst maintaining or improving on potency and solubility. Additionally analogs containing a methyl group on the thienopyrimidine core (**54**-**55**) showed that it was possible to inhibit both mTOR and class 1 PI3Ks simultaneously.[51, 52]

When the indazole group in **52** was replaced with 2-aminopyrimidine **58**, a 20-fold increase in mTOR activity was observed (from 570 nM to 29 nM). However, this change didn't dramatically change the proliferation potency. The microsomal stability data correlated well with *in vivo* data except in dog pharmacokinetic studies, where a methyl substitution on the core was required to improve dog clearance **59** (GNE-477, PI3Kα IC_{50} = 4 nM, mTOR IC_{50} = 21 nM).[52]

However, these structural changes led to solubility issues and the design focus moved to improving compound solubility whilst maintaining the good biological and pharmacokinetic properties. This was achieved by considering changes to the solvent exposed sulfonamide. A

series of piperazine amides were prepared to maintain the neutral charge of the distal amine using both amino and hydroxy acids, with and without substitution at the 7-position to modulate metabolic stability (Scheme 5).

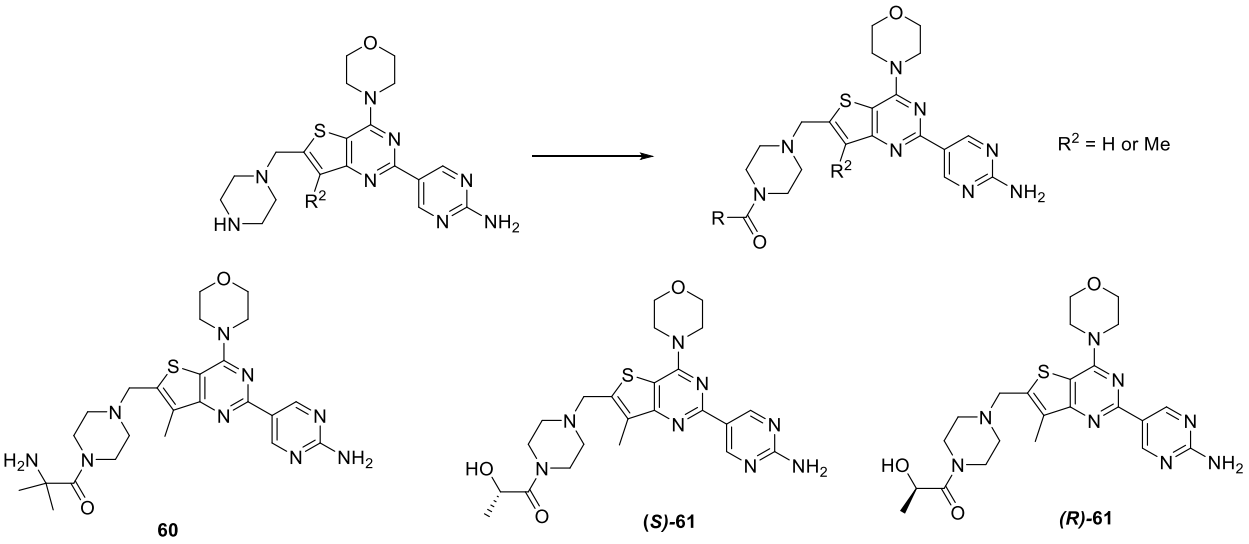

Scheme 5. Chemical exploration of the piperizine group through amidation to deliver ***(S)*-61 (**apitoloisib)

Amine-based analogs all had good potency **60** (PI3Kα IC_{50} = 1.0 nM, mTOR IC_{50} = 14 nM) and showed good improvement in solubility (1.0 mg/mL pH 6.5). However,bioavailability was poor (F = 6%). The alcohol-based amides, such as ***(S)*-61** and ***(R)*-61** showed much better PK properties giving reasonable solubility (0.084 mg/mL pH 6.5), low to moderate predicted human clearance (3.1 – 6.5 mg/min/kg), and good oral bioavailability (F = 77 – 100%). The enantiomer ***(R)*-61** demonstrated reduced biochemical activity and increased microsomal stability than ***(S)*-61** and was chosen for further study due to its low predicted clearance in human (3.1 ml/min/kg), its low *in vivo* clearance in rat (15 ml/min/kg) and its high oral bioavailability (F% = 100%).

The *in vivo* profile of ***(S)*-61** was characterized through PK studies conducted in several different species. Clearance was low (predicted Cl_h 33 mL/min/kg, Cl_p 9.2 mL/min/kg), PPB was low (71%), solubility was good (0.084 mg/mL pH 6.5) and the volume of distribution was 1.7 L/kg. The maximum tolerated dose of ***(S)*-61** was found to be 7.5 mg/kg and at this dose tumor stasis or regression was observed in PC-3 and MCF-7 neo/HER2 mouse xenograft models. This is likely due to the high cellular potency, low plasma clearance and relatively high free-fraction of the drug *in vivo*. ***(S)*-61** was found to show a high degree of selectivity over off-target kinases even while maintaining dual inhibition of mTOR and the PI3K isoforms. This was confirmed by Invitrogen's SelectScreen panel. Of the 240 kinases in the panel, only 5 other kinases consistently showed greater than 60% inhibition when treated with 1 μM (Fgr 697 nM, Mlk1 232 nM, PAK4, Syk 134 nM, and Yes1). ***(S)*-61** was highly selective over closely related PIKK family kinases: C2α (1300 nM), C2β 794 nM, VPS34 2000 nM and DNA-PK 623 nM and ***(S)*-61** (GDC-0980, Apitolisib) was advanced into development and is currently in phase I and II clinical trials.[51]

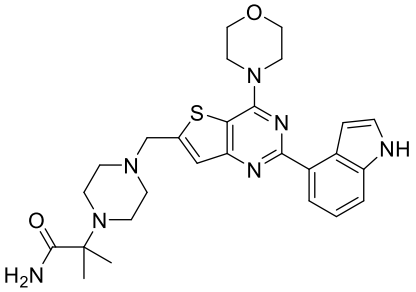

62

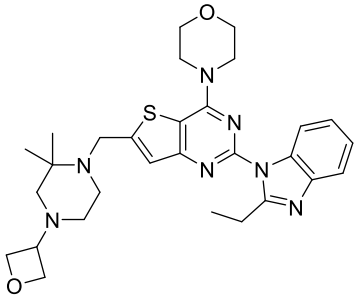

63

Having disclosed a pan-PI3K and a pan PI3K/mTOR inhibitor, Genentech scientists disclosed the development of a series of PI3Kδ-selective compounds [53] including **62** (PI3Kδ = 1.8 nM, δ/α = 129, δ/β = 104, δ/γ = 1444) which used a 4-substituted indole as the phenol bioisostere

replacement. They hypothesized that, although the residues in the affinity pocket are highly conserved between the PI3K isoforms, disruption of the strong hydrogen bond between the indazole nitrogen atom and Tyr867, could radiate and extend past the conserved affinity pocket resulting in undesirable conformational changes for the anti-targets (α, β, γ), thereby providing PI3Kδ specificity when the indazole is replaced with an indole. Although this bioisosteric replacement led to improvements in selectivity they also observed dramatic differences in time-dependent CYP3A4 inhibition, which could lead to auto-inhibition and poor drug-drug interactions. They employed several strategies to reduce this time-dependent inhibition to develop **63** (PI3Kδ = 12.3 nM, δ/α = 50, δ/β = 815, δ/γ = 112). Unfortunately, they were unsuccessful in identifying an indole containing compound with the combination of reduced time-dependent inhibition, acceptable potency, selectivity and drug-like properties.

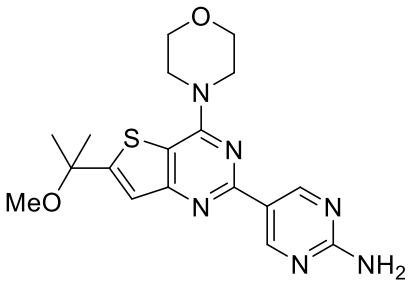

64

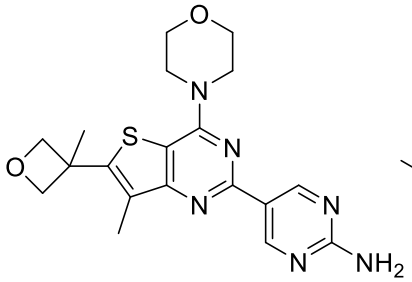

65

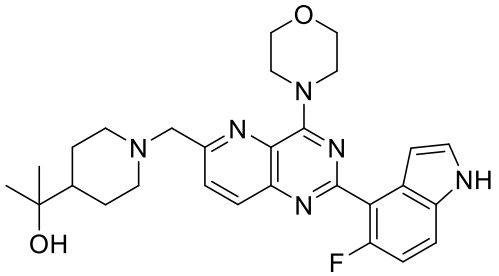

66

After their previous programs that led to the discovery of **52** and ***(S)*-61**, Heffron *et al.* extended the study towards brain penetrant inhibitors.[54] Compound **52** ($[brain]_u/[Plasma]_u$ = <0.05), and ***(S)*-61** ($[brain]_u/[Plasma]_u$ = <0.05) were found to poorly penetrate the blood-brain-barrier (BBB), which was attributed to efflux by the two most prevalent transporters in the BBB, P-glycoprotein (P-gp) and breast cancer resistance protein (Bcrp1). The properties of these compounds are markedly different from marketed drugs that target the CNS, where the median

values are: MW = 305, HBD = 1, TPSA = 45, and cLogP = 2.8. In order to bring these properties in-line with the median, they initially truncated the solvent exposed regions of the compounds, showing that the compounds retained biological activity. Additionally, using a central nervous system multi-parameter optimization (CNS MPO) scoring system (a score of 0-6) which was shown to display a correlation between higher CNS MPO score and low Pgp efflux, they prioritized the synthesis of compounds that have a CNS MPO score of ≥4.5 for their study. Of the molecules they made prior to implementing an *in silico* evaluation, 53% had high efflux mediated by P-gp and 66% by Bcrp1. After employing the CNS MPO score of ≥4.5 as a filter, new compounds were more than twice as likely as those made before to have low efflux as a result of either P-gp or Bcrp1 transporters. This design strategy led to the discovery of **64** ($[brain]_u/[Plasma]_u$ = 0.5, PI3Kα = 1 nM, mTOR = 10 nM) and **65** ($[brain]_u/[Plasma]_u$ = 0.4, PI3Kα = 2 nM, mTOR = 9 nM). Both compounds were highly potent brain penetrant PI3K/mTOR inhibitors. Furthermore, compounds **64** and **65** were evaluated in a panel of 59 kinases provided by Invitrogen's SelectScreen service. Only **65** inhibited any kinase in the panel by >75% at 1 μM concentration of the test compound (PI3KC2β, 77%).

By utilizing the highly-selective substituted indole group as a bioisostere for the phenol group, Sutherlin *et al.* reported a highly selective PI3Kδ compound, **66** (PI3Kδ = 3.8 nM, δ/α = 340, δ/β = 200, δ/γ = 410). [55] Additionally, they reported that the methyl groups of the tertiary alcohol of **66** could form hydrophobic contacts with the face of Trp760. This interaction would allow them to specifically target the space created by the Thr750 side chain in PI3Kδ, which is electronically and structurally distinct from the residues found in PI3Kα, β, and γ (Arg770, Lys771, and Lys802, respectively). This hydrophobic region present in PI3Kδ is often referred to as the "tryptophan shelf". Compound **66** was progressed to *in vivo* studies in mouse and rat, and

showed moderate hepatic clearance (53 mL/min/kg and 59 mL/min/kg respectively). Reasonable half-lives were observed upon oral dosing (2.6 - 5 h and 2.6 - 4 h respectively) as well as good oral bioavailability (80% and 90% respectively).

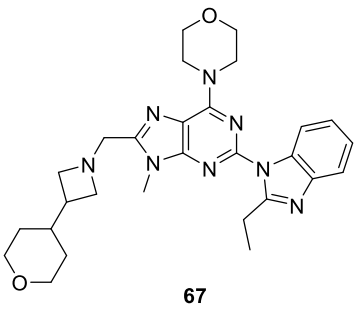

67

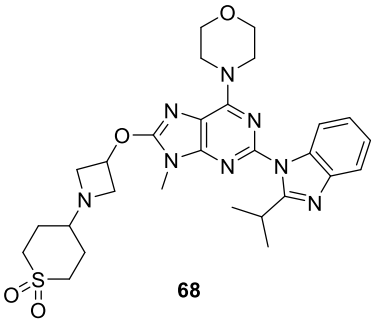

68

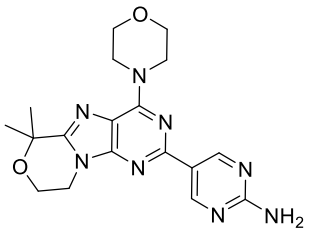

69

Murray *et al.* identified benzimidazole-based inhibitors of PI3Kδ with improved selectivity against other PI3K isoforms as well as improved *in vitro* and *in vivo* pharmacokinetic properties.[56] They initially looked at modification of the central heterocycle, which they hypothesized would allow them to tune the interaction of the solvent region of the inhibitors with the "tryptophan shelf". They explored a range of heterocyclic replacements and found that purines were interesting replacements for the thienopyrimidine, as these inhibitors were inactive against PI3Kγ and only weak inhibitors of PI3Kβ. The calculated ground state conformation of the purines indicated that a low-energy conformation is adopted in which the purine and benzimidazole rings are coplanar. Further optimization of PI3Kδ selectivity was achieved by increasing interactions with Trp760 through substitution of the solvent exposed group with alternative sterically demanding amines, compounds containing a hydrophobic groups attached to the piperazine ring, bulky amine groups and azetidines. Although substitution with the 4-methanesulfonylpiperazine of **52** resulted in a significant increase in activity versus PI3Kα and PI3Kγ. **67** (PI3Kδ = 2 nM, δ/α = 100, δ/γ = 260) is a representative example of the series; it is soluble in aqueous solution (sol. at pH 6.5 = 338 μg/mL) and has good permeability in a standard

MDCK assay (Papp = 16 × 10−6 cm/s). Rat (90%) and human (91%) plasma protein binding were moderate/good. There was no reversible or time-dependent CYP inhibition associated with **67** in testing against five CYP isoforms. Additionally, very weak inhibition (less than 25% inhibition at 1 μM) was observed against a panel of 55 diverse kinases. Pharmacokinetic profiling of **67** indicated that it had moderate to low clearance, CL (rat) = 34 mL/min/kgand a V_{ss} of 6.5 L/kg, and $T_{1/2}$ = 2.6 h.

Safina *et al.* reported [57] that inhibitors such as **67** were found to induce micronuclei formation in both the micronucleus test (MNT) and human chromosome aberration (HCA) assays in the absence of compound metabolism using the liver S9 fraction (-S9). However, it was determined to be non-genotoxic in the Ames test, suggesting that neither the MNT nor HCA result was directly linked to DNA mutation. They reported that genotoxicity SAR suggested that it was the combination of the purine core with the benzimidazole moiety that was responsible for the observed genotoxicity. Initially compounds that tested negative in the MNT assay were successfully identified through modifications of the molecular volume of the 2-benzimidazole. However, whilst they were exploring the conformational preferences required for selectivity towards PI3Kδ they simultaneously explored the effects of substitution and conformational restriction on genotoxicity. They designed analogs that altered the dihedral angle between the amine group and the purine N-7, mainly by substitution of the methylene carbon with heteroatoms. Through crystallographic and docking studies, the preferred dihedral angle was determined to be 10–30°. This led to the discovery of **68**, where an isopropyl group increases the molecular volume of the 2-benzimidazole and an oxygen linker favors a torsional angle of <30°. **68** tested negative in the HCA assay and exhibited excellent PI3K isoform selectivity (PI3K δ = 0.47 nM, δ/α = 256, δ/β = 420, δ/γ = 219) and broad kinase selectivity through Invitrogen's 239

kinase panel at 1 μM, only B-Raf was inhibited at 61% and PI4Kβ at 71%. Additionally, **68** possessed favorable pharmacokinetic properties with low predicted hepatic clearance in human (1.7 mL/min/kg) and moderate permeability (MDCK P_{app} A to B 8.23 x 10^{-6}) which led to high oral absorption across species (F = 82–100%) and acceptable half-lives ($T_{1/2}$ = 2.59–11.6 h).

Unfortunately, the series of thienopyrimidine containing brain penetrant PI3K inhibitors were deemed not suitable for clinical development due to projected poor metabolic human stability. With the knowledge that desirable metabolic stability was attainable with a purine scaffold they evaluated purine-based analogs of their previous thienopyrimidine series, ultimately resulting in **69** (GDC-0084 PI3Kα = 2nM, mTOR = 0.07 μM). **69** exhibited excellent human metabolic stability in microsomal and hepatocyte incubations (CL (mouse) = 19 mL/min/kg) and had good oral bioavailability in mouse (F = 75%). **69** was shown to penetrate the BBB through determination of the brain-to-plasma ratio in mouse, where $[Brain]_u/[Plasma]_u$ = 0.4. Additionally, **69** was studied in a subcutaneous U87 tumor xenograft model of glioblastoma in mice, showing a dose-dependent tumor growth inhibition. As a consequence, **69** was progressed to clinical development.

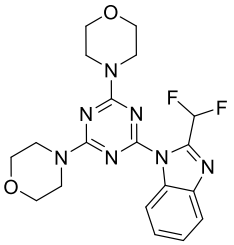

70

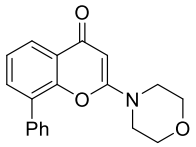

71

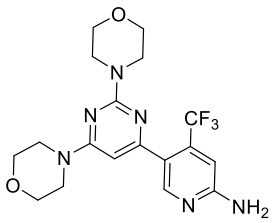

72

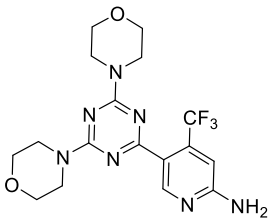

73

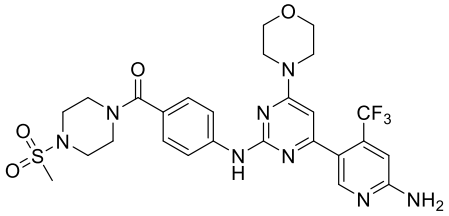

74

ZSTK474 (**70**) was discovered as a library hit by the Japanese Foundation for Cancer Research and showed strong anti-proliferative activity.[58] However, its molecular target and therefore its potential as a novel anticancer drug was unknown at that time. They initially observed that the cellular potencies of **70** against a panel of cell-lines closely correlated with the cellular potencies of LY294002 (**71**) so they examined the ability of **70** to inhibit PI3K, observing that **70** was 20-fold more active (PI3Kα = 8.9 nM, PI3Kβ = 17 nM, PI3Kγ = 53 nM, PI3Kδ = 16 nM) than LYS294002 (**71**) against PI3K and did not substantially inhibit the activity of 139 other protein kinases.

In 2011, Burger *et al.* reported the identification of **72** (buparlisib, NVP-BKM120), (PI3Kα = 52 nM, PI3Kβ = 166 nM, PI3Kγ = 262 nM, PI3Kδ = 116 nM). Their original hit came from a high throughput screen on a series of 2-morpholino 6-(3-hydroxyphenyl) pyrimidines identified from a solid phase combinatorial library of 2, 4, 6-trisubstituted pyrimidines in the same chemical class as **70**.[59, 60] After further modification the compounds *per se* had good oral bioavailability, low or sub-nanomolar biochemical potency and sub-micromolar cellular potency

against PI3Kα, however had high clearance in rat. Their goal was to decrease clearance while maintaining and optimizing potency, solubility, permeability and safety. Initially improved clearance was achieved through substituting with an aminoquinoline in the solvent exposed region. In addition to increase potency they made substitutions in the activity pocket. In changing the pyrimidyl group to a pyridyl group they found that the biochemical potency increased upon the addition of an electron withdrawing group in the C-4 position of the pyridine, forcing the group out of plane to slightly improving aqueous solubility. This did not compromise the PK properties however, the compounds still exhibited low aqueous solubility and low Caco-2 permeability. From previous work it was known that substitution of the C-4 position on the pyrimidine core could tolerate a wide range of moieties. Additionally, it was known that a morpholine group at the C-4 position of the core maintained reasonable potency while improving solubility relative to the aminoquinoline, and thus the aminoquinoline was substituted for a morpholine to give **72**. The additional morpholine at the C-4 position did not compromise the rat PK parameters and solubility was improved.

The biochemical activity of **72** was assessed across related lipid kinases and against more than 200 protein kinases (VPS34 (2.4 μM), mTOR (4.6 μM), DNAPK (>5 μM), PIK4β (>25 μM)). No significant activity was observed against the protein kinases tested. The *in vivo* profile of **72** was characterized through PK studies conducted in several different species including: mouse, rat, dog, and monkey. With the favorable cellular potency, kinase selectivity, pre-clinical pharmacology and rodent, dog and monkey pharmacokinetics, physical properties and preclinical safety profile, **72** was advanced into clinical trials in 2008. It was later reported that **72** exhibited an off-target activity at high concentrations that is not related to PI3K inhibition. This off-target

activity was found to be linked to mitosis and ultimately found to be due to inhibition of tubulin polymerization.[61]

In order to overcome tubulin binding of **72**, Bohnacke *et al.* from the University of Basel described the discovery of **73** (bimiralisib, PQR309).[62] They reported the crystal structure of **72** bound to tubulin (PDB 5M7E) and showed that high affinity binding of **72** to tubulin occurs *via* the pyrimidine core C–H group which is oriented towards βMet259 of tubulin. **73** was found to not bind to tubulin, which can be explained by the core C-H being replaced with a nitrogen atom. **73** was found to be highly potent (PI3Kα = 15 nM, PI3Kβ = 11 nM, PI3Kγ = 25 nM, PI3Kδ = 25 nM) and showed a satisfactory PK profile *in vitro* showing low clearance in rat, dog and human liver microsomes. **73** was progressed to *in vivo* studies in rodents and dogs, where it was found to be orally bioavailable and brain penetrable. The *in vivo* profile and a PC3 xenograft model in nude rats validated **73** as a clinical candidate and thus **73** was advanced through phase I clinical trials and is currently in phase II studies in relapsed and refractory lymphoma and advanced solid tumors.

Zhang *et. al.,* contrary to SAR studies conducted by Novartis and The University of Basel on the 4- and 6- positions, designed derivatives by replacing the C-2 morpholine with various aliphatic or long-chain substituted aromatic amines. Their work led to the discovery of **74** as a potent PI3K inhibitor (PI3Kα = 18 nM, PI3Kβ = 2014 nM, PI3Kδ = 13 nM, PI3Kγ = 80 nM) that showed comparable bioactivity with **70**.[63]

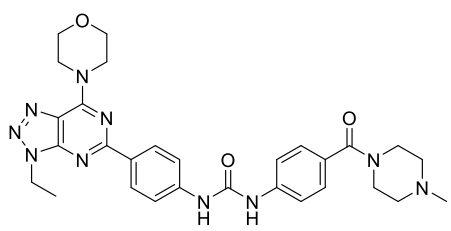

75

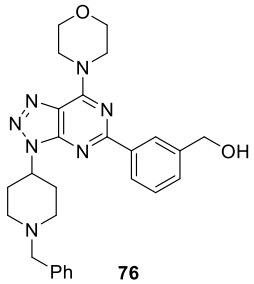

76

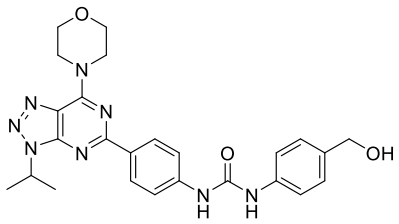

77

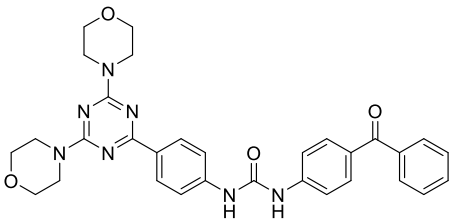

78

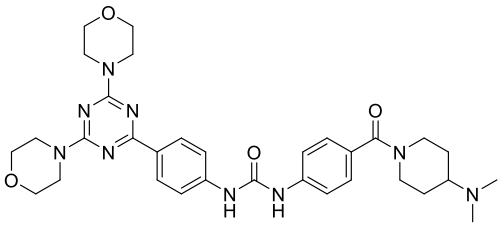

79

The discovery of **79** (Gedatolisib, PKI-587 or PF05212384)[64] by Wyeth (later Pfizer) followed on from the discovery of **75** (PKI-402).[65] The initial lead compound was a triazolopyrimidine **76** that exhibited good potency against PI3Kα (IC_{50} = 83 nM), PI3Kγ (IC_{50} = 435 nM), and mTOR (IC_{50} = 50 nM). However, activity, particularly against mTOR, and microsomal stability was improved by replacement of a benzylic alcohol with a substituted urea. The urea containing compound **77** was highly potent against PI3Kα (IC_{50} = 3.5 nM), PI3Kγ (IC_{50} = 24.8 nM), and mTOR (IC_{50} = 0.32 nM), however the compound exhibited very poor solubility. In order to increase solubility, basic amines were introduced onto the urea, giving compounds such as **75.** However, solubility issues still persisted and advanced studies were halted until modifications to **75** were implemented to decrease the overall lipophilicity of the series. In addition, another morpholine group was included to address a reported morpholine metabolic liability *via* oxidation α to the morpholine ring oxygen causing loss of potency. This morpholine change to the bismorpholino-1, 3, 5- triazine scaffold, such as **78**, led to potent PI3Kα, PI3Kγ, and mTOR inhibitory activity but only moderate potency in cell proliferation assays, attributed to poor

solubility and permeability. Due to the retention of biochemical potency, they probed the SAR to improve cellular potency. They observed a drop in PI3K activity when substituting the phenyl moiety of the urea with an alkyl group. However, the compounds maintained mTOR potency and incorporating basic amines onto the phenyl ring, as in the case of **79**, led to excellent biochemical and cell potencies. These analogs had good microsomal stability across species and exhibited good to moderate solubility. On the basis of enhanced potency (PI3Kα = 0.4 nM, PI3Kβ = 6.0 nM, PI3Kγ = 8 nM, PI3Kδ = 6 nM, mTOR = 1.6 nM), solubility (14 μg/mL pH 7.4), microsomal stability and a lack of Cyp inhibition, **79** was chosen for further *in vivo* evaluations, showing low plasma clearance (7 mL/min/kg), high volume of distribution (7.2 L/kg), and long half-life ($T_{½}$ = 14.4 h). **79** was also evaluated against a panel of 236 human protein kinases at 10 μM, where it was found to be highly selective for PI3K and mTOR. **79** progressed to phase I and II clinical trials.

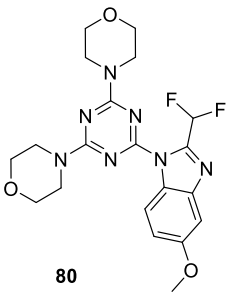

80

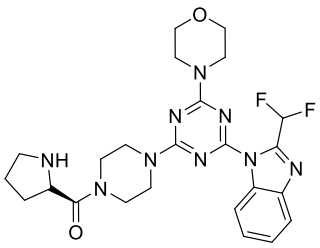

81

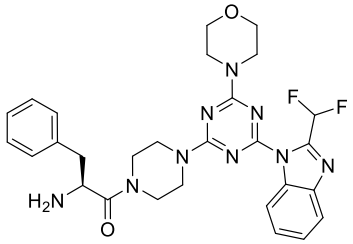

82

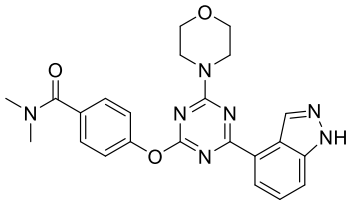

83

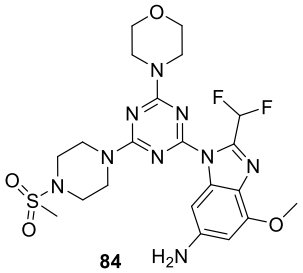

84

Miller *et. al.* reported a series of inhibitors in the same structural class as **63**, although they were consistently less potent.[66] Compound **80** (PI3Kα IC_{50} = 375 nM, PI3Kβ IC_{50} = 214 nM, PI3Kγ IC_{50} = >10 μM, PI3Kδ IC_{50} = 110 nM) is representative of that series. Overall, they found that substitution in the 5-position was consistently ~10-fold more potent than substitution at the 6-position. In a subsequent paper the morpholine in the solvent exposed region was replaced with piperazine amides derived from amino acids, **81** is representative of the series.[67] They sought to form interactions with Asn836 of PI3Kδ to gain selectivity towards PI3Kδ but found that **81** was a β/δ inhibitor (PI3Kα IC_{50} = 2611 nM, PI3Kβ IC_{50} = 36 nM, PI3Kγ IC_{50} = 5859 nM, PI3Kδ IC_{50} = 12 nM). In a subsequent publication, Pinson *et al.* highlighted **82** as a compound with high PI3Kβ isoform selectivity (PI3Kα IC_{50} = 4700 nM, PI3Kβ IC_{50} = 63 nM, PI3Kγ IC_{50} = >100 μM, PI3Kδ IC_{50} = 2200 nM) through targeting the non-conserved Asp862 on PI3Kβ. Compound **82** showed strong inhibition of cellular Akt phosphorylation and growth of PTEN-deficient MD-MBA-468 cells.[68]

Also, in the same structural class are a series of inhibitors reported by Dugar *et al.* from Sphaera Pharma.[69] Compound **83** was identified as their candidate compound for further development exhibiting good potency towards PI3Kα (IC_{50} = 60 nM) and good cellular potency (IC_{50} = 500 nM). **83** also showed a high level of microsomal stability, excellent oral bioavailability (AUC = 5.2 μM/h), no *h*ERG liability and minimal inhibition activity for CYP3A4, CYP2C19, and CYP2D6 at 10 μM concentrations. Gamage *et al.* produced extensive SAR on analogs of **70**, replacing one of the morpholine groups with a sulphonamide containing substituents lead to a series of PI3K inhibitors.[70] Most compounds synthesized suffered solubility issues, however **84** (PI3Kα IC_{50} = 22 nM, PI3Kβ IC_{50} = 116 nM, PI3Kδ IC_{50} = 13 nM), as the methanesulfonate salt, showed suitable solubility (3.82 μg/mL) to be progressed *in vivo*.

Compound **84** was evaluated in a mouse study using U87MG human glioblastoma tumor xenografts in $Rag1^{-/-}$ mice at a dose of 60 mg/kg qd x 10 by i.p. injection effectively slowed tumor growth over the 10 day dosing period.

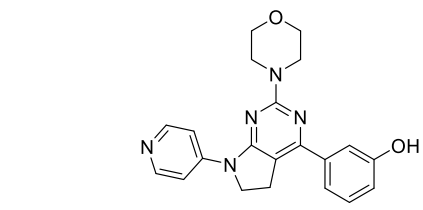

85

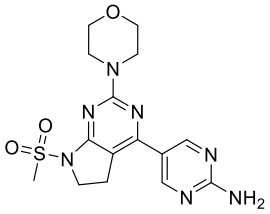

86

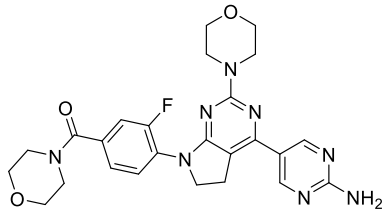

87

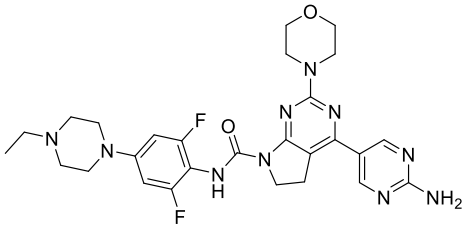

88

Ohwada *et al.* from Chugai Pharmaceutical Co. superimposed compounds **57** and **71**. The structure based design led to a phenol and morpholine containing lead **85,** which showed excellent activity (PI3Kα IC_{50} = 8.6 nM) but exhibited poor metabolic stability in human microsomes and poor oral bioavailability in mouse mainly due to rapid glucuronidation of the phenol.[71, 72] They sought to address the metabolic instability through bioisosteric replacement of the phenol with an aminopyrimidine moiety, which showed a slight reduction in PI3Kα activity but exhibited good antitumor activity *in vivo* in a human prostate cancer PC3 xenograft model, as a result of improved metabolic stability and oral bioavailability. With room for improvement in terms of its physicochemical and ADME profile, they embarked upon modification of the solvent exposed region to ultimately lead to the discovery of **86** (CH5132799), a clinical candidate that showed good activity against PI3Kα (IC_{50} = 14 nM), good oral bioavailability in mouse (F =

101%), good human liver microsomal stability and *in vivo* antitumor activity in the PC3 xenograft model (TGI: 101% at 25 mg/kg, 11 days). **86** selectively inhibits class I PI3Ks and showed less inhibition of class II PI3Ks (C2α = >10 μM, C2β = 5.3 μM), class III PI3K (Vps34 = >10 μM) and mTOR (IC_{50} = 1.6 μM) . Additionally, **86** showed no inhibitory activity (IC_{50} >10 μM) against 26 other protein kinases.

After the development of **86**, Kawada *et al.* made changes to further improve the PK profile. The chemistry focused on introducing a solubilizing group in the solvent exposed region to give compound **87**.[73] Additionally, **87** incorporates an *ortho*-substituent which disrupts the molecular planarity and improves water solubility. The pharmacokinetic profile of **87** in mouse showed a good clearance (CL = 11.1 mL/min/kg) and oral bioavailability (F = 86%), without significant loss of inhibitory activity (PI3Kα = 42 nM).

In a follow up paper, Kawada *et al.* from Chugai Pharmaceutical Co reported that the introduction of an urea functionality, as in the case of **88,** enhanced PI3Kα activity (22 nM).[74] They proposed that this observation was due to the urea acting as a spacer, placing the aromatic ring close enough to the Trp760 to make a favorable interaction, thus enhancing the inhibitory activity. This change however introduced a solubility issue, due to intermolecular hydrogen bonding between the urea and the pyrimidine core, resulting in a flat conformation that increases the crystallization propensity. They attempted to disrupt the planarity by introducing a methyl group to the *ortho*-position on the amino-pyrimidine however, this led to an 8-fold reduction of potency as disrupting the planarity in this region of the inhibitor was not acceptable for keeping key interactions in the affinity pocket. They then shifted attention back to the urea region introducing *ortho*-substituents to the phenyl ring and including solubilizing amines such as ethyl piperazine. However,this was not enough to improve the solubility to a satisfactory level.

Incorporating an *ortho*-fluorine on the phenyl ring in which electrostatic repulsion between the fluorine atom and the urea carbonyl can be expected, resulted in a flat conformation and thus poor solubility. However, evaluation of the difluoro compound showed a modest increase to the solubility as this compound prefers a twisted conformation that avoids the electrostatic repulsion of the second fluorine atom with the urea carbonyl group. Liver microsomal stability of **88** was good in both mouse (7.6 μL/min/mg) and human (2.2 μL/min/mg) and permeability was also acceptable (1.1 x 10^{-6} cm/sec in PAMPA).

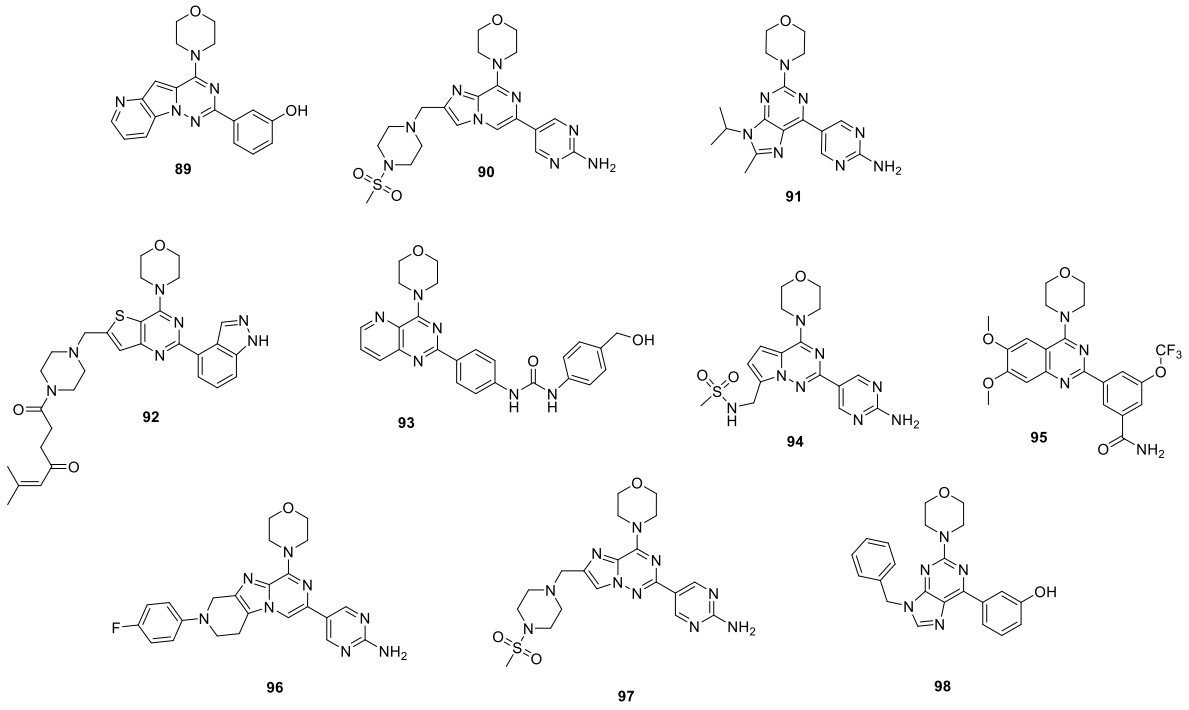

Wang *et al.* from the Chinese Academy of Sciences utilized the structural information of **57** to design a series of 4-(2-arylpyrido[30,20:3,4]pyrrolo[1,2-f][1,2,4]triazin-4-yl)morpholine derivatives containing phenolic esters.[75] The compounds had comparable PI3Kα activity to **57**. All of the compounds showed selectivity over 15 protein kinases and anti-proliferative activity at

micromolar concentration against several cancer cell lines. An example of the series is compound **89** (PI3Kα IC_{50} = 33.6 nM).

González *et al.* from the Spanish National Cancer Research Centre developed **90** (ETP-46321), employing a similar strategy to the Genentech team in the development of **52**. Through a rational design exercise, they replaced the C-C unit between the pyrimidine ring and the thiophene with a C-N unit.[76] In an effort to optimize potency and *in vivo* properties, they explored a variety of hetero-aromatic groups at the imidazo [1, 2-a] pyrazine C-6 position, leading to the discovery of **90** (PI3Kα IC_{50} = 2.3 nM, PI3Kβ IC_{50} = 170 nM, PI3Kγ IC_{50} = 179 nM, PI3Kδ IC_{50} =14.2 nM). Compound **90** was shown to be a potent PI3K α/δ inhibitor that was highly selective over mTOR (IC_{50} = 4.88 μM) and 288 representative kinases and demonstrated a good pharmacokinetic profile in mice (CL = 0.6 L/h/kg, F = 90%). Compound **90** was selected for preliminary *in vivo* evaluation in a lung tumor mouse model driven by a K-RasG12V oncogenic mutation and showed significant tumor growth inhibition (ca. 51%). In a later publication[76] they applied a conformational restriction strategy to enable the exploration of the solvent-exposed region. **96** (PI3Kα IC_{50} = 0.5 nM) is an example of the series and was progressed to a preliminary *in vivo* PK study and showed similar results to **90**. Additionally González *et al.* reported a scaffold hopping strategy to replace the core moiety of **90** to produce compounds such as **97 (**PI3Kα IC_{50} = 1.52 nM, PI3Kβ IC_{50} = 155 nM).[77]

With the goal of developing a dual mTOR/pan PI3K inhibitor, structure and ligand-based design was used to develop the lead structure **98** from **91** (VS-5584; SB2343). Using the SAR of compounds **57**, **71** and **70,** in combination with core modification, they developed a lead structure **98,** possessing a purine core substituted with a morpholine ring, a phenol head group and a hydrophobic substituent.[76] Compound **98** showed good potency against PI3Kα (IC_{50} = 89

nM) and mTOR (IC_{50} = 400 nM), however the phenol group posed a metabolic liability through glucoronidation. In order to overcome the metabolic liability, bioisoteric replacement of the phenol was employed resulting in substitution of the phenol for an amino-pyrimidine head group. The amino-pyrimidine head group was found to be equipotent with the phenol in inhibiting mTOR (300 nM) but introduced an imbalance in the inhibitory activity between mTOR and PI3Kα, being 10-fold more potent toward PI3Kα (IC_{50} = 34 nM). Optimization of the 8- and 9-position side chains led to the discovery of **91**, a compound with improved mTOR potency (IC_{50} = 37 nM) and PI3K activity (PI3Kα IC_{50} =16 nM, PI3Kβ IC_{50} = 68 nM, PI3Kδ IC_{50} = 42 nM, and PI3Kγ IC_{50} = 25 nM). **91** was selected for further profiling and found to have excellent PK and ADME properties, as well as being active in animal models. **91** progressed to phase I trials in patients with advanced non-hematologic malignancies or lymphoma.

Nacht *et al.* from Celgene Avilomics Research described **92** (CNX-1351), the first example of a targeted covalent inhibitor of the lipid kinase family that is an isoform-selective inhibitor of PI3Kα.[78] After examining the ATP binding site and nearby residues of PI3Kα to identify opportunities for selective covalent modification they identified Cys862, which is unique to PI3Kα, as a promising amino acid to target for covalent inhibition. Using the core of **52** in combination with a series of design cycles exploring both linker spacing and electrophilic functional groups they identified **92** and, although useful as a tool compound, the pharmacokinetic properties were suboptimal and thus they are currently focusing their efforts on improving the oral bioavailability.

Saurat *et al.* described a series of dual mTOR/PI3K inhibitors based on a pyridopyrimidine scaffold that have nanomolar enzymatic and cellular activities with an acceptable kinase

selectivity profile. **93** (PI3Kα IC_{50} = 58 nM, mTOR IC_{50} = 5 nM) is a representative example of the series.[79]

Starting from a morpholino-pyrrolotriazine heterocyclic lead, Dugar *et al.* from Sphaera Pharma Pte. Ltd developed their pre-clinical compound **94**.[80] **94** (PI3Kα IC_{50} = 20 nM) was found to be inactive in a panel of close homology kinases, except for other isoforms of PI3K (PI3Kβ 54% inhibition at 1 μM, PI3Kδ 67% inhibition at 1 μM) and mTOR (85% inhibition at 1 μM).

Wang *et al.* described a series of compounds based on a quinazoline scaffold. **95** (PI3Kα IC_{50} = 96 nM, PI3Kβ IC_{50} = 128 nM, PI3Kδ IC_{50} = 330 nM, and PI3Kγ IC_{50} = 465 nM) is representative of the series. **95** showed anti-proliferative effects *in vitro* and was found to induce apoptosis. Western blots suggested that **95** can block the PI3K/AKT/mTOR pathway. Additionally, **95** inhibited tumor growth on a mouse S180 homograft model.[81]

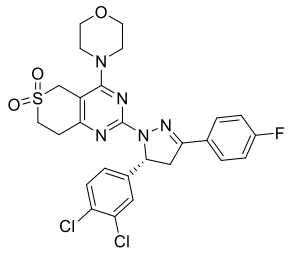

99

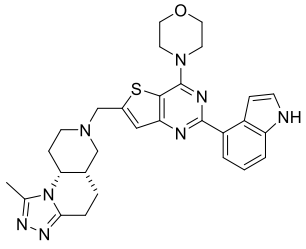

100

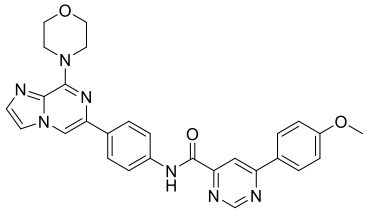

101

Wang *et al.* synthesized a series of inhibitors based on a thiopyrano-pyrimidine core such as compound **99** (PI3Kα IC_{50} = 8.38 μM). These compounds showed cytotoxicity against four cancer cell lines (IC_{50} = 6.02–10.27 μM).[82] In a later publication they incorporated the core from **97** to produce a series of compounds, where **101** (PI3Kα IC_{50} = 1.25 μM) is representative of the series.[83]

Considering **52** as the chemical starting point, Schwehm *et al.* investigated the incorporation of a tricyclic molecular scaffold leading to the discovery of a series of potent and highly-selective PI3Kδ inhibitors.[84] Compound **100** includes a 4-substituted indole group in the activity pocket, which was reported to give rise to good PI3Kδ selectivity.[55] Additionally, they reported that an overlay of the available crystal structures of the class I PI3K isoforms reveals a potential key π−cation interaction present in the structures of the PI3Kα (Arg770), PI3Kβ (Lys771), and PI3Kγ (Lys802) isoforms with Trp760 (δ-numbering) that is not present in PI3Kδ (Thr750). They reported that this may suggest that their inhibitors might be able to form an extra Van der Waals π−π face to face interaction with Trp760, an interaction that is obstructed in the case of the other isoforms. These effects coupled together produced a synergistic group effect, to introduce high δ-selectivity. The physicochemical properties of compound **100** were calculated (PI3K δ (pIC_{50} = 9.1), MW 540.7, cLogP 3.9, clogD 2.5, TPSA 88 $Å^2$, solubility at pH 7.4 in water: 0.02 mg/mL, solubility category: Low, LIPE = 5.2) and they report that the properties may not be ideal for oral drug likeness, however the compounds may fulfil inhalation delivery criteria.[85]

The remainder of the perspective will examine the medicinal chemistry design and evaluation based on a core chemical structure categorized by scaffold class.

Pyrrolo[2,1-f][1,2,4]triazin-4-amines

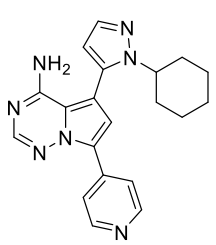

102

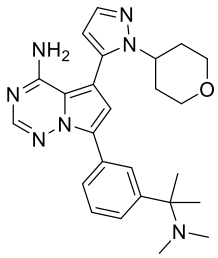

103

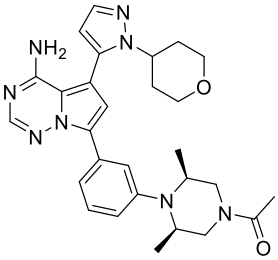

104

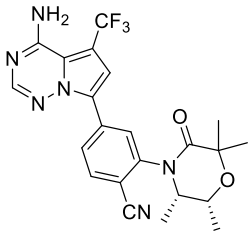

105

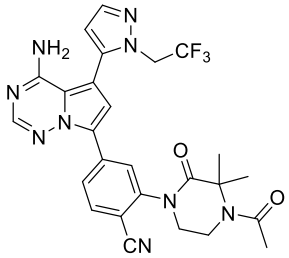

106

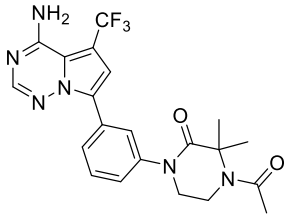

107

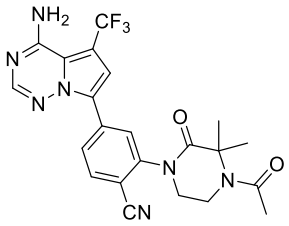

108

A novel series of pyrrolo[2,1-f][1,2,4]triazin-4-amines have been reported by researchers from Bristol-Myers Squibb, resulting in the identification of selective PI3Kδ inhibitors. Bhide *et al.* reported on the identification of **102** (PI3Kδ IC_{50} = 22 nM) from a kinase-directed screen.[86] However, **102** was shown to be non-selective against other PI3K isoforms (fold selectivity PI3K α/β/γ = 4/120/0.4) and a potent CYP inhibitor which was attributed to the 4-pyridyl moiety as well as poor microsomal stability due, in part, to the lipophilic cyclohexyl ring. Extensive SAR aimed at changing the cyclohexyl group and the pyridine ring resulted in the identification of **103** (PI3Kδ IC_{50} = 2 nM, fold selectivity PI3K α/β/γ = 665/800/130), a compound with improved metabolic stability (58% remaining @ 0.5 μM 10 min incubation) and good pharmacokinetics (mouse PK CL 82.1 mL/kg/Kg; V_{ss} 6.2 L/kg, F = 46%) that subsequently demonstrated *in vivo* efficacy in a mouse Keyhole Limpet Hemocyanin (KLH) and collagen-induced arthritis (CIA) model, when dosed at 100 mg/kg. The efficacy was reported to be better than that of methotrexate at 1mg/kg. Qin *et al.* reported on the optimization of the ADMET properties of the

compounds leading to the identification of **104** (PI3Kδ IC_{50} = 1.3 nM, fold selectivity PI3K α/β/γ = 611/1443/44), a compound with reduced *h*ERG activity (18% @ 10 μM – patch clamp) and metabolic stability. **104** progressed to a 4-day exploratory toxicity study in mice dosed up to 300 mg/kg/day (QD) and was found to be well tolerated at all doses. In addition, **2** showed efficacy in the KLH model when dosed at 3 mg/kg, reflecting the improvement in whole cell potency and pharmacokinetic properties, compared to **103**.[87] Running in parallel, Marcoux *et al.* reported further SAR studies to improve the physical and pharmacokinetic properties of **104**. Further exploration of the substituted piperazine and the replacement of the substituted pyrazole with smaller moieties resulted in the identification of the highly isoform-selective PI3Kδ inhibitor **105** (PI3Kδ PIC_{50} = <0.2 nM, fold selectivity PI3K α/β/γ = >1000) that was highly potent in a human B cell proliferation assay (IC_{50} = 1 nM). In addition, **105** was shown not to inhibit any CYPS or ion channels. It possessed very good permeability but unfortunately exhibited poor stability towards liver microsomes where it was determined that the morpholine ring was extensively metabolized and was not progressed further.[88] Liu *et al.* finally reported on the identification of a pre-clinical candidate **108** identified after further extensive SAR studies to improve on the pharmacokinetic properties within the evolving series. Guided by X-ray crystallography of **106** (PI3Kδ IC_{50} = 2.4 ± 0.8nM, fold selectivity PI3K γ = 270), in PI3Kδ (Figure 9), the polar pyrazole group was replaced with either a simple chlorine atom or a trifluoromethyl group, which led to **107** (PI3Kδ IC_{50} = 3 ± 1 nM, fold selectivity PI3K α/γ =110/37), a compound with improved Caco-2 permeability, reduced *h*ERG activity (12% @ 3 μM – patch clamp) and increased selectivity profile, while maintaining potency in the CD69 *h*WB assay.

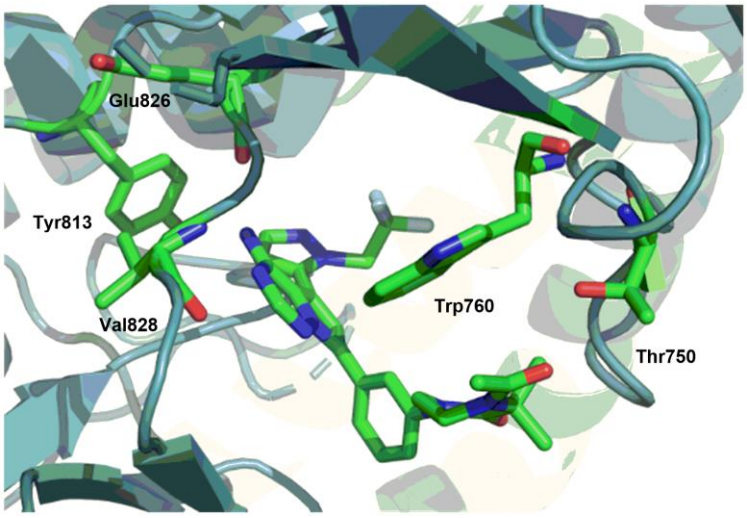

Figure 9. X-ray co-crystal structure of **106** bound into PI3Kδ. Key interactions between **106** and the hinge included Val828 and Glu826 and a close interaction between the carbonyl of the acetamide group and Thr750. The pyrazole group of **106** filled a hydrophobic pocket formed by Ile825 (not shown) and participated in an edge-to-face interaction with Tyr813 (PDB 5VLR)

Final optimization of the aryl substitution identified **108** (PI3Kδ IC_{50} = 1.9 ± 0.9 nM, fold selectivity PI3K α/β/γ =700/1443/>5000), where it was shown that the 4-CN group led to an improved human/rodent scaling in microsomal metabolic stability and excellent cross species pharmacokinetics (e.g. rat PK CL = 2.3 ± 0.3 mL/min/kg; Vss = 0.5 ± 0.1 L/kg; F = 71%). **108** proved highly efficacious in a mouse collagen-induced arthritis model for 42 days. Although lower than expected exposures were observed for **108**, a dose-dependent reduction of the clinical score was observed where doses of 2 and 5 mg/kg showed greater than 50% suppression of paw swelling. Taking the exposure into consideration, an EC_{50} of 10 nM at 24 h (ED_{50} of ~1.25 mg/kg) was derived.[89]

Amino triazine-based hinge binders

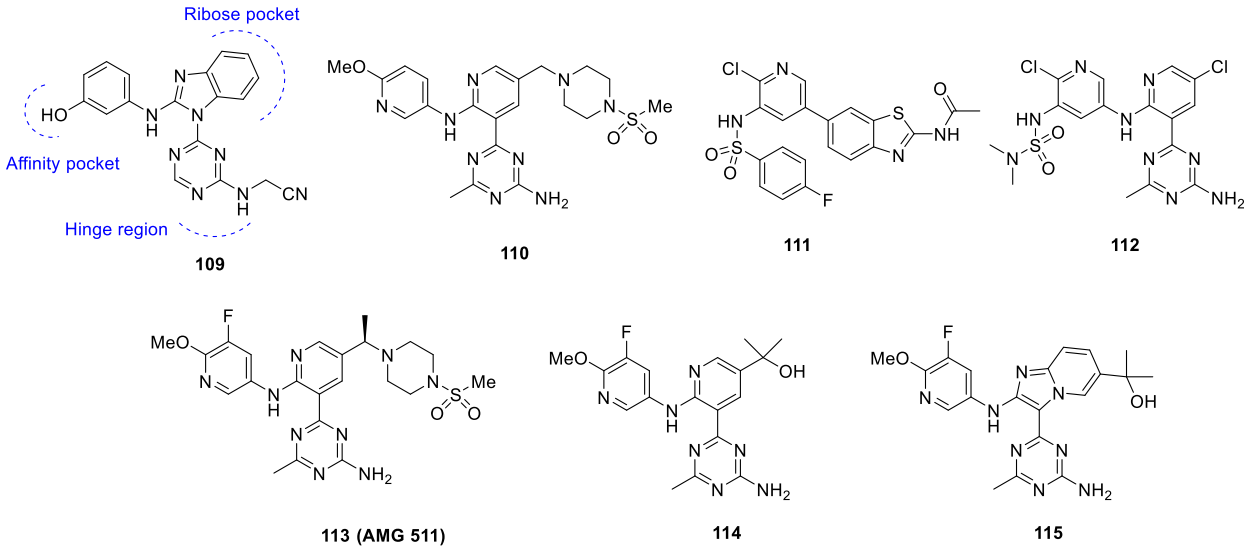

Figure 10. Amino triazine-based hinge binders

In a series of publications scientists from Amgen reported on the optimization of a novel series of substituted amino triazines culminating in the identification of **113** (AMG 511, Figure 10). In their first paper, Smith *et al.* discussed the optimization of a benzimidazole triazine **109** obtained from a HTS screen.[90] **109** had favorable properties (PI3Kα IC_{50} = 0.32 μM; PI3Kβ IC_{50} = 0.38 μM; PI3Kδ IC_{50} = 0.24 μM; PI3Kγ IC_{50} = 0.1 μM, mTOR IC_{50} = 0.097 μM) and a co-crystal structure was determined in PI3Kγ, demonstrating that **109** bound in the ATP binding site. Optimization of **109** led to **110** (PI3Kα IC_{50} = 9 nM; PI3Kβ IC_{50} = 5 nM; PI3Kδ IC_{50} = 2 nM; PI3Kγ IC_{50} = 4 nM, mTOR IC_{50} = 4.8 μM), where the substituted piperazine was making interactions with the ribose pocket and the metabolically-labile 3-phenol was replaced with a substituted pyridine. **110** had good oral exposure in mice (F = 95%, 25 mg/kg p.o.) and inhibited HGF-stimulated PI3K signaling in a mouse liver PD assay where a 75 mg/kg dose was able to maintain sufficient plasma concentrations for 24 h to provide at least 64% target coverage over a 24 h period (plasma free fraction concentration = 68 nM at 24 h). Subsequently, **110** caused a

dose-dependent inhibition of tumor growth with an ED_{50} of 6.0 mg/kg ($AUC_{0–24\ h}$ = 7.6 μM/h) in CD1 nude mice and tumor stasis was achieved at 25 mg/kg QD. However, it was concluded that continuous robust inhibition of PI3K over 14 days may be poorly tolerated.[91] Wurtz *et al.* reported on the hybridization of compounds; combining the amino triazines, such as **110** with a series of substituted aminobenzthiazoles **111** (PI3Kα IC_{50} = 1.2 nM; mTOR IC_{50} = 2.1 nM) [92] to generate **112** (PI3Kα IC_{50} = 7.7 nM; PI3Kβ IC_{50} = 0.4 nM; PI3Kδ IC_{50} = 2 nM; PI3Kγ IC_{50} = 1 nM, mTOR IC_{50} = 163 μM), which exhibited good oral bioavailability in rats (F = 63%) and showed a dose dependent reduction in the phosphorylation of Akt in a U87 tumor pharmacodynamic model with a plasma EC_{50} = 193 nM.[93] Norman *et al.* reported on further optimization of **110** to identify **113**, a potent pan inhibitor of class I PI3Ks with a superior pharmacokinetic profile (PI3Kα K*i* = 4 nM; PI3Kβ K*i* = 6 nM; PI3Kδ K*i* = 2 nM; PI3Kγ K*i* = 1 nM).[94] **113** was shown to potently block the targeted PI3K pathway in a mouse liver pharmacodynamic model as indicated by a dose-dependent decrease in phosphorylated AKT (p-AKT) at Ser473 and a nonlinear regression analysis revealed a plasma EC_{50} of 228 ng/mL. It was shown that inhibition of AKT phosphorylation directly correlated with plasma concentrations. **113** inhibit tumor growth in a U87 malignant glioma glioblastoma xenograft model where treatment at 1 mg/kg QD resulted in significant inhibition of tumor growth of approximately 70% compared to the vehicle control group. Tumor stasis was observed in the cohort treated with 3 mg/kg, and tumor regression was observed in the 10 mg/kg cohort. The ED_{50} of compound **113** was 0.6 mg/kg, with an AUC at EC_{50} of 3.6 μg·h/mL. On the basis of its excellent *in vivo* efficacy and pharmacokinetic profile, compound **113** was selected for further evaluation as a clinical candidate. However, to date no further information has been reported.

In a subsequent paper, Lanman *et al.* reported on studies to replace the piperazine sulfonamide portion of **113** with an array of primary alcohols to reduce molecular weight and improve interaction within the ribose binding pocket, leading to the identification of **114** (PI3Kα K*i* = 23 nM), a compound with much reduced MWt compared to **113** (327 Da for **114** vs 518 Da for **113**). **114** demonstrated a similar pharmacokinetic profile to that of **113** with oral bioavailability slightly reduced (37% vs 57%) and clearance elevated (1.1 vs 0.45 L/h/kg). **114** was further evaluated in a mouse liver pharmacodynamic model that measured the inhibition of hepatocyte growth factor (HGF)-induced Akt phosphorylation at Ser473 in female CD1 nude mice and it significantly suppressed PI3K signaling at 10 and 30 mg/kg bringing about a dose-dependent decrease in p(S473)Akt. A nonlinear regression analysis established an EC_{50} of 239 ng/mL, comparable to that obtained from compound **113** (EC_{50} = 240 ng/mL). The biological activity of the significantly truncated analog **114** relative to **113** highlights both the efficiency of the 2-hydroxypropyl group as a ribose pocket binding group however, compounds from this class were unable to replicate the enzymatic potency of the piperazine sulfonamide series.[95] Stec *et al.* investigated the use of the imidazo[1,2-a]pyridine ring system as a scaffold and identified **115** as a potent dual phosphoinositide-3-kinase (PI3K)/mammalian target of rapamycin (mTOR) inhibitor (PI3Kα K*i* = 11 nM; PI3Kβ K*i* = 17 nM; PI3Kδ K*i*= 0.6 nM; PI3Kγ K*i* = 5.3 nM) mTOR IC_{50} = 206 nM). When dosed orally in rats (2 mg/kg), **115** showed good oral bioavailability (51%) and moderate plasma exposure (AUC = 640 ng·h/mL). The *in vivo* activity of compound **115** was evaluated in the mouse liver pharmacodynamic assay and showed significant inhibition of AKT phosphorylation at all three doses with a maximum inhibition of 56% at the 30 mg/kg dose. The calculated ED_{50} relative to vehicle was 11 mg/kg.[96]

2,3-Dihydroimidazo[1,2-c]quinazolin-5-yl)pyrimidine-based inhibitors (copanlisib)

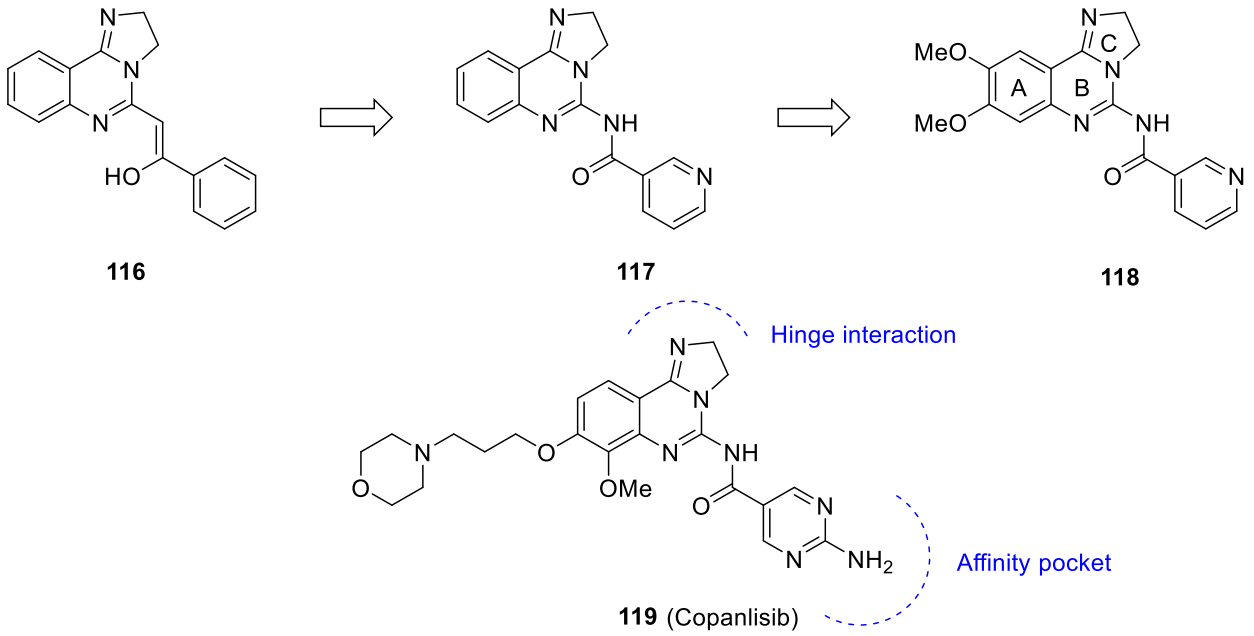

Scheme 6. Discovery of **119** (copanlisib) a PI3K inhibitor with potential antineoplastic activity

Scott *et al.* recently reported on the identification of **119** (copanlisib), a selective PI3Kα/β inhibitor that has been granted an accelerated approval as a treatment for patients with relapsed follicular lymphoma who have received at least 2 least prior systemic therapies (Scheme 6).[97, 98] HTS on a series of PI3Kγ-active leads led to the discovery of the structurally novel 2,3-dihydroimidazo[1,2-c]quinazoline **116** (PI3Kγ IC_{50} = 810 nM, PI3Kβ IC_{50} = 4000 nM). In the lead optimization phase, the enol moiety of **116** could be replaced with an amide moiety giving **117** (PI3Kγ IC_{50} = 60 nM, PI3Kβ IC_{50} = 1 nM) and further substitutions on the phenyl ring led to **118** (PI3Kγ IC_{50} = 60 nM, PI3Kβ IC_{50} = 1700 nM) and both were shown to have an effect on isoform selectivity. Therefore, a program to optimize the PI3Kβ and PI3Kα activity of the 2,3-dihydroimidazo[1,2-c]quinazoline lead for potential use in cancer therapies was undertaken. Scott *et al.* reported on extensive SAR studies where multiple substitutions on the A ring in combination to changes in the B and C rings eventually led to the discovery of **119**

(copanlisib).[97] An X-ray crystal structure showed that the imidazoline N-1 nitrogen atom formed a critical hydrogen bond to Val882 in the adenine hinge pocket and the 4-aminopyrimiding group interacted in the affinity pocket forming hydrogen bonds with Asp836 and Asp841 through the amino group, and with Lys833 through a pyrimidine nitrogen atom (PDB 5G2N). Copanlisib was shown to be a potent PI3K inhibitor (PI3Kα IC_{50} = 0.5 nM, PI3Kβ IC_{50} = 3.7 nM, PI3Kγ IC_{50} = 6.4 nM, PI3Kβ IC_{50} = 45 nM) as well as inhibiting mTOR (IC_{50} = 45 nM) and has potent cellular mechanistic activity, inhibiting both IGF-1-stimulated AKT phosphorylation in S473 cells, and basal AKT phosphorylation in KPL4 cells. The intravenous first-in-human phase I study of copanlisib in patients with advanced solid tumors and non-Hodgkin's lymphomas (NHL) showed that it was well tolerated with a MTD of 0.8 mg/kg. Copanlisib exhibited dose-proportional pharmacokinetics and promising anti-tumor activity, particularly in patients with NHL.[99]

4,6-Disubstituted indazole-based inhibitors (GSK2269557 & GSK2292767)

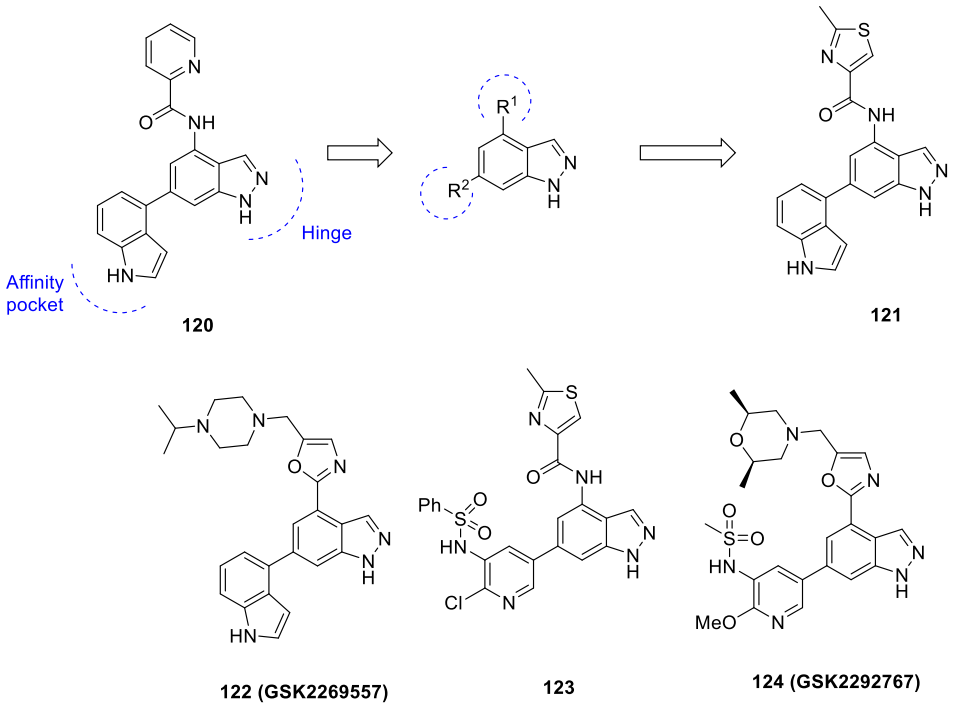

Scheme 7. Identification of **120** and the evolution to **122** (GSK2269557) and **124** (GSK2292767)

Down *et al.* reported on the discovery of a series of selective indazole-based PI3Kδ inhibitors for the treatment of respiratory diseases, culminating in the discovery of the development compound **122** (GSK2269557) and the back-up clinical candidate **124** (GSK2292767) (Scheme 7).[100] Compound **120** was selected as a lead due to its favorable selectivity profile for PI3Kδ (PI3Kδ pIC_{50} = 7.0; PI3Kβ pIC_{50} = 5.2; PI3Kα pIC_{50} = 5.0; PI3Kγ pIC_{50} = 5.2) and, to avoid any potential negative impact of broad systemic inhibition of this biology, a lead optimization program was initiated with the aim of delivering an inhaled clinical candidate. Inhibition of PI3K enzymatic activity was determined using a homogeneous time-resolved fluorescence (HTRF) assay format and to measure cellular activity for compounds of interest. In addition, a peripheral blood mononuclear (PBMC) assay was used using cytostim to stimulate cytokine production from the T-lymphocyte compartment. Interferon γ (IFNγ) was selected as an optimal

analyte owing to robust stimulation by cytostim and exquisite sensitivity to PI3Kδ inhibition. The target profile was established of high potency, which is a requirement for inhaled delivery due to dose limitations and the target PK profile was intended to minimize systemic circulation after inhaled delivery. Therefore, moderate to high intrinsic clearance was required in order to ensure removal of drug once absorbed through the lung into the plasma and low oral bioavailability was required to limit absorption of the swallowed fraction of the inhaled dose. Exploration of the SAR at the two positions of substitution on the indazole core was examined, where initially group R_2 was fixed as indole and exploration of R_1 pursued. A set of 4-position amide modifications were prepared while keeping the 6-indole substituent fixed. Extensive SAR showed that in this position a planar amide conformation was important for potency and isoform selectivity, as typified by **121** (PI3Kδ pIC_{50} = 7.3; PI3Kβ pIC_{50} = 5.0; PI3Kα pIC_{50} <4.6; PI3Kγ pIC_{50} = 5.4). The requirements for planarity to balance both isoform potency and pharmacokinetics led to the application of heteroaromatic bioisosteric replacements for the co-planar amide substitutent R^1, leading to the eventual discovery of **122** (PI3Kδ pK_i = 9.9; PI3Kβ pK_i = 5.8; PI3Kα pK_i = 5.3; PI3Kγ pK_i = 5.2), a compound with excellent cellular activity (PBMC IFNγ pK_i 9.7). The rat PK profile of **122** was encouraging, with low oral bioavailability (F = 2%) and *in vivo* clearance of 28 mL min^{-1} kg^{-1}, which met the criteria for progression. Importantly, due to the dibasic nature of **122** in combination with its moderate lipophilicity (clogP = 4.4), **122** also had a high volume of distribution of 6.3 L/kg, which suggested a beneficial tissue retention when delivered topically to the lung. **122** was progressed to a human lung parenchyma assay where finely chopped lung tissue was incubated with the plant lectin phytohemagglutinin (PHA) for 72 h to induce production of cytokines including IFNγ and IL-2. This response was inhibited by **122** in a concentration-dependent manner, returning pIC_{50} values

of 8.2 (IFNγ) and 8.1 (IL-2). In a disease relevant brown Norway rat acute OVA model of Th2 driven lung inflammation, **122** was shown to protect against eosinophil recruitment, with an ED_{50} of 67 μg/kg. In addition, the activity of **122** was assessed using other end points in this model, including leukocyte recruitment to the lung (neutrophils, macrophages, CD4 and CD8 T-lymphocytes at 48 h) and Th2 cytokines such as IL-13. Importantly, **122** was shown to dose-dependently reduce recruitment of all leukocyte sub-populations and IL-13 in the lungs. In light of all the data, **122** progressed to clinical evaluation as GSK2269557. In phase I studies, inhaled GSK2269557 had an acceptable safety profile for progression into larger studies in COPD patients and resulted in suppression of sputum IL-8 and IL-6 levels, consistent with the known anti-inflammatory activity of a PI3Kδ inhibitor and further clinical trials are on-going.[101] Replacing the indole in **121** with a pyridyl methylsulfonamide gave **123** (PI3Kδ pIC_{50} = 8.7; PI3Kβ pIC_{50} = 6.0; PI3Kα pIC_{50} = 6.5; PI3Kγ pIC_{50} = 7.3). Although this replacement resulted in a greater than 10-fold increase in potency for PI3Kδ, potency at the other PI3K isoforms was also significantly enhanced, such that compound **123** was no more selective than compound **121**. However, further evolution of the sulfonamide group and bioisosteric replacement of the secondary amide resulted in **124** ((PI3Kδ pKi = 10.1; PI3Kβ pKi = 6.2; PI3Kα pKi = 6.3; PI3Kγ pKi = 6.3), with excellent cellular activity (PBMC IFNγ pKi = 9.2). In a human lung parenchyma assay, **124** inhibited both IFNγ and IL-2 production in a concentration-dependent manner, with pIC_{50} values of 8.7 and 8.5, respectively. In the brown Norway rat acute OVA model of Th2 driven inflammation in the lungs, **124** was shown to protect against eosinophil recruitment with an ED_{50} of 35 μg/kg, similar to compound **122**. A PK study in rat, demonstrated a high *in vivo* clearance of 50 mL min^{-1} kg^{-1} which was significantly higher than that for compound **122** and fitted well for the target profile for a follow-up inhaled candidate. In addition, the oral

bioavailability was low (F < 2%), in line with the data observed for compound **122** and therefore **124** was progressed into preclinical development as a back-up for **122**.

1,3-Dihydro-2H-imidazo[4,5-c][1,5]naphthyridin-2-ones (BEZ235) - inspired inhibitors

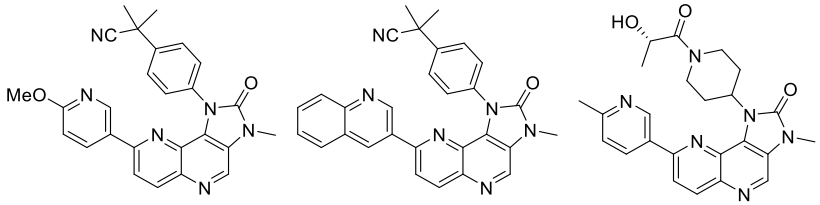

Starting from **125** (BEZ235, dactolisib),[61] the first PI3K inhibitor to enter clinical trials in 2006, Chen *et al.* from Pfizer reported on a fast-follower approach to discover **126**, which exhibited excellent properties (mouse PI3Kα Ki = 1.41 nM, which translates to a ligand efficiency (LE) of 0.354). When tested in an mTOR kinase domain *in vitro* biochemical assay, **126** exhibited good activity with a K_i of 4.51 nM. However, in a BT20 cell assay, measuring inhibition of AKT phosphorylation at S473, **126** exhibited only moderate cellular potency with an IC_{50} of 144 nM, which relates to a cell-based LipE of 2.15, due to high lipophilicity (cLogP 4.69). Unsurprisingly, the combination of lack of sp^3 atoms and lipophilicity led to the reported poor solubility (2.0 μM). [102] SAR studies, directed to increasing both PI3Kα and mTOR activity whilst reducing lipophilicity led to the discovery of **127** (PF-04979064), as a structurally diverse back-up to their first development compound **79**.[64] Compound **127** (PI3Kα K_i = 0.3 nM; mTOR K_i = 1.42 nM) and, due in part to the reduction in lipophilicity (cLogP = 1.27) and increase in solubility (539 μM), had very good cellular potency (IC_{50} = 9.1 nM), which relates to a cell-based improved LipE of 6.8. **127** progressed to pharmacokinetic studies (rat PK CL = 19.3 ml/min/kg; V_{dss} = 5.23 L/kg; F = 61%) and progressed to mouse *in vivo* xenograft efficacy

studies, where it exhibited dose proportional tumor growth inhibition (TGI) in a U87MG mouse xenograft model, achieving 88% TGI at the highest tolerated dose, 40 mg/kg QD.

2,8-Disubstituted pyrido[3,2-d]pyrimidine and substituted 5,6,7,8-tetrahydropyrido[4,3-d]pyrimidine inhibitors (leniolisib)

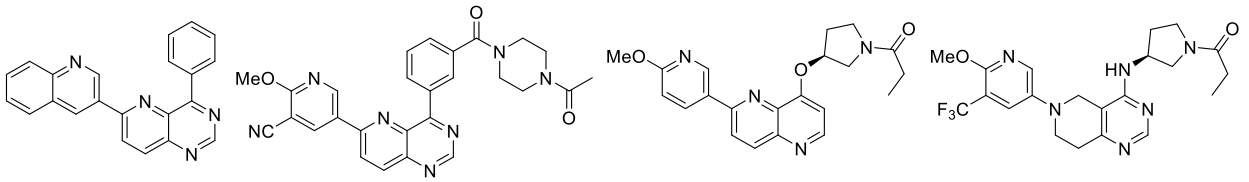

128 **129** **130** **131**

Hoegenauer *et al.* from Novartis also used **125** as a starting point for the discovery of **131**.[103] In their first disclosure they reported on efforts to synthesize a PI3Kδ inhibitor. Guided by docking studies they deconstructed the imidazolquinoline present in **125,** which they considered was contributing to the affinity of **125** for mTOR (mTOR IC_{50} = 6 nM), to the simplified quinazoline fragment **128** (PI3Kα IC_{50} = 0.65 μM; PI3Kδ IC_{50} = 8.1 μM; PI3Kβ/γ and mTOR IC_{50} = >10μM). Further SAR studies led to **129** (PI3Kα IC_{50} = 0.262 μM; PI3Kδ IC_{50} = 9 nM; PI3Kβ IC_{50} = 1.65 μM; PI3Kγ IC_{50} = 4.63 μM, cell activity PI3Kδ IC_{50} = 0.049 μM). In rats, **129** showed a moderate 22% oral bioavailability. While a higher total exposure could be reached with increasing the dose to 30 mg/kg, this overall gain was not dose-linear and bioavailability dropped to 10%, likely due to solubility limited absorption. However, in dogs the overall pharmacokinetic properties for **129** were similar but with a better 42% oral bioavailability at 0.3 mg/kg. PK/PD studies were performed in rodents following a single oral dose of compound **129** (30 mg/kg) in male Lewis rats. Blood was collected at various time points and changes for two PD biomarker expression profiles as well as drug levels were determined. A clear relationship of drug exposure, inhibition of Akt

phosphorylation and anti-IgM/rIL-4-induced CD86 expression was observed.[104] Further SAR was reported by Hoegenauer *et al.* to improve physicochemical properties of the quinazoline series, as typified by **129**, through reducing the MWt and fsp^3 which are known drivers of poor physicochemical properties. Further SAR studies resulted in the identification of **130** (PI3Kα IC_{50} = 0.424 μM; PI3Kδ IC_{50} = 22 nM; PI3Kβ IC_{50} = 1.03 μM; PI3Kγ IC_{50} = 2.94 μM). However, the improvement in physicochemical properties did not lead to an increase in cellular activity (IC_{50} = 0.022 μM), due in part, to the reduction in PI3Kδ activity.[105] In their final publication, further optimization led to the discovery of **131** (leniolisib PI3Kα IC_{50} = 0.244 μM; PI3Kδ IC_{50} = 11 nM; PI3Kβ IC_{50} = 0.424 μM; PI3Kγ IC_{50} = 2.23 μM). **131** demonstrated 30-fold cell activity over PI3Kα (PI3Kδ IC_{50} = 56 nM). **131** was tested in a mouse ozone-induced lung inflammation model where it dose-dependently inhibited the increase in bronchoalveolar lavage (BAL) neutrophil and macrophage numbers with ED_{50} values of 16 mg/kg and 40 mg/kg, respectively. In a rat model of collagen-induced arthritis (*r*CIA) it significantly inhibited pathogenic anti-rat collagen antibodies, paw swelling, inflammatory cell infiltration, proteoglycan loss and joint erosion when dosing started, before disease onset and full efficacy was also observed with low doses (3 mg/kg bid). In a therapeutic setting when **131** was administered when significant paw swelling was present, a dose of 10 mg/kg bid significantly ameliorated disease parameters.[103] Currently **131** is undergoing Phase II/III studies for Activated PI3Kδ syndrome and Primary Sjögren syndrome.[106]

Xin *et al.* reported on the synthesis of a range of 4-anilinequinazoline derivatives as PI3Kδ inhibitors designed as a fast follower approach.

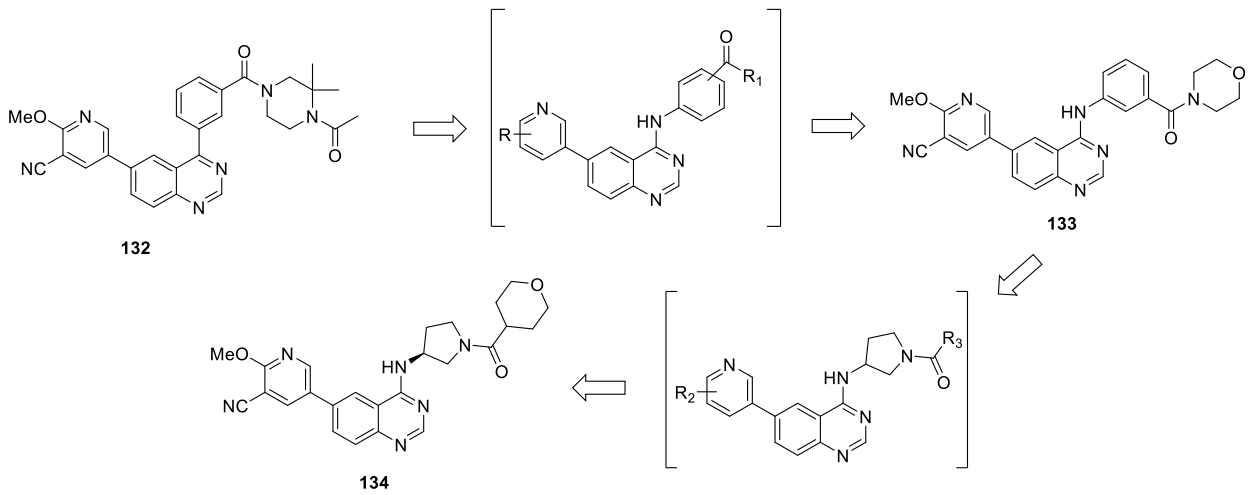

Scheme 8: 2,8-Disubstituted pyrido[3,2-d]pyrimidine inhibitors

Changing the aromatic linkage present in the Novartis compound **132** generated a new series of 6-aryl substituted 4-anilinquinazoline derivatives (Scheme 8), which resulted in the identification of **133** (PI3Kδ IC_{50} = 9.3 nM). **133** demonstrated similar anti-proliferative profiles to idelalisib in several human B cell lines (e.g RPMI-8226 IC_{50} = 6.61 μM; idelalisib IC_{50} = 5.49 μM).[107] Further studies, changing the aniline group for less lipophilic moieties resulted in the identification of **134** (PI3Kδ IC_{50} = 2.7 nM; PI3Kα IC_{50} = 25.6 nM; PI3Kβ IC_{50} = 263.8 nM; PI3Kγ IC_{50} = 174.2 nM).[108] **134** showed significant potent anti-proliferative activity against human B cell line Ramos (IC_{50} = 0.57 μM), moderate anti-proliferation against RPMI-8226 (IC_{50} = 4.34 μM) and SU-DHL-6 (IC_{50} = 4.55 μM), but no activity against Raji (IC_{50} > 10 μM).

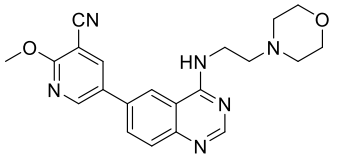

135

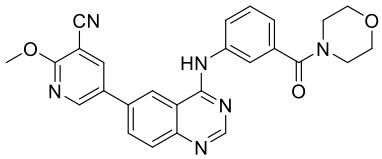

36

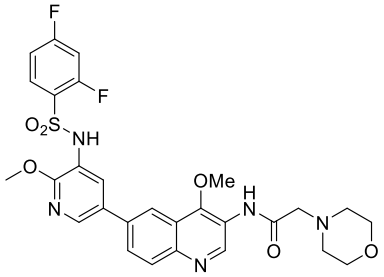

137

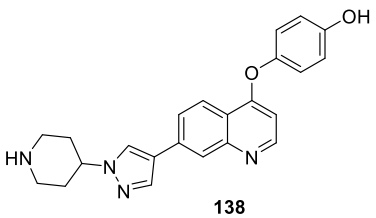

138

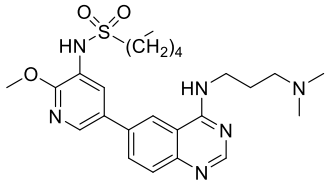

139

Hei *et al.* reported on a series of 4,6-disubstituted quinazoline derivatives, as typified by **135**, which displayed high potency against PI3K enzymes (PI3Kα IC_{50} = 465 nM, PI3Kδ IC_{50} = 37 nM) and anti-proliferative activities against both HCT-116 (IC_{50} = 0.51 μM) and MCF-7 (IC_{50} = 2.10 μM) and could efficaciously inhibit tumor growth in a mice S-180 model.[109] In a similar series of compounds, Xin *et al.* demonstrated that **136** had good PI3K enzyme activity (PI3Kδ IC_{50} = 9.3 nM) and showed similar anti-proliferative profiles to idelalisib in human B cell lines [e.g. RPMI-8226 cells IC_{50} = 6.61 μM, idelalisib 5.49 μM].[110] Zhang *et al.* reported on **137**, a potent PI3K/mTOR dual inhibitor which significantly inhibit Class I PI3Ks **(**PI3Kδ IC_{50} = 0.87 nM; PI3Kβ $IC_{50=}$ 3.9 nM; PI3Kα IC_{50} = 1.7 nM; PI3Kγ IC_{50} = 8.4 nM), mTOR (IC_{50} = 10 nM) and phosphorylation of pAkt(Ser473) at low nanomolar level.[111] Moreover, **137** displayed high potency in an anti-proliferative assay in PC-3 cells (IC_{50} = 80 nM) and showed acceptable *in vivo* pharmacokinetic properties in mice after oral administration at 5 mg/kg as a crystalline suspension in 0.5% methylcellulose [CL = 0.42 L/h/kg, V_d, = 1.0 L/kg, plasma terminal half-life ($T_{1/2}$, 1.6 h)]. Mah *et al.* reported the identification of 4-phenoxyquinoline based inhibitor for L1196M

mutant of anaplastic lymphoma kinase as typified by **138** discovered by a fragment growing strategy.[112] **138** exhibited significant anti-proliferative effects on H2228 CR crizotinib-resistant cells by decreasing PI3K/AKT and MAPK signaling. Fan *et al.* highlighted compound **139** with potent anti-proliferative activity without cytotoxicity to human normal cells. **139** was reported to be selective for PI3K*a* (IC_{50} = 13.6 nM. Selectivity ~10-fold) and, in a western blot assay, **138** demonstrated inhibition of cell proliferation *via* suppression of PI3Kα kinase activity (IC_{50} of 13.6 nM) and subsequently blocked PI3K/Akt pathway activation in HCT116 cells.[113]

7,9-Disubstituted-2-morpholino-4H-pyrido[1,2-a]pyrimidin-4-one-based inhibitors – evolution of AZD6482 and AZD8186

TGX-221 (**140**) was disclosed as a selective PI3Kβ inhibitor by Kinaacia Ply Ltd, a spin out from Monash University, and has served as the inspiration of several drug discovery programs looking for potent and selective PI3Kβ inhibitors (Scheme 9).

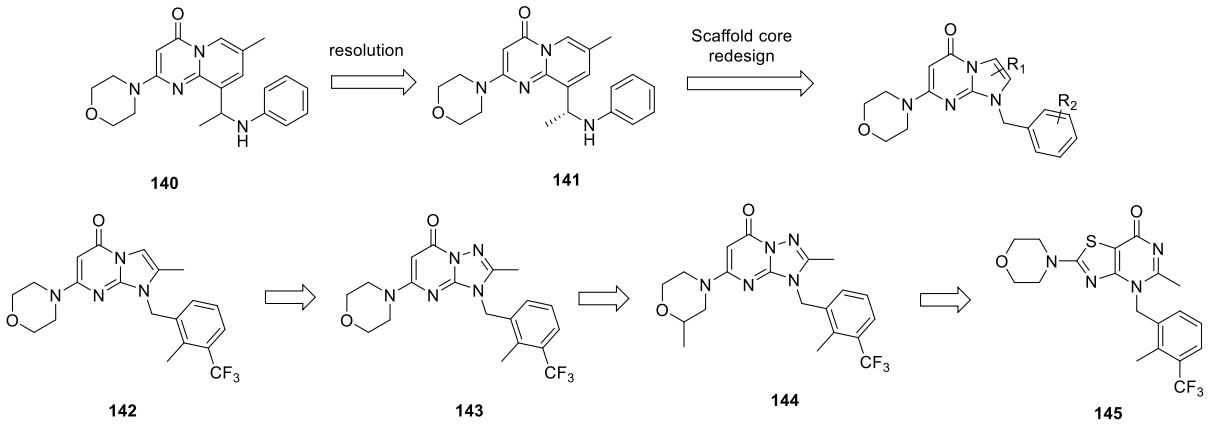

Scheme 9. Evolution of 7,9-disubstituted-2-morpholino-4H-pyrido[1,2-a]pyrimidin-4-one-based inhibitors

Scientists at GSK separated the enantiomers by chiral HPLC and discovered that the biological activity resided in one enantiomer, with the *(R)*-enantiomer **141** (PI3Kβ IC_{50} = 6 nM) being ~30-fold more potent than the *(S)*-enantiomer (PI3Kβ IC_{50} = 200 nM), suggesting that the aniline plays an important role in the interaction with PI3Kβ.[114] It was suggested that imadazo[1,2-a]-pyrimidine-5(1*H*)-one, with a *N*-1 substituted benzyl group, would be a replacement scaffold and SAR demonstrated that a 2, 3-disubstituted benzyl group was optimal for balancing potency and PI3Kβ isoform selectivity **142** (PI3Kβ = 1 nM; PI3Kα = 2 μM; PI3Kδ = 8 nM; PI3Kγ = 1 μM), as well as demonstrating potent cell growth inhibition (EC_{50} = 0.14 μM) against a PTEN-deficient breast cancer cell line (MDA-MB-468). In a follow on publication, the core imadazo[1,2-a]-pyrimidine-5(1*H*)-one was changed to a 1,2,4-triazolo[1,5-a]pyrimidin-7(3*H*)-one with similar activity, **143** (PI3Kβ = 1.5 nM; PI3Kδ = 4 nM), as well as demonstrating good cell growth inhibition (EC_{50} = 0.1 μM) against a PTEN-deficient breast cancer cell line (MDA-MB-468). Substituting the morpholine ring with a 2-methyl group substantially increased potency and cell-based activity **144** (PI3Kβ = 0.3 nM; PI3Kδ = 4 nM; EC_{50} = 0.5 nM). Unfortunately, the series of compounds suffered high rat clearance and was not progressed.[115] In light of the poor rat metabolic stability, a core change to a new thiazolopyrimidinone series was evolved.[114] Once more extensive SAR studies identified **145** (PI3Kβ = 0.6 nM; PI3Kα = 2.5 μM; PI3Kδ = 20 nM; PI3Kγ = 0.79 μM; cell: MDA-MB-468 pAKT IC_{50} 24 nM; proliferation gIC_{50} = 0.103 μM). Importantly, **145** showed good pharmacokinetics (mouse PK CL 29.6 mL/min/kg); Vd_{ss} 2.8 L/kg; F 49%) and progressed to a PTEN-deficient PC-3 prostate carcinoma xenograft mouse model, where it was dosed once-daily for 21 days at 100 and 300 mg/kg, demonstrating complete tumor growth inhibition relative to vehicle treated mice, with no effect on body weight. However, the authors conclude by stating that other unknown activities of PI3Kβ may be

contributing to the effects on tumor growth. However, these studies represented a significant milestone towards validating PI3Kβ as a potential target for proliferative disorders.

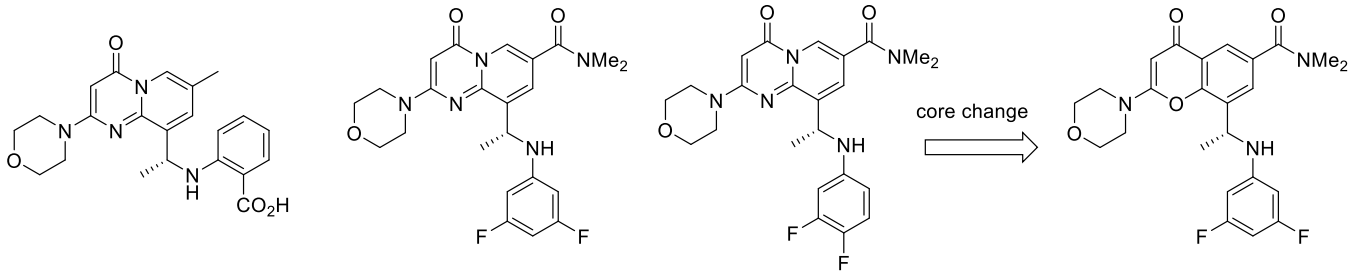

Scheme 10. Chemical modifications on **146** to deliver AZD8186 a PI3Kβ Inhibitor for use in treating patients with advanced solid tumors with PTEN or PIK3CB mutations that are metastatic or cannot be removed by surgery

Once more taking inspiration from **141** and **146** (AZD6482), Barlaam *et al.* reported on the discovery of 9-(1-anilinoethyl)-2-morpholino-4-oxo-pyrido[1,2-a]pyridine carboxamides as selective PI3Kβ/δ inhibitors for the treatment of PTEN-deficient tumors.[116] With an aim of reducing lipophilicity and balancing PI3Kβ enzyme and cellular activity through increasing permeability, a series of 6-substituted carboxamides were synthesized which resulted in the identification of **147** (PI3Kβ IC_{50} = 5 nM; PI3Kα IC_{50} = 0.075 μM; PI3Kδ IC_{50} = 32 nM; PI3Kγ IC_{50} = 0.51 μM; cell: MDA-MB-468 pAKT IC_{50} = 3 nM, mouse PK CL = 82 mL/min/kg; F = 31%)). **147,** a compound with low/medium metabolic stability, showed profound pharmacodynamic modulation of phosphorylated Akt in a PC3 prostate tumor xenograft after a single oral dose. In addition, **148** (PI3Kβ IC_{50} = 7 nM; PI3Kα = 0.34 μM; PI3Kδ IC_{50} = 45 nM; PI3Kγ IC_{50} = 3.0 μM; cell: MDA-MB-468 pAKT IC_{50} = 34 nM, mouse PK CL = 74 mL/min/kg; F = 35%) demonstrated significant inhibition of tumor growth in the PC3 prostate xenograft model after chronic oral dosing. In order to address the low/medium metabolic stability, improve

solubility and increase bioavailability, a reduction in lipophilicity was explored, where the core was changed to a 2-morpholino-4-oxo-4H-chromene-6-carboxamide scaffold to generate, after extensive SAR studies, **149** (PI3Kβ IC_{50} = 4 nM; PI3Kα IC_{50} = 35 nM; PI3Kδ IC_{50} = 12 nM; PI3Kγ IC_{50} = 0.675 μM; cell: MDA-MB-468 pAKT IC_{50} = 3 nM, mouse PK CL = 77 mL/min/kg; F = 18%) (Scheme 10).[117] **149** proved to be efficacious for p-Akt in PTEN-deficient PC3 prostate tumor bearing mice after oral administration and showed complete inhibition of tumor growth in a mouse PTEN-deficient PC3 prostate tumor xenograft model. **149** was selected as a clinical candidate for patients with advanced castrate-resistant prostate cancer (CRPC), squamous non-small cell lung cancer (sqNSCLC), triple negative breast cancer (TNBC) and known PTEN-deficient / mutated or PIK3CB mutated / amplified advanced solid malignancies as a monotherapy and in combination with vistusertib or abiraterone acetate. Further clinical studies are on-going.

Marshall *et al.* reported on further SAR evaluation of pyrido[1,2-a]pyrimidinone-based class 1 PI3K inhibitors (Scheme 11).[118] Extensive SAR, such as replacement of the group X of by CH_2O and CH_2S decreased both potency and selectivity as well as constraining the group X with $NHSO_2$, NHCO or CONH moieties confirming the structural requirements for these "T-shaped" inhibitors.[117] Interestingly, in this report the *N*-methyl analogue **150** showed the best potency (PI3Kβ IC_{50} = 20 nM) but was not tested in a cell-based assay.

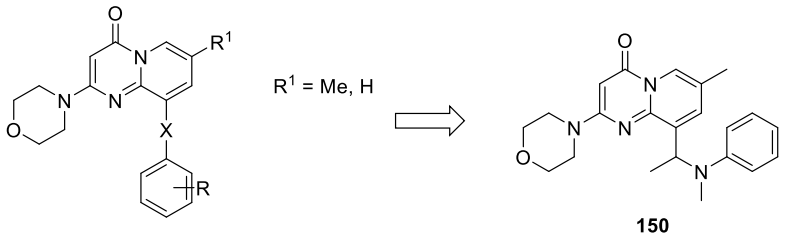

150

Scheme 11. Pyrido[1,2-a]pyrimidinone-based class 1 PI3K inhibitors

146 is an ATP-competitive PI3Kβ inhibitor and the first human target validation of PI3Kβ inhibition with **2** was reported following a 3 h infusion of seven different doses of **146**; a wide separation between anti-thrombotic effect and bleeding was observed, demonstrating that previous pharmacodynamic findings in dog translated well to man. Whereas **146** was well tolerated in man, a weak but significant concentration-dependent increase in plasma insulin and corresponding homeostasis model analysis (HOMA) index was recorded. In the plasma concentration range tested, it was suggested that such an effect could be ascribed to the compound's ability to inhibit PI3Kα (IC_{50} = 0.87 μM). In addition, **146** had a short plasma half-life (5–43 min) due to high metabolic clearance and a relatively small distribution volume (40–68 L).[117] Thus the pharmacokinetic and pharmacodynamic profile of **146** might limit its use to parenteral administration in situations where a low bleeding risk is desirable. Giordanetto *et al.* reported fragment-based drug discovery approaches [119,120] to reduce the PI3Kα inhibitory activity through investigating the requirement of the aromatic carboxylic acid, the linking group to the aniline and the incorporation of a group to improve water solubility. This extensive SAR resulted in **151** (PI3Kβ IC_{50} = 100 nM; PI3Kα IC_{50} = 3.5 μM; PI3Kδ IC_{50} = 0.4 μM; PI3Kγ IC_{50} = 83 μM; dog PK CL = 8 mL/min/kg; F = 31%) as a novel orally bioavailable PI3Kβ inhibitor. **151** inhibited platelet activation in plasma and whole blood, was highly soluble and metabolically stable. Furthermore, no significant inhibition of Cyp450 enzymes and ion channels involved in cardiac function was recorded. Efficacy versus bleeding in anaesthetized dogs showed **151** elicited a concentration-dependent inhibition of platelet aggregation *ex vivo* (EC_{80} = 0.69 ± 0.06 μM), which well predicted its inhibition of thrombosis *in vivo* (EC_{80}: 0.6 ± 0.05 μM). Importantly, no significant increase in bleeding time and blood loss was recorded at the observed

maximum compound concentration (24.1 ± 2.3 μM). Finally, no significant increase of the homeostasis model analysis (HOMA-index) from baseline was apparent at the maximum compound concentration (20.4 ± 2.1 μM). Therefore, the safety margin to compound concentrations resulting in full antithrombotic effect was acceptable and **151** was selected as a preclinical candidate for further development (Scheme 12).[121]

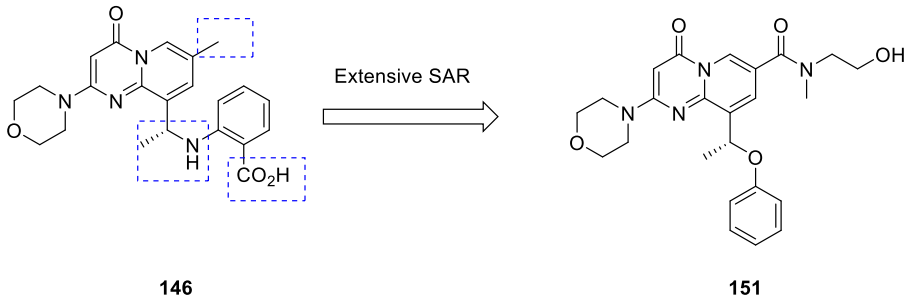

Scheme 12. Extensive SAR to deliver **151**

Starting from a high throughput screening campaign, Certal *et al.* identified **152** as an interesting lead due to its selectivity for PI3Kβ versus other PI3K isoforms (PI3Kβ IC_{50} 42-2133 nM in various screens and >10 μM on PI3Kα,δ,γ). Chemistry to exchange the potentially labile amide bond with heterocyclic replacements gave **153** (PI3Kβ IC_{50} = 158 nM) and **154** (PI3Kβ IC_{50} = 82nM) and further SAR optimization resulted in **155** (PI3Kβ IC_{50} = 99 nM; PI3Kδ IC_{50} = 1395 nM and >10 μM on PI3Kα,γ), a compound with adequate *in vitro* pharmacokinetic properties and was shown to potently inhibit Akt phosphorylation in PTEN-deficient PC3 prostate carcinoma cell line when dosed at 300 mg/kg b.i.d. for 9 days.[122]

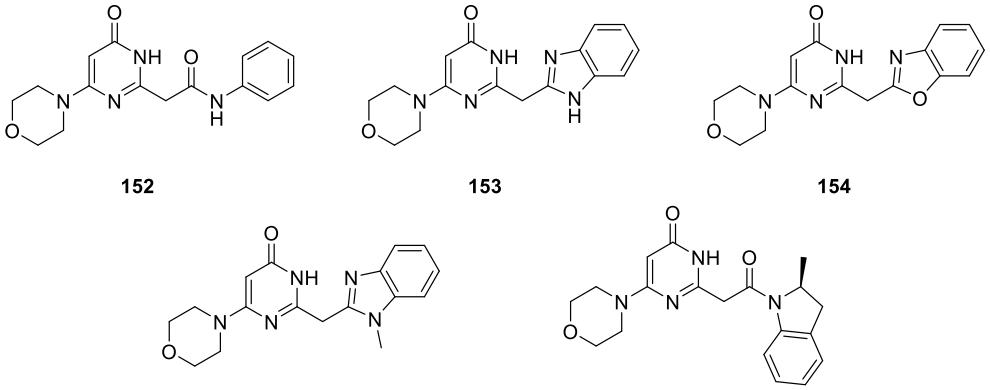

152 **153** **154**

155 **156** (SAR260301)

In a continuation of their studies, Certal *et al.* reported on the identification of the clinical candidate **156** (SAR260301), a low molecular weight compound (MW 354 cLogP 1.5) with improved physicochemical and *in vitro* pharmacokinetic properties (PI3Kβ IC_{50} = 23 nM; PI3Kα IC_{50} = 1.5 μM; PI3Kδ IC_{50} = 0.47 μM; PI3Kγ IC_{50} = >10 μM; dog PK CL = 0.4 L/h/kg; F = 67%). The first X-ray co-crystal structure of p110β with the selective inhibitor **156** bound to the ATP site demonstrated the "T-shaped" nonplanar binding mode. The X-ray showed that the morpholine oxygen accepts a H-bond from Val-848 in the hinge region.[123] The aniline generates an induced fit in the P-loop at the top of the ATP binding site creating a lipophilic pocket lined with Met771 and Trp781 and this was the reason for the β-isoform selectivity (Figure 11).

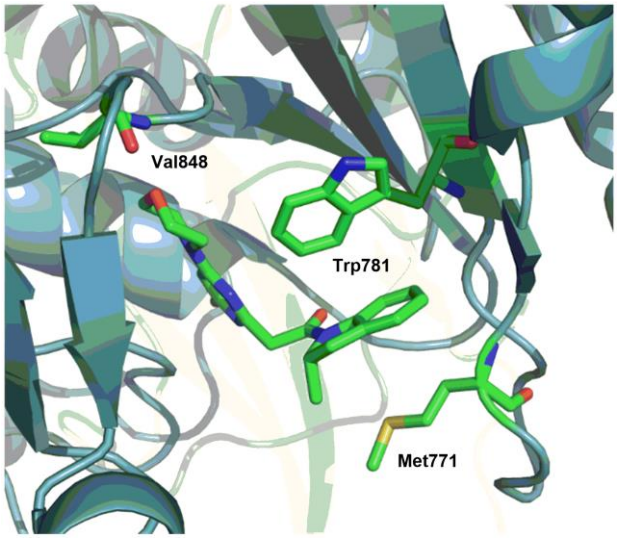

Figure 11. Binding of **156** to the ATP binding site of *p*110β (PDB 4BFR) – visualized in PyMol

Compound **156** demonstrated significant *in vivo* activity in a mouse UACC-62 xenograft model and entered phase I/Ib clinical trials in patients with advanced cancer where **156** had an acceptable safety profile, but exposure sufficient to inhibit the PI3K pathway was unachievable because of rapid clearance, and clinical development was terminated.[124]

Benzoxazepin-based PI3Kδ Inhibitors

In 2011, Staben *et al.* identified a benzopyran-based inhibitor **157** from a HTS.[125]

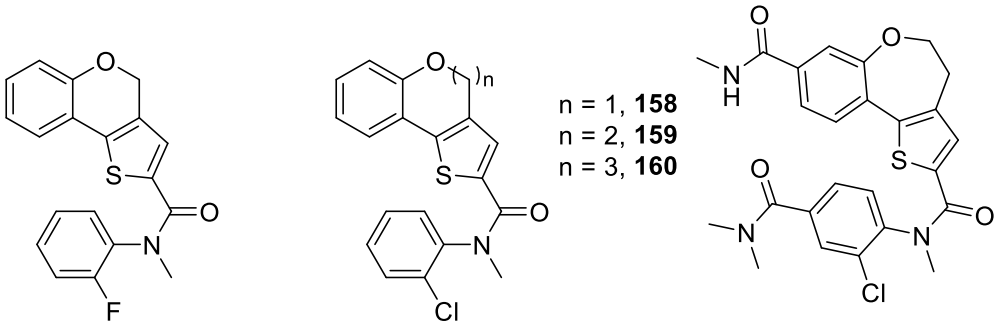

157 **161**

Compound **157** exhibited reasonable potency for PI3Kα (IC_{50} = 0.254 μM), however the physicochemical properties were not ideal (cLogP = 4.1, LE = 0.39, LipE = 2.5, MW = 356). Due to the structural novelty of the scaffold, a SAR study was initiated where the aryl substituent on the aniline amide revealed the importance of the *ortho*-halogen for PI3Kα activity. Additionally, a crystal structure of **158** (PI3Kα = 0.108 μM) indicated that the *N*-methylaniline amide bound in a *cis*-fashion in the activity pocket, and that the hinge binding interaction of the pyran oxygen was suboptimal, and could be potentially improved upon through ring expansion. This led to a 7-membered ring with a 4-fold increase in potency (PI3Kα = 0.024 μM) and subsequent expansion to an 8-membered ring, **159**, reduced potency drastically (>10 μM). Comparison of the crystal structures of **157** and **159** confirmed a shorter hydrogen bond and better angle for interaction with the hinge Val882 (Figure 12). Although potency had increased, the rate of clearance proved consistently high across the series of analogs. A metabolite ID experiment in human hepatocytes revealed hydrolysis of the aniline amide and an oxidative metabolite resulting from demethylation, aromatic oxidation and glucoronindation of the aniline. *Para*-substitution with an electron withdrawing polar amide **161** (GNE-614) reduced lipophilicity (clogP = 2.7), blocked *para*-oxidation, and decreased clearance in rat (36 mL/min/kg). Compound **161** exhibited good potency towards the class I PI3Ks (PI3Kα IC_{50} = 4.6 nM, PI3Kβ IC_{50} = 60 nM, PI3Kγ IC_{50} = 5 nM, PI3Kδ IC_{50} = 1.7 nM) and was relatively inactive against mTOR (IC_{50} = 530 nM). However, **161** showed only a moderate PK profile: rat (CL = 36 mL/min/kg, F = 50%, AUC = 39 μM/h), mouse (CL = 15 mL/min/kg, F = 28%, AUC = 330 μM/h), and dog (CL = 5 mL/min/kg, F = 120%, AUC = 17 μM/h) and was found to inhibit DNA-PK (IC_{50} = 6 nM), a structurally similar counter target.

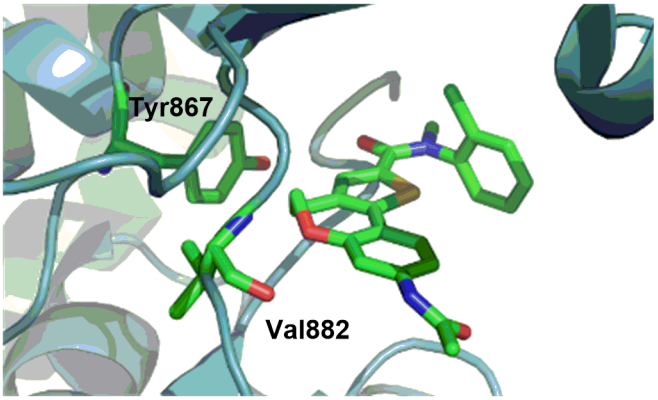

Figure 12. The X-ray crystal structures of **157** showing a shorter hydrogen bond and better angle for interaction with the hinge Val882 (PDB 3R7R)

In a follow-up paper, Staben *et al.* aimed to improve the upon the PK profile of **161** by replacing the metabolically liable *cis*-*N*-methyl anilide with an appropriate bioisostere. After extensive SAR they discovered that replacing the aryl group with an alkyl group was not tolerated. However, replacement with heteroaryl groups led to the discovery of **162** (PI3Kα IC_{50} = 4 nM) which showed improved properties for further optimization (rat CL = 13 mL/min/kg), AUC = 5.7 - 17.8 μM/h).[126]

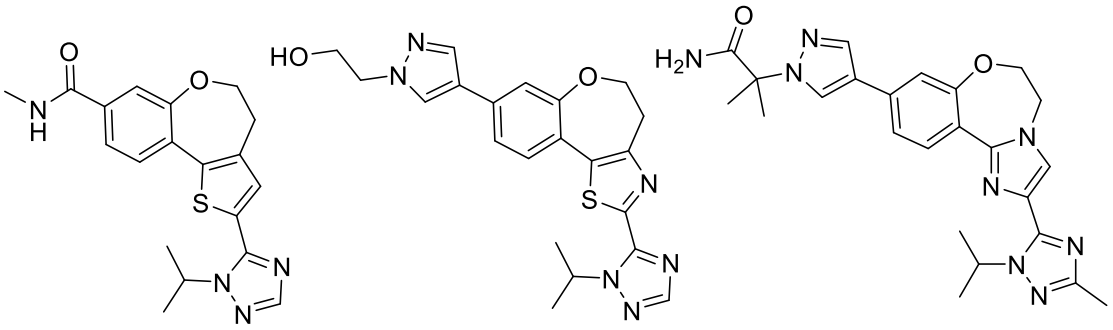

162 **163** **164**

Following the discovery of **162**, Staben *et al.* set out to further decrease the lipophilicity of the series by modification of the thiophene.[127] In addition, replacement of the thiophene would

remove the potential oxidative metabolism of this group. After identifying a number of suitable heteroaryl groups the group opted to select the thiazole, **163** for further development. **163** was highly potent towards the class I PI3Ks (PI3Kα IC_{50} = 0.27, PI3Kβ IC_{50} = 15 nM, PI3Kγ IC_{50} = 0.55 nM, PI3Kδ IC_{50} = 0.61 nM), although they observed that potency towards PI3Kβ was consistently lower with specific substitutions at the 8-position of the benzoxepin. They hypothesized that this was due to a different conformation (in PI3Kβ) of the tryptophan residue that makes up the tryptophan shelf in the case of PI3Kδ. Compound **163** showed a suitable PK profile for further advancement as it had low clearance and high bioavailability in rodents (rat CL = 5.4 mL/min/kg, F = 83%, mouse CL = 9.5 mg/mL/kg, F = 110%), acceptable PK in dog (CL = 14 mL/min/kg, F = 22%) and moderate predicted clearance in human (hepatocyte Clp = 12 mL/min/kg). In addition, **163** showed modest tumor growth inhibition in an MCF7-neo/HER2 xenograft breast cancer model and activity against counter targets were also reduced (mTOR IC_{50} >4.3 μM and DNA-PK IC_{50} = 0.34 μM).

With **163** showing only modest tumor growth inhibition in a MCF7-neo/HER2 xenograft breast cancer model despite being highly potent and exhibiting a moderate PK profile, Staben *et al.* aimed to increase the unbound exposure by further reducing the lipophilicity. An extensive screen of heteroaryl isosteres was performed, with focus on lowering the lipophilicity, leading to the discovery of **164** (GDC-0032, clogD 2.5). Compound **164** showed good activity towards the class I PI3Ks, with decreased PI3Kβ activity (PI3Kα IC_{50} = 0.29 nM, PI3Kβ IC_{50} = 9.1 nM, PI3Kγ IC_{50} = 0.12 nM, PI3Kδ IC_{50} = 0.97 nM). In addition, against a panel of 235 kinases, only 2 (not including the Class I PI3Ks) exhibiting greater than 50% inhibition at 10 μM concentration: C2β (80.4%), and Vps34 (69.9%). **164** also had a good PK profile, exhibited low *in vivo*

clearance in rat with high oral bioavailability (F = 99%). After toxicological and safety evaluations, **164** was progressed to clinical trials for PI3K-related cancers.[128]

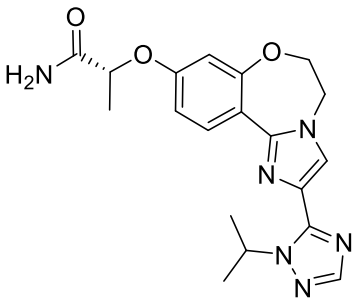

165

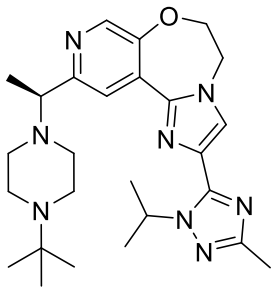

166

Having only reported pan or so-called β-sparing benzoxepins, in 2016, Heffron *et al.* moved the focus of their program towards the development of selective PI3Kα inhibitors. [129] At the onset of their PI3Kα program, a crystal structure of one of their benzoxepin inhibitors was obtained, revealing two residues unique to the α-isoform, Gln859 and His855. From molecular modelling evidence the team decided to target Gln859 in order to gain selectivity towards PI3Kα. Extensive SAR, and monitoring of torsion angle at the 8-position, focused on optimizing hydrogen bonding with Gln859. This led to the discovery of **165** (GDC-0326), where the primary amide makes 3 concerted hydrogen bonds with Gln859 (Figure 13). **165** is a PI3Kα-selective inhibitor (PI3Kα IC_{50} = 0.2 nM, α/β = 133, α/γ = 51, α/δ= 20) and showed a comparable PK profile to **164** and was selected for further study, although it has not yet progressed into the clinic at the time of writing.

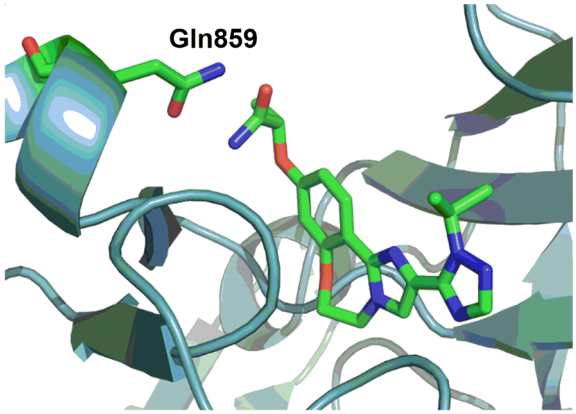

Figure 13. **165** X-ray crystal structure in PI3Kα where the primary amide makes 3 concerted hydrogen bonds with Gln859 (PDB 5DXT)

In their most recent publication, Safina *et al.* used their previous experience with the design of selective PI3Kδ inhibitors in order to build-in PI3Kδ selectivity into the benzoxepin core.[130] Since the benzoxepin core was a result of ADME optimization it possessed favorable drug-like properties and therefore this was an attractive endeavor. They discovered **166** as a PI3Kδ-selective inhibitor (PI3Kδ IC_{50} = 1.9 nM, δ/α = 113) through interaction *via* the tryptophan shelf.[130] Compound **166** had low lipophilicity (clogD 1.29), yet maintained good permeability (MDCK A to B = 10 × 10^{-6} cm/s).

Amino thiazole and aminobenzthiazole urea-based inhibitors

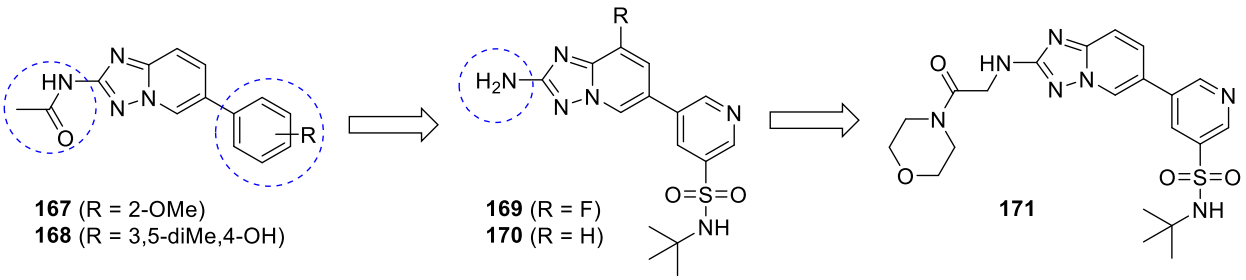

Scheme 13. Discovery of the urea-based inhibitor **171** from early HTS of a kinase focused library

In 2012, scientists from Cellzome reported **167** (PI3Kα pIC_{50} < 4, PI3Kβ pIC_{50} < 4, PI3Kγ pIC_{50} = 5.4, PI3Kδ pIC_{50} = 4.5) and **168** (PI3Kα pIC_{50} = 4.9, PI3Kβ pIC_{50} = 4.7, PI3Kγ pIC_{50} = 5.7, PI3Kδ pIC_{50} = 5.2) as hits from an HTS of a kinase focused library of 16000 compounds (Scheme 13).[131–133] SAR around the core led to **169** (CZC19945, PI3Kα pIC_{50} = 5.6, PI3Kγ pIC_{50} = 7.6, PI3Kδ pIC_{50} = 5.8). Further SAR on the central core led to **170** (CZC24832, PI3Kα pIC_{50} < 5, PI3Kγ pIC_{50} = 7.6, PI3Kδ pIC_{50} = 5.1). **170** showed moderate PK properties in mouse (CL = 11.5 mL/min/kg, F = 37%), showed no inhibition of *h*ERG up to 100 μM, no CYP inhibition and was negative in the Ames test. In addition, **170** demonstrated efficacy in a chronic model of inflammation, although poor aqueous solubility (5 μg/mL) made pre-clinical development problematic. Crystallographic studies show that these compounds bound to the hinge region of PI3Kγ *via* the donor/acceptor motif of the triazolopyridine with the pyridine sulphonamide interacting with the activity pocket. In a further publication, Ellard *et al.* detailed more SAR at the solvent exposed region, leading to PI3Kγ/δ compounds such as **171** (PI3Kα pIC_{50} 6.4, PI3Kγ pIC_{50} = 8.4, PI3Kδ pIC_{50} = 7.8, PI3K pIC_{50} = 6.3), although poor physicochemical properties precluded them from oral absorption.[134]

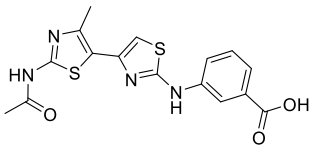

172

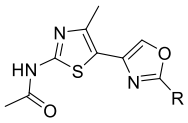

173 (R = CH_2CF_3)
174 (R = tBu)

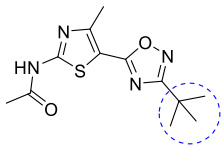

175

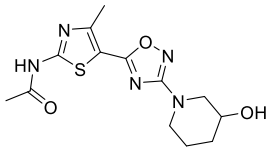

176

In parallel, Oka *et al.* identified **172** as a hit in their HTS with excellent enzymatic potency (PI3Kγ IC_{50} = 5 nM). Through structural modification, struggling initially with permeability issues, they developed **173** (PI3Kγ IC_{50} = 10 nM, α/γ = 4) and **174** (PI3Kγ IC_{50} = 3 nM, α/γ = 5).

However, although both demonstrated improved permeability leading to improved cellular potency, they showed low selectivity over PI3Kγ.[135] In a later publication, it was reported that the de-acetylated version of **173** was positive in the Ames test.[136] Although the de-acetylated product was not found to be a major metabolite, they sought to mitigate mutagenic risk by replacing the oxazole ring with more π-electron deficient heterocycles. This led to the 2-amino-5-oxadiazolyl thiazole **175**, where both the acetylated and de-acetylated analogs were negative in the Ames test. Being approximately equipotent in terms of PI3Kγ potency to **174**, they were able to explore **175** further, leading to the discovery of **176** (TASP0415914, PI3Kγ IC_{50} = 29 nM). **176** exhibited a better PK profile, showed no CYP inhibition and was progressed to *in vivo* studies in a mouse collagen-induced arthritis model and was effective in a dose-dependent manner.

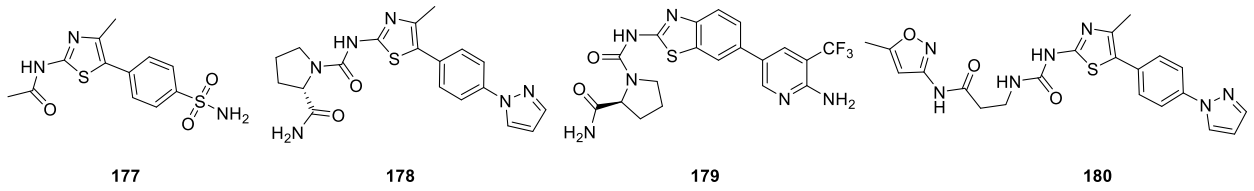

177 **178** **179** **180**

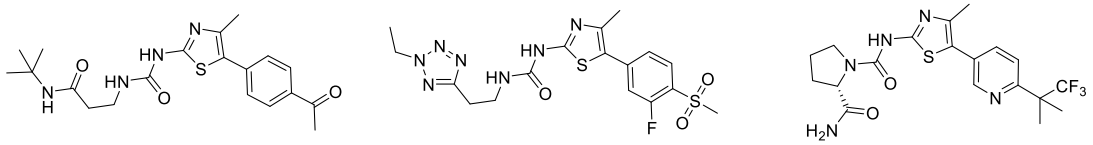

181 **182** **183**

Also, in 2012, Bruce *et al.* revealed **177** as a hit from a HTS targeting PI3Kγ.[137] A docking study involving **177** showed that the thiazole nitrogen and amide hydrogen form a bidentate donor–acceptor pair with the hinge region, and the sulfonamide interacts with the activity pocket. They observed that residues lining the binding pocket were less conserved and hypothesized that isoform selectivity might be achievable by extending or replacing the acyl moiety with diverse substituents to exploit these differences. After developing a method of thiazole synthesis

amenable to automation, they were able to generate approximately 400 analogs with replacements for the acyl moiety. Most of these compounds were found to be either inactive or weak pan-PI3K inhibitors. However, 3 types of amines were identified which led to potent isoform selective inhibitors. For example, (*S)*-pyrrolidine carboxamides such as **178** (NVS-PI3-1, PI3Kα K_i = 0.005 μM, PI3Kβ K_i = 2.0 μM, PI3Kγ K_i = 0.53 μM, PI3Kδ K_i = 0.22 μM) and **179** (NVS-PI3-2, PI3Kα IC_{50} = 0.04 μM, PI3Kβ IC_{50} = 22.94 μM, PI3Kγ IC_{50} = 1.19 μM, PI3Kδ IC_{50} = 0.54 μM) were the optimal compounds. A structurally related benzothiazole was shown to be selective towards PI3Kα, due to the carboxamide making favorable interactions with the non-conserved Gln859 of PI3Kα. Aminopropionic acid derivatives such as **180** (NVS-PI3-3, PI3Kα K_i = 0.15 μM, PI3Kβ K_i = 0.34 μM, PI3Kγ K_i = 1.02 μM, PI3Kδ K_i = 0.004 μM), **181** (NVS-PI3-4, PI3Kα K_i = 1.89 μM, PI3Kβ K_i = 0.25 μM, PI3Kγ K_i = 0.088 μM, PI3Kδ K_i = 0.74 μM) and **182** (NVS-PI3-5, PI3Kα K_i = 1.40 μM, PI3Kβ K_i = 0.32 μM, PI3Kγ K_i = 0.036 μM, PI3Kδ K_i = 0.47 μM) led to PI3Kδ-selective (**180**) and PI3Kγ-selective (**181** and **182**). The authors suggested that the PI3Kδ and PI3Kγ selectivity was most likely derived from interactions between the terminal functional groups of the urea side chain and non-conserved amino acids at the outer edge of the binding site. Additionally, all examples in the series were much less potent towards PI3Kβ than the other isoforms. However, the PK properties of **178-182** were not adequate for further progression, but this work led to some interesting observations towards selective inhibitors.

Following this in 2013, Furet *et al.* disclosed the discovery of the PI3Kα selective inhibitor **183**, Alpelisib (NVP-BYL719).[138] Addressing the poor PK and isoform selectivity within the series to date, extensive SAR studies around **178** led to the discovery of **183** (PI3Kα IC_{50} = 0.005 μM, PI3Kβ IC_{50} = 1.2 μM, PI3Kγ IC_{50} = 0.25 μM, PI3Kδ IC_{50} = 0.29 μM). Crystallographic

evidence of **183** in complex with PI3Kα shows that **183** exhibited its excellent selectivity towards PI3Kα by exploiting the non-conserved Gln859 of PI3Kα. **183** had a suitable PK profile (rat CL = 10 mL/min/kg, Vss = 1.9 L/kg) and showed no significant CYP or related-kinase inhibition, and was progressed to clinical development.

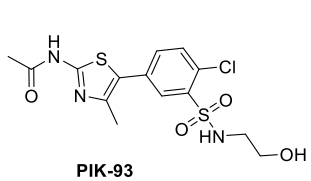

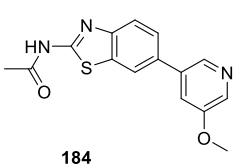

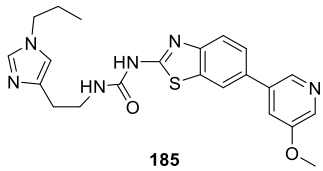

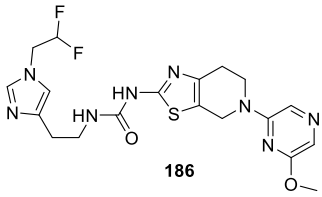

In 2014, Collier *et al.* analyzed the crystal structure of PIK-93 and observed that there was sufficient space in the ATP binding pocket to allow for a ring fusion of the thiazole into a benzothiazole where hinge binding could be achieved through the donor-acceptor motif of the nitrogen atoms of the aminobenzothiazole. **184** (PI3Kγ K_i = 0.004 μM, α/γ =1, β/γ = 10, and δ/γ = 3) and **185 (**PI3Kγ K_i = 0.002 μM, α/γ = 66, β/γ = 21, and δ/γ = 61) were compounds which exhibited isoform selectivity towards PI3Kγ.[139] After obtaining an X-ray crystal structure for **185** in PI3Kγ (Figure 14, PDB 4PS3), they hypothesized that this selectivity was a result of two non-conserved residues within the binding site. The first is Ala885, which is unique to PI3Kγ. In PI3Kα, β, and δ this is a serine residue where the OH of serine is involved in hydrogen bonding with the hinge valine residue. They proposed that introduction of urea functionality allows for the urea carbonyl to form an additional hydrogen bond to the hinge valine, which in-turn breaks the serine-valine hydrogen bond, freeing up the OH group thereby introducing a steric clash with the lipophilic side chain. This steric clash is unfavorable in the anti-targets and does not happen in the case of PI3Kγ. The second non-conserved residue is Gly829, a glutamic acid residue in PI3Kα. This aids selectivity over PI3Kα upon increasing the length of the terminal alkyl chain.

These compounds were not progressed further, however they were useful in determining important residues for identifying new approaches for PI3K isoform selectivity.

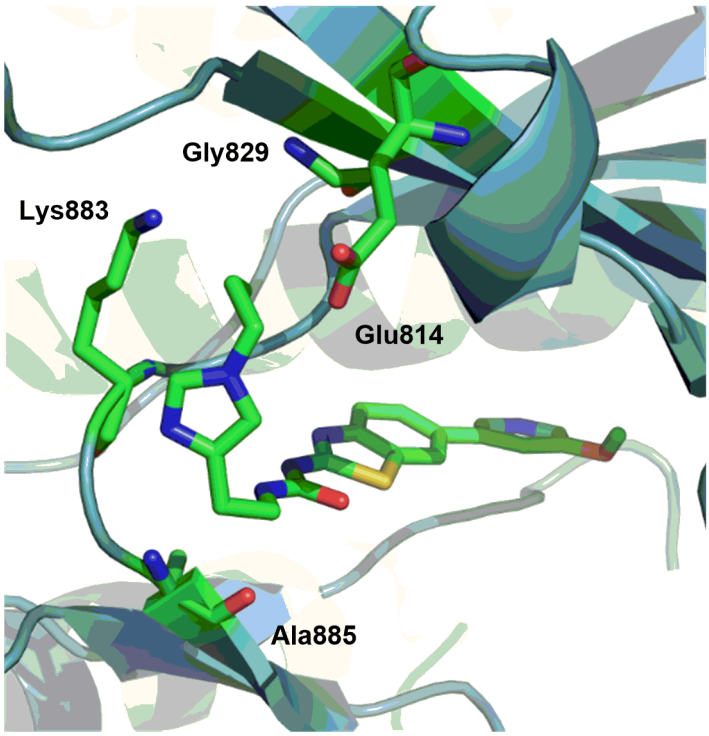

Figure 14. X-ray crystal structure of **185** in PI3Kγ, demonstrating new key interactions generating isoform selectivity (PDB 4PS3)

To improve the overall physicochemical properties (as typified by **185**), Collier *et al.* aimed to reduce the overall lipophilicity in combination with increasing the fraction of Sp3 atoms (FSp3) within the series.[140] In order to accomplish this, they replaced the central benzothiazole core with a thiazolopiperidine, leading to **186** (PI3Kγ K_i = 0.002 μM, α/γ = 228, β/γ = 105, and δ/γ = 395). In **186** they suggested that incorporating fluorine atoms onto the terminal alkyl chain increased selectivity markedly through increasing affinity for PI3Kγ, due to a C−F···C=O interaction with Thr827. Additionally, they suggested that the increase in selectivity was driven by a favorable interaction of the acidic methine proton of the fluoroethyl group with Glu814, a residue unique to

PI3Kγ. Compound **186** showed no significant inhibition in a screen of structurally related kinases.

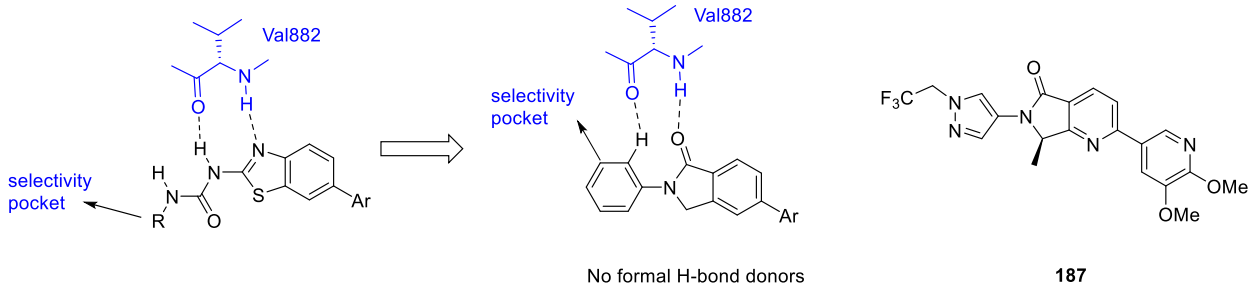

Figure 15. Strategy employed to reduce the number of H-bond donor groups to aid CNS penetration and compound **187**.

In a recent publication, Come *et al.* disclosed further refinement of the core structure with a view to increasing blood-brain barrier penetration. The authors highlighted the general difficulty in designing CNS-penetrant kinase inhibitors due, in part, to the property space characteristics of the ATP-competitive kinase inhibitors, where hydrogen bond donor moieties are essential pharmacophoric elements required to bind to the kinase hinge region. They proposed a very elegant solution where an isoindolinone carbonyl group would provide a hydrogen bond acceptor to the backbone NH of the hinge residue Val882 and, in addition, an aromatic proton would be positioned in place of the urea NH donor (Figure 15). Further functionalization gave **187** as a selective, brain penetrant inhibitor of PI3Kγ (PI3Kγ K_i = 4 nM, α/γ = 60, β/γ = 10, and δ/γ = 14). **187** was an orally bioavailable compound (rat PK CL = 20 (mL/min)/kg, F = 100%, $T_{1/2}$ = 5.1 h) that showed efficacy in murine experimental autoimmune encephalomyelitis (EAE), a preclinical model of multiple sclerosis.[141]

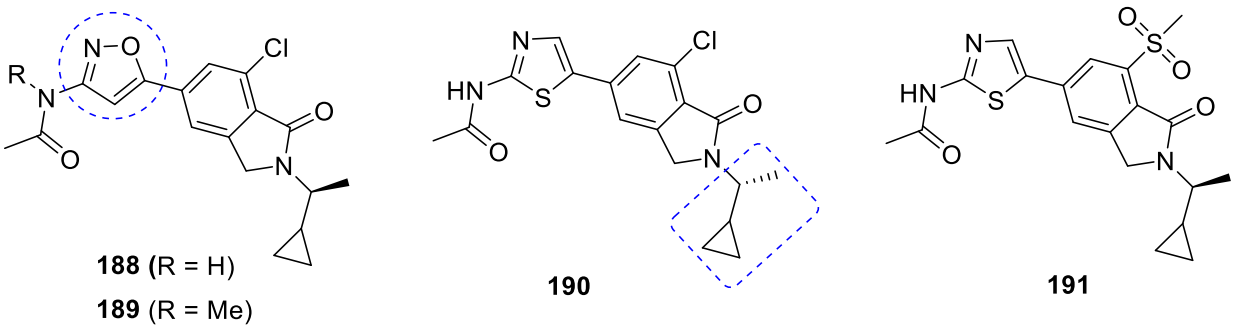

Pemberten *et al.* discovered **188** (PI3Kγ pIC_{50} = 6.8) from a HTS. They showed that methylation of the acetamide **189** led to a large reduction in potency, suggesting that the acetamido-substituted isoxazole was the hinge binding motif.[142] SAR to replace the isoxazole with amino heterocycles that are typical kinase hinge-binding motifs lead to replacement of the isoxazole with a thiazole, **190** *(R)*-enantiomer PI3Kγ pIC_{50} = 8.9. Failing to co-crystallize inhibitors of the series in PI3Kγ, the team looked to co-crystallize inhibitors in PI3Kδ. Successfully crystallizing **190** within PI3Kδ they confirmed the aminothiazole forms hydrogen bonds to the hinge residue Val828 and that the carbonyl of the lactam interacts with Lys779. The *N*-alkyl tail is oriented perpendicular to the isoindolinone core and extends deep into the ATP-binding pocket. An interesting observation was that removal of the *N*-alkyl group led to a 100-fold decrease in PI3Kγ activity and a corresponding 15-fold increase in PI3Kα potency, suggesting that PI3Kγ selectivity seems to originate from the *N*-alkyl tail extending deep into the ATP-binding pocket. Compound **190** exhibited poor properties for oral administration due to a combination of poor solubility, high *in vitro* clearance and high lipophilicity. Introduction of a sulfone led to the discovery of **191**, with excellent isoform selectivity (PI3Kα $pIC_{50} < 4.5$, PI3Kβ $pIC_{50} < 4.5$, PI3Kγ pIC_{50} = 8.1, PI3Kδ pIC_{50} = 6.0) and good bioavailability (F = 51%) and low *in vivo* clearance (rat 6.3 mL/min/kg). In a kinase screen only related kinases C2β (84%) and C2γ (71%) showed significant inhibition at 10 μM concentration. In a rat LPS-induced acute

inflammation model, oral administration of **191** resulted in a dose-dependent inhibition of airway neutrophilia in rats.

PI3K dual pharmacology compounds

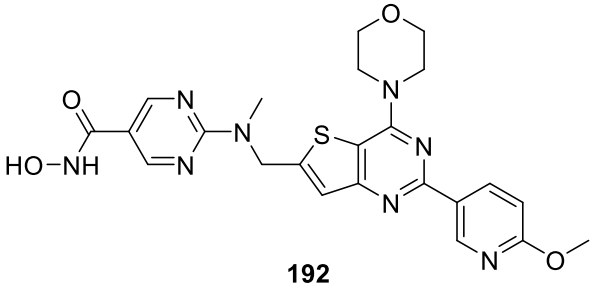

192

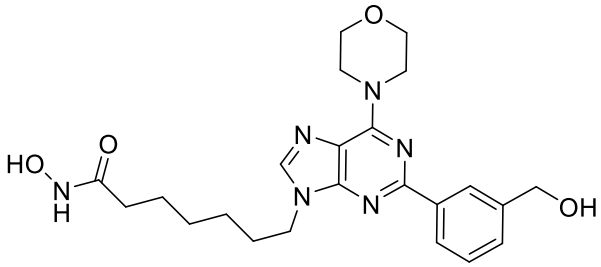

193

Qian *et al.* observed synergistic effects between PI3K inhibitors and HDAC inhibitors and therefore synthesized a novel series of dual-acting PI3K and HDAC inhibitors by incorporating HDAC inhibitory functionality into a PI3K inhibitor pharmacophore.[143] They incorporated the morpholine-pyrimidine core from **85** and **70** for PI3K inhibition and the hydroxamic acid from SAHA (Vorinostat), LBH-589 (Panobinostat) and JNJ-16241199 for HDAC inhibition to produce **192** (CUDC-907).[144,145] They reported that **192** displayed potent anticancer activity in both cultured cancer cells and xenograft models and may offer therapeutic benefits in multiple cancers, through broad signaling network disruption. **192** is currently in phase I and II clinical trials. In a similar fashion, Chen *et al.* once more combined the PI3K and HDAC pharmacophores to generate a series of dual inhibitors typified by **193** (PI3Kα = 28 nM, HDAC1 = 1.1 nM, HDAC6 = 4.2 nM). Compound **193** demonstrated target modulation in cancer cell lines and in mice bearing MV4-11 and HepG2 tumors and, in particular, showed significant single agent oral efficacy in hypervascular liver cancer models (e.g., HepG2, HuH-7, and Hep3B) and was well-tolerated.[146]

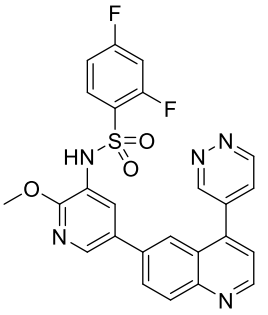

Omipalisib

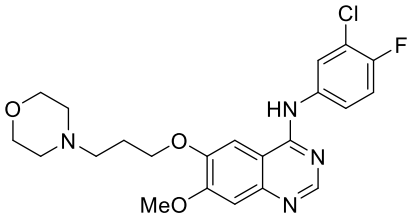

Gefitinib

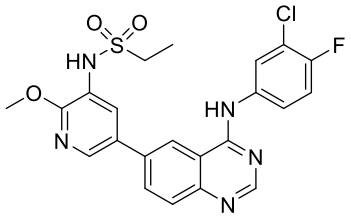

194

Ding *et al.* reported novel 4-aminoquinazolines as dual target inhibitors of EGFR-PI3Kα. Based on the structural similarity to omipalisib and gefitinib, compound **194** was shown to possess reasonable PI3Kα activity (IC_{50} = 317 nM) in combination with very high EGFR activity (IC_{50} = 2.4 nM). Compound **194** could induce cell cycle arrest in G1 phase and apoptosis in BT549 cells. The western blot assay indicated that **194** inhibited the proliferation of BT549 cell through EGFR and PI3Ka/Akt signaling pathway, suggesting that compound **194** could be a potential dual inhibitors of EGFR and PI3Kα.[147]

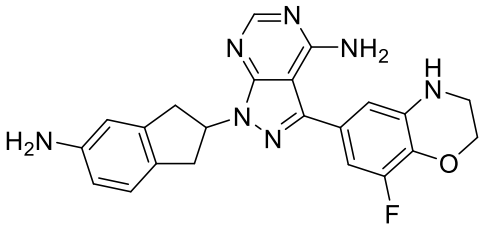

195

Pujala *et al.* reported a range of pyrazolopyrimidine derivatives, such as **195**, as dual inhibitors of Bruton's tyrosine kinase (BTK, IC_{50} = 32 nM) and PI3Kδ (IC_{50} = 16 nM). **195** had a reasonable mouse pharmacokinetic profile [10 mg/kg PO, CL = 0.59 L/h/kg, V_z = 3.44 L/kg, plasma terminal half-life = 1.3 h, F = 40%)]. No *in vivo* results were shown for the compound.[148]

Conclusion and perspective comment:

The PI3K pathway has attracted enormous industrial and academic interest as a therapeutic target for clinical conditions, such as cancer, diabetes and asthma. Idelalisib was the first PI3K inhibitor approved by the US Food and Drug Administration (FDA) and is utilized in the treatment of relapsed/refractory chronic lymphocytic leukemia/small lymphocytic lymphoma and follicular lymphoma.[149] However, the use of idelalisib may come with toxicities that are distinct from the side effects of immunochemotherapy and, as such, co-dosing strategies with steroids are currently being investigated in the clinic. [150,151] Subsequently, copanlisib was approved for relapsed follicular lymphoma in patients who have received at least two prior systemic therapies.[152] In addition, there is a wealth of PI3K agents currently in clinical development (38 at this present time), which target various combinations of the PI3K isoforms. While idelalisib has proven to be efficacious for patients, unexpected infectious and autoimmune toxicities have demonstrated the need for careful development and monitoring of new agents.

The phosphatidylinositol 3-kinase family consists of highly conserved enzymes that are part of the intracellular PI3K/Akt/mammalian target of rapamycin (mTOR) signaling axis. As such, early medicinal chemistry strategies concentrated on the discovery of non-selective PI3K inhibitors. However, the identification of "propeller-shaped" PI3K inhibitors signaled a step-change in the design of isoform selective PI3Kδ inhibitors. This led to the identification of idelalisib, the first FDA-approved PI3K inhibitor.

Concerns over isoform toxicity has led to groups exploring structural modification to synthesize compounds with PI3K isoform selectivity through subtle change in chemical structure. This led to the explosion of structural variation, with many changes to the core of the molecules, mainly to secure intellectual property, but has also, in some cases leading to subtle changes in isoform selectivity. In general, the initial pan PI3K inhibitors suffered from poor

physicochemical properties, such as poor solubility and permeability from the combination of multiple aromatic rings and lack of sp^3 carbons leading to compounds with poor pharmacokinetic properties.[153,154] These early issues were rapidly solved by medicinal chemists, through decreasing lipophilicity and adding ionizeable groups to deliver compounds with excellent permeability and good oral pharmacokinetic properties. Drug delivery has also been considered, with various groups exploring the design of compounds with improved pharmacokinetics for topical lung delivery, thus removing some of the safety issues involved with systemic exposure of the high affinity inhibitors.

Running in parallel with the discovery of the propeller shaped inhibitors, the identification of "flat-shaped" pan PI3K inhibitors has resulted in the delivery of many potent clinical candidates. However, their inherent lack of 3 dimensional structure resulted in compounds with higher lipophilicity leading again to poor water solubility. These physicochemical properties resulted in compounds with reduced cellular potency and off-target toxicity in pre-clinical studies. Once more concerns over pan-PI3K inhibition has, through careful consideration of ligand-bound X-ray structures, led to the creative design of inhibitors with good to excellent isoform selectivity. However, these highly selective inhibitors have generally gained their selectivity at a consequence of increased molecular weight resulting, in the case of PI3Kδ inhibitors, movement towards topical (i.e. inhaled) delivery.

Bivalent or dual pharmacology inhibitors have been disclosed, where secondary pharmacology has been built into the original PI3K core scaffold, such as the dual PI3K/HDAC inhibitors and more recently EGFR-PI3K dual inhibitors utilizing solvent-exposed positions of the PI3K scaffold to incorporate the secondary pharmacology.

Finally, it should be noted the extremely positive effect that ligand-bound X-ray crystallography has had on the design and synthesis on new isoform selective PI3K inhibitors. Outputs from these studies has enabled medicinal chemistry groups to thoroughly explore structural diversity in pursuit of gaining freedom to operate in a very congested and narrow field. In addition, the often non-predictive subtle targeting of specific residues inducing isoform selectivity was made possible through information gleaned from multiple ligand-bound X-ray crystal data, once more highlighting the importance of structure based drug design for to increase isoform selectivity.

In conclusion, it is disappointing that many PI3K inhibitors have not met their true clinical potential due to: the absence of reliable and effective biomarkers, the limited efficacy as single agents and the lack of development of rational therapeutic combinations, off-target effects, and suboptimal therapeutic exposures.[7] Therefore, it is hoped that with regard to current PI3K inhibitors in late-stage clinical trials, the identification of appropriate efficacy biomarkers and the development of optimal combination regimens will lead to future successful FDA drug approvals.

Bibliographies:

Aimie E. Garces received her first class Master's degree in Chemistry (M.Sci) from The University of Nottingham (U.K.) in 2015. During those studies, she undertook PI3K and αv integrin collaborative projects between GSK and The University of Nottingham. Currently she is a doctoral student within the Division of Biomolecular Science and Medicinal Chemistry at the University of Nottingham (U.K.) under the supervision of Dr. Michael Stocks and Dr. Tracey

Bradshaw. Her current research focuses on the development of bi-functional prodrugs, incorporating PI3K inhibitors, for oncology use.

Michael J. Stocks is an Associate Professor in Medicinal Chemistry within the School of Pharmacy at The University of Nottingham. He has over 20 years of industrial experience in drug discovery within Fison's Pharmaceuticals, Astra Pharma and AstraZeneca and was the lead scientist on multiple pre-clinical research projects. Since joining the School of Pharmacy in 2012, Michael has focused his research on the medicinal chemistry design and synthesis of compounds to study and modulate the function of biological targets. His recent research interests lie in: combining chemical structures to discover dual inhibitors for cancer therapy; identification of inhibitors for disrupting bacterial quorum sensing; generation of fluorescent ligands to study GPCR function, topical drug delivery and serine protease inhibitor design.

ASSOCIATED CONTENT

Supporting Information.

The following files are available free of charge.

Supplementary material.pdf – chemical structures of PI3K inhibitors in clinical development (Table ST1)

AUTHOR INFORMATION

Corresponding Author

*michael.stocks@nottingham.ac.uk

Author Contributions

The manuscript was written through contributions of all authors.

Funding Sources

This work was supported by the UK Medical Research Council-funded PhD research studentship AEG (ref. number 1648176).

ABBREVIATIONS

AUC area under the curve; BTK Bruton tyrosine kinase; CIA collagen-induced arthritis; EMA he European Medicines Agency; F bioavailability; FDA US Food and Drug Administration; GPCR G protein-coupled receptor HDAC histone deacetylase; *h*ERG human Ether-à-go-go-Related Gene; LE ligand efficiency; LIPE lipophilic ligand efficiency; mTOR mammalian target of rapamycin; PBS phosphate-buffered saline; PDB protein data bank; PI3Ks phosphatidylinositol 3-kinases; PIKK phosphatidylinositol like kinase; PK pharmacokinetics; SAR structure activity relationship; TPSA topological polar surface area.

REFERENCES

(1) Toker, A.; Cantley, L. C. Signalling through the Lipid Products of Phosphoinositide-3-OH Kinase. *Nature* **1997**, *387* (6634), 673–676.

(2) Fruman, D. A.; Rommel, C. PI3K and Cancer: Lessons, Challenges and Opportunities. *Nat. Rev. Drug Discov.* **2014**, *13* (2), 140–156.

(3) Zhao, W.; Qiu, Y.; Kong, D. Class I Phosphatidylinositol 3-Kinase Inhibitors for Cancer Therapy. *Acta Pharm. Sin. B* **2017**, *7* (1), 27–37.

(4) Zhao, H.; Wang, J.; Shao, W.; Wu, C.; Chen, Z.; To, S. T.; Li, W. Recent Advances in the Use of PI3K Inhibitors for Glioblastoma Multiforme: Current Preclinical and Clinical Development. *Mol. Cancer* **2017**, *16* (1), 100.

(5) Thorpe, L. M.; Yuzugullu, H.; Zhao, J. J. PI3K in Cancer: Divergent Roles of Isoforms, Modes of Activation and Therapeutic Targeting. *Nat. Rev. Cancer* **2015**, *15* (1), 7–24.

(6) Stark, A. K.; Sriskantharajah, S.; Hessel, E. M.; Okkenhaug, K. PI3K Inhibitors in Inflammation, Autoimmunity and Cancer. *Curr. Opin. Pharmacol.* **2015**, *23*, 82–91.

(7) Janku, F. Phosphoinositide 3-Kinase (PI3K) Pathway Inhibitors in Solid Tumors: From Laboratory to Patients. *Cancer Treat. Rev.* **2017**, *59*, 93–101.

(8) Knight, Z. A.; Gonzalez, B.; Feldman, M. E.; Zunder, E. R.; Goldenberg, D. D.; Williams, O.; Loewith, R.; Stokoe, D.; Balla, A.; Toth, B.; Balla, T.; Weiss, W. A.; Williams, R. L.; Shokat, K. M. A Pharmacological Map of the PI3-K Family Defines a Role for P110α in Insulin Signaling. *Cell* **2006**, *125* (4), 733–747.

(9) Huang, X.; Liu, G.; Guo, J.; Su, Z. The PI3K/AKT Pathway in Obesity and Type 2 Diabetes. *Int. J. Biol. Sci.* **2018**, *14* (11), 1483–1496.

(10) Jackson, S. P.; Schoenwaelder, S. M.; Goncalves, I.; Nesbitt, W. S.; Yap, C. L.; Wright, C. E.; Kenche, V.; Anderson, K. E.; Dopheide, S. M.; Yuan, Y.; Sturgeon, S. A.; Prabaharan, H.; Thompson, P. E.; Smith, G. D.; Shepherd, P. R.; Daniele, N.; Kulkarni, S.; Abbott, B.; Saylik, D.; Jones, C.; Lu, L.; Giuliano, S.; Hughan, S. C.; Angus, J. A.; Robertson, A. D.; Salem, H. H. PI 3-Kinase P110β: A New Target for Antithrombotic Therapy. *Nat. Med.* **2005**, *11* (5), 507–514.

(11) JACKSON, S. P.; SCHOENWAELDER, S. M. Antithrombotic Phosphoinositide 3-Kinase β Inhibitors in Humans: A 'Shear' Delight! *J. Thromb. Haemost.* **2012**, *10* (10), 2123–2126.

(12) Cushing, T. D.; Metz, D. P.; Whittington, D. A.; McGee, L. R. PI3Kδ and PI3Kγ as Targets

for Autoimmune and Inflammatory Diseases. *J. Med. Chem.* **2012**, *55* (20), 8559–8581.

(13) Rowan, W. C.; Smith, J. L.; Affleck, K.; Amour, A. Targeting Phosphoinositide 3-Kinase δ for Allergic Asthma. *Biochem. Soc. Trans.* **2012**, *40* (1), 240–245.

(14) Yoo, E. J.; Ojiaku, C. A.; Sunder, K.; Panettieri, R. A. Phosphoinositide 3-Kinase in Asthma: Novel Roles and Therapeutic Approaches. *Am. J. Respir. Cell Mol. Biol.* **2017**, *56* (6), 700–707.

(15) Lucas, C. L.; Kuehn, H. S.; Zhao, F.; Niemela, J. E.; Deenick, E. K.; Palendira, U.; Avery, D. T.; Moens, L.; Cannons, J. L.; Biancalana, M.; Stoddard, J.; Ouyang, W.; Frucht, D. M.; Rao, V. K.; Atkinson, T. P.; Agharahimi, A.; Hussey, A. A.; Folio, L. R.; Olivier, K. N.; Fleisher, T. A.; Pittaluga, S.; Holland, S. M.; Cohen, J. I.; Oliveira, J. B.; Tangye, S. G.; Schwartzberg, P. L.; Lenardo, M. J.; Uzel, G. Dominant-Activating Germline Mutations in the Gene Encoding the PI(3)K Catalytic Subunit P110δ Result in T Cell Senescence and Human Immunodeficiency. *Nat. Immunol.* **2014**, *15* (1), 88–97.

(16) Angulo, I.; Vadas, O.; Garcon, F.; Banham-Hall, E.; Plagnol, V.; Leahy, T. R.; Baxendale, H.; Coulter, T.; Curtis, J.; Wu, C.; Blake-Palmer, K.; Perisic, O.; Smyth, D.; Maes, M.; Fiddler, C.; Juss, J.; Cilliers, D.; Markelj, G.; Chandra, A.; Farmer, G.; Kielkowska, A.; Clark, J.; Kracker, S.; Debre, M.; Picard, C.; Pellier, I.; Jabado, N.; Morris, J. A.; Barcenas-Morales, G.; Fischer, A.; Stephens, L.; Hawkins, P.; Barrett, J. C.; Abinun, M.; Clatworthy, M.; Durandy, A.; Doffinger, R.; Chilvers, E. R.; Cant, A. J.; Kumararatne, D.; Okkenhaug, K.; Williams, R. L.; Condliffe, A.; Nejentsev, S. Phosphoinositide 3-Kinase Gene Mutation Predisposes to Respiratory Infection and Airway Damage. *Science (80-.).* **2013**, *342* (6160), 866–871.

(17) Kracker, S.; Curtis, J.; Ibrahim, M. A. A.; Sediva, A.; Salisbury, J.; Campr, V.; Debré, M.; Edgar, J. D. M.; Imai, K.; Picard, C.; Casanova, J.-L.; Fischer, A.; Nejentsev, S.; Durandy, A. Occurrence of B-Cell Lymphomas in Patients with Activated Phosphoinositide 3-Kinase δ Syndrome. *J. Allergy Clin. Immunol.* **2014**, *134* (1), 233–236.e3.

(18) Coulter, T. I.; Chandra, A.; Bacon, C. M.; Babar, J.; Curtis, J.; Screaton, N.; Goodlad, J. R.; Farmer, G.; Steele, C. L.; Leahy, T. R.; Doffinger, R.; Baxendale, H.; Bernatoniene, J.; Edgar, J. D. M.; Longhurst, H. J.; Ehl, S.; Speckmann, C.; Grimbacher, B.; Sediva, A.; Milota, T.; Faust, S. N.; Williams, A. P.; Hayman, G.; Kucuk, Z. Y.; Hague, R.; French, P.; Brooker, R.; Forsyth, P.; Herriot, R.; Cancrini, C.; Palma, P.; Ariganello, P.; Conlon, N.; Feighery, C.; Gavin, P. J.; Jones, A.; Imai, K.; Ibrahim, M. A. A.; Markelj, G.; Abinun, M.; Rieux-Laucat, F.; Latour, S.; Pellier, I.; Fischer, A.; Touzot, F.; Casanova, J.-L.; Durandy, A.; Burns, S. O.; Savic, S.; Kumararatne, D. S.; Moshous, D.; Kracker, S.; Vanhaesebroeck, B.; Okkenhaug, K.; Picard, C.; Nejentsev, S.; Condliffe, A. M.; Cant, A. J. Clinical Spectrum and Features of Activated Phosphoinositide 3-Kinase δ Syndrome: A Large Patient Cohort Study. *J. Allergy Clin. Immunol.* **2017**, *139* (2), 597–606.e4.

(19) Elkaim, E.; Neven, B.; Bruneau, J.; Mitsui-Sekinaka, K.; Stanislas, A.; Heurtier, L.; Lucas, C. L.; Matthews, H.; Deau, M.-C.; Sharapova, S.; Curtis, J.; Reichenbach, J.; Glastre, C.; Parry, D. A.; Arumugakani, G.; McDermott, E.; Kilic, S. S.; Yamashita, M.; Moshous, D.; Lamrini, H.; Otremba, B.; Gennery, A.; Coulter, T.; Quinti, I.; Stephan, J.-L.; Lougaris, V.; Brodszki, N.; Barlogis, V.; Asano, T.; Galicier, L.; Boutboul, D.; Nonoyama, S.; Cant, A.; Imai, K.; Picard, C.; Nejentsev, S.; Molina, T. J.; Lenardo, M.; Savic, S.; Cavazzana, M.; Fischer, A.; Durandy, A.; Kracker, S. Clinical and Immunologic Phenotype Associated with Activated Phosphoinositide 3-Kinase δ Syndrome 2: A Cohort Study. *J. Allergy Clin.*

Immunol. **2016**, *138* (1), 210–218.e9.

(20) Conte, E.; Gili, E.; Fruciano, M.; Korfei, M.; Fagone, E.; Iemmolo, M.; Lo Furno, D.; Giuffrida, R.; Crimi, N.; Guenther, A.; Vancheri, C. PI3K P110γ Overexpression in Idiopathic Pulmonary Fibrosis Lung Tissue and Fibroblast Cells: In Vitro Effects of Its Inhibition. *Lab. Investig.* **2013**, *93* (5), 566–576.

(21) Fruman, D. A.; Chiu, H.; Hopkins, B. D.; Bagrodia, S.; Cantley, L. C.; Abraham, R. T. The PI3K Pathway in Human Disease. *Cell* **2017**, *170* (4), 605–635.

(22) Workman, P.; van Montfort, R. L. M. Revealing the Delta Lady. *Nat. Chem. Biol.* **2010**, *6*, 82.

(23) Berndt, A.; Miller, S.; Williams, O.; Le, D. D.; Houseman, B. T.; Pacold, J. I.; Gorrec, F.; Hon, W.-C.; Ren, P.; Liu, Y.; Rommel, C.; Gaillard, P.; Rückle, T.; Schwarz, M. K.; Shokat, K. M.; Shaw, J. P.; Williams, R. L. The P110δ Structure: Mechanisms for Selectivity and Potency of New PI(3)K Inhibitors. *Nat. Chem. Biol.* **2010**, *6* (2), 117–124.

(24) The PyMOL Molecular Graphics System, Version 2.0 Schrödinger, LLC.

(25) Proschak, E.; Stark, H.; Merk, D. Polypharmacology by Design: A Medicinal Chemist's Perspective on Multitargeting Compounds. *J. Med. Chem.* **2018**, DOI: 10.1021/acs.jmedchem.8b00760, Publication Date (Web): July 23, 2018

(26) Chen, J. Potential Value and Limitation of Dual Inhibitors of PI3K and MTOR in the Treatment of Cancer. *Curr. Cancer Drug Targets* **2013**, *13* (2), 117–120.

(27) Sarbassov, D. D. Phosphorylation and Regulation of Akt/PKB by the Rictor-MTOR Complex. *Science (80-.).* **2005**, *307* (5712), 1098–1101.

(28) Schenone, S.; Brullo, C.; Musumeci, F.; Radi, M.; Botta, M. ATP-Competitive Inhibitors of MTOR: An Update. *Curr. Med. Chem.* **2011**, *18* (20), 2995–3014.

(29) PubChem https://pubchem.ncbi.nlm.nih.gov/.

(30) Fowler, K. W.; Huang, D.; Kesicki, E. A.; Ooi, H. C.; Oliver, A. R.; Ruan, F.; Treiberg, J. Preparation of Purine Quinazolinones as Inhibitors of Human Phosphatidylinositol 3-Kinase Delta. WO2005113556A1., December 1, 2005.

(31) Somoza, J. R.; Koditek, D.; Villaseñor, A. G.; Novikov, N.; Wong, M. H.; Liclican, A.; Xing, W.; Lagpacan, L.; Wang, R.; Schultz, B. E.; Papalia, G. A.; Samuel, D.; Lad, L.; McGrath, M. E. Structural, Biochemical, and Biophysical Characterization of Idelalisib Binding to Phosphoinositide 3-Kinase δ. *J. Biol. Chem.* **2015**, *290* (13), 8439–8446.

(32) Ramanathan, S.; Jin, F.; Sharma, S.; Kearney, B. P. Clinical Pharmacokinetic and Pharmacodynamic Profile of Idelalisib. *Clin. Pharmacokinet.* **2016**, *55* (1), 33–45.

(33) Patel, L.; Chandrasekhar, J.; Evarts, J.; Haran, A. C.; Ip, C.; Kaplan, J. A.; Kim, M.; Koditek, D.; Lad, L.; Lepist, E.-I.; McGrath, M. E.; Novikov, N.; Perreault, S.; Puri, K. D.; Somoza, J. R.; Steiner, B. H.; Stevens, K. L.; Therrien, J.; Treiberg, J.; Villaseñor, A. G.; Yeung, A.; Phillips, G. 2,4,6-Triaminopyrimidine as a Novel Hinge Binder in a Series of PI3Kδ Selective Inhibitors. *J. Med. Chem.* **2016**, *59* (7), 3532–3548.

(34) Patel, L.; Chandrasekhar, J.; Evarts, J.; Forseth, K.; Haran, A. C.; Ip, C.; Kashishian, A.; Kim, M.; Koditek, D.; Koppenol, S.; Lad, L.; Lepist, E.-I.; McGrath, M. E.; Perreault, S.; Puri, K. D.; Villaseñor, A. G.; Somoza, J. R.; Steiner, B. H.; Therrien, J.; Treiberg, J.; Phillips, G. Discovery of Orally Efficacious Phosphoinositide 3-Kinase δ Inhibitors with

Improved Metabolic Stability. *J. Med. Chem.* **2016**, *59* (19), 9228–9242.

(35) Perreault, S.; Chandrasekhar, J.; Cui, Z.-H.; Evarts, J.; Hao, J.; Kaplan, J. A.; Kashishian, A.; Keegan, K. S.; Kenney, T.; Koditek, D.; Lad, L.; Lepist, E.-I.; McGrath, M. E.; Patel, L.; Phillips, B.; Therrien, J.; Treiberg, J.; Yahiaoui, A.; Phillips, G. Discovery of a Phosphoinositide 3-Kinase (PI3K) β/δ Inhibitor for the Treatment of Phosphatase and Tensin Homolog (PTEN) Deficient Tumors: Building PI3Kβ Potency in a PI3Kδ-Selective Template by Targeting Nonconserved Asp856. *J. Med. Chem.* **2017**, *60* (4), 1555–1567.

(36) Turiso, F. G. De; Shin, Y.; Brown, M.; Cardozo, M.; Chen, Y.; Fong, D.; Hao, X.; He, X.; Henne, K.; Hu, Y.; Johnson, M. G.; Kohn, T.; Lohman, J.; Mcbride, H. J.; Mcgee, L. R.; Medina, J. C.; Metz, D.; Miner, K.; Mohn, D.; Pattaropong, V.; Seganish, J.; Simard, J. L.; Wannberg, S.; Whittington, D. A.; Yu, G.; Cushing, T. D. Discovery and in Vivo Evaluation of Dual PI3K β / δ Inhibitors. *J. Med. Chem.* **2012**, *55*, 7667–7685.

(37) Cushing, T. D.; Hao, X.; Shin, Y.; Andrews, K.; Brown, M.; Cardozo, M.; Chen, Y.; Duquette, J.; Fisher, B.; Gonzalez-Lopez de Turiso, F.; He, X.; Henne, K. R.; Hu, Y.-L.; Hungate, R.; Johnson, M. G.; Kelly, R. C.; Lucas, B.; McCarter, J. D.; McGee, L. R.; Medina, J. C.; San Miguel, T.; Mohn, D.; Pattaropong, V.; Pettus, L. H.; Reichelt, A.; Rzasa, R. M.; Seganish, J.; Tasker, A. S.; Wahl, R. C.; Wannberg, S.; Whittington, D. A.; Whoriskey, J.; Yu, G.; Zalameda, L.; Zhang, D.; Metz, D. P. Discovery and in Vivo Evaluation of (S)- N -(1-(7-Fluoro-2-(Pyridin-2-Yl)Quinolin-3-Yl)Ethyl)-9 H -Purin-6-Amine (AMG319) and Related PI3Kδ Inhibitors for Inflammation and Autoimmune Disease. *J. Med. Chem.* **2015**, *58* (1), 480–511.

(38) Shin, Y.; Suchomel, J.; Cardozo, M.; Duquette, J.; He, X.; Henne, K.; Hu, Y.; Kelly, R. C.;

McCarter, J.; McGee, L. R.; Medina, J. C.; Metz, D.; San Miguel, T.; Mohn, D.; Tran, T.; Vissinga, C.; Wong, S.; Wannberg, S.; Whittington, D. A.; Whoriskey, J.; Yu, G.; Zalameda, L.; Zhang, X.; Cushing, T. D. Discovery, Optimization, and in Vivo Evaluation of Benzimidazole Derivatives AM-8508 and AM-9635 as Potent and Selective PI3Kδ Inhibitors. *J. Med. Chem.* **2016**, *59* (1), 431–447.

(39) Bui, M.; Hao, X.; Shin, Y.; Cardozo, M.; He, X.; Henne, K.; Suchomel, J.; McCarter, J.; McGee, L. R.; San Miguel, T.; Medina, J. C.; Mohn, D.; Tran, T.; Wannberg, S.; Wong, J.; Wong, S.; Zalameda, L.; Metz, D.; Cushing, T. D. Synthesis and SAR Study of Potent and Selective PI3Kδ Inhibitors. *Bioorg. Med. Chem. Lett.* **2015**, *25* (5), 1104–1109.

(40) Gonzalez-Lopez de Turiso, F.; Hao, X.; Shin, Y.; Bui, M.; Campuzano, I. D. G.; Cardozo, M.; Dunn, M. C.; Duquette, J.; Fisher, B.; Foti, R. S.; Henne, K.; He, X.; Hu, Y.-L.; Kelly, R. C.; Johnson, M. G.; Lucas, B. S.; McCarter, J.; McGee, L. R.; Medina, J. C.; Metz, D.; San Miguel, T.; Mohn, D.; Tran, T.; Vissinga, C.; Wannberg, S.; Whittington, D. A.; Whoriskey, J.; Yu, G.; Zalameda, L.; Zhang, X.; Cushing, T. D. Discovery and in Vivo Evaluation of the Potent and Selective PI3Kδ Inhibitors 2-((1S)-1-((6-Amino-5-Cyano-4-Pyrimidinyl)Amino)Ethyl)-6-Fluoro-N-Methyl-3-(2-Pyridinyl)-4-Quinolinecarboxamide (AM-0687) and 2-((1S)-1-((6-Amino-5-Cyano-4-Pyrimidinyl)Amino)Eth. *J. Med. Chem.* **2016**, *59* (15), 7252–7267.

(41) Erra, M.; Taltavull, J.; Greco, A.; Bernal, F. J.; Caturla, J. F.; Gracia, J.; Dominguez, M.; Sabate, M.; Paris, S.; Soria, S.; Hernandez, B.; Armengol, C.; Cabedo, J.; Bravo, M.; Calama, E.; Miralpeix, M.; Lehner, M. D. Discovery of a Potent, Selective, and Orally Available PI3Kδ Inhibitor for the Treatment of Inflammatory Diseases. *ACS Med. Chem.*

Lett. **2017**, *8* (1), 118–123.

(42) Wei, M.; Zhang, X.; Wang, X.; Song, Z.; Ding, J.; Meng, L.-H.; Zhang, A. SAR Study of 5-Alkynyl Substituted Quinazolin-4(3H)-Ones as Phosphoinositide 3-Kinase Delta (PI3Kδ) Inhibitors. *Eur. J. Med. Chem.* **2017**, *125*, 1156–1171.

(43) Evans, C. A.; Liu, T.; Lescarbeau, A.; Nair, S. J.; Grenier, L.; Pradeilles, J. A.; Glenadel, Q.; Tibbitts, T.; Rowley, A. M.; DiNitto, J. P.; Brophy, E. E.; OHearn, E. L.; Ali, J. A.; Winkler, D. G.; Goldstein, S. I.; OHearn, P.; Martin, C. M.; Hoyt, J. G.; Soglia, J. R.; Cheung, C.; Pink, M. M.; Proctor, J. L.; Palombella, V. J.; Tremblay, M. R.; Castro, A. C. Discovery of a Selective Phosphoinositide-3-Kinase (PI3K)-γ Inhibitor (IPI-549) as an Immuno-Oncology Clinical Candidate. *ACS Med. Chem. Lett.* **2016**, *7* (9), 862–867.

(44) Srinivas, M.; Singh Pathania, A.; Mahajan, P.; Verma, P. K.; Chobe, S. S.; Malik, F. A.; Nargotra, A.; Vishwakarma, R. A.; Sawant, S. D. Design and Synthesis of 1,4-Substituted 1H-1,2,3-Triazolo-Quinazolin-4(3H)-Ones by Huisgen 1,3-Dipolar Cycloaddition with PI3Kγ Isoform Selective Activity. *Bioorg. Med. Chem. Lett.* **2018**, *28* (6), 1005–1010.

(45) Perry, M. W. D.; Björhall, K.; Bonn, B.; Carlsson, J.; Chen, Y.; Eriksson, A.; Fredlund, L.; Hao, H.; Holden, N. S.; Karabelas, K.; Lindmark, H.; Liu, F.; Pemberton, N.; Petersen, J.; Rodrigo Blomqvist, S.; Smith, R. W.; Svensson, T.; Terstiege, I.; Tyrchan, C.; Yang, W.; Zhao, S.; Öster, L. Design and Synthesis of Soluble and Cell-Permeable PI3Kδ Inhibitors for Long-Acting Inhaled Administration. *J. Med. Chem.* **2017**, *60* (12), 5057–5071.

(46) Cooper, A. E.; Ferguson, D.; Grime, K. Optimisation of DMPK by the Inhaled Route: Challenges and Approaches. *Curr. Drug Metab.* **2012**, *13* (4), 457–473.

(47) Stocks, M. J.; Alcaraz, L.; Bailey, A.; Bonnert, R.; Cadogan, E.; Christie, J.; Dixon, J.; Connolly, S.; Cook, A.; Fisher, A.; Flaherty, A.; Humphries, A.; Ingall, A.; Jordan, S.; Lawson, M.; Mullen, A.; Nicholls, D.; Paine, S.; Pairaudeau, G.; Young, A. Discovery of AZD3199, An Inhaled Ultralong Acting β 2 Receptor Agonist with Rapid Onset of Action. *ACS Med. Chem. Lett.* **2014**, *5* (4), 416–421.

(48) Folkes, A. J.; Ahmadi, K.; Alderton, W. K.; Alix, S.; Baker, S. J.; Box, G.; Chuckowree, I. S.; Clarke, P. A.; Depledge, P.; Eccles, S. A.; Friedman, L. S.; Hayes, A.; Hancox, T. C.; Kugendradas, A.; Lensun, L.; Moore, P.; Olivero, A. G.; Pang, J.; Patel, S.; Pergl-Wilson, G. H.; Raynaud, F. I.; Robson, A.; Saghir, N.; Salphati, L.; Sohal, S.; Ultsch, M. H.; Valenti, M.; Wallweber, H. J. A.; Wan, N. C.; Wiesmann, C.; Workman, P.; Zhyvoloup, A.; Zvelebil, M. J.; Shuttleworth, S. J. The Identification of 2-(1 H -Indazol-4-Yl)-6-(4-Methanesulfonyl-Piperazin-1-Ylmethyl)-4-Morpholin-4-Yl-Thieno[3,2- d]Pyrimidine (GDC-0941) as a Potent, Selective, Orally Bioavailable Inhibitor of Class I PI3 Kinase for the Treatment of Cancer †. *J. Med. Chem.* **2008**, *51* (18), 5522–5532.

(49) Hayakawa, M.; Kaizawa, H.; Moritomo, H.; Koizumi, T.; Ohishi, T.; Okada, M.; Ohta, M.; Tsukamoto, S.; Parker, P.; Workman, P.; Waterfield, M. Synthesis and Biological Evaluation of 4-Morpholino-2-Phenylquinazolines and Related Derivatives as Novel PI3 Kinase P110α Inhibitors. *Bioorg. Med. Chem.* **2006**, *14* (20), 6847–6858.

(50) Andrs, M.; Korabecny, J.; Jun, D.; Hodny, Z.; Bartek, J.; Kuca, K. Phosphatidylinositol 3 - Kinase (PI3K) and Phosphatidylinositol 3 - Kinase-Related Kinase (PIKK) Inhibitors: Importance of the Morpholine Ring. *J. Med. Chem.* **2015**, *58*, 41–71.

(51) Sutherlin, D. P.; Bao, L.; Berry, M.; Castanedo, G.; Chuckowree, I.; Dotson, J.; Folks, A.;

Friedman, L.; Goldsmith, R.; Gunzner, J.; Heffron, T.; Lesnick, J.; Lewis, C.; Mathieu, S.; Murray, J.; Nonomiya, J.; Pang, J.; Pegg, N.; Prior, W. W.; Rouge, L.; Salphati, L.; Sampath, D.; Tian, Q.; Tsui, V.; Wan, N. C.; Wang, S.; Wei, B.; Wiesmann, C.; Wu, P.; Zhu, B.-Y.; Olivero, A. Discovery of a Potent, Selective, and Orally Available Class I Phosphatidylinositol 3-Kinase (PI3K)/Mammalian Target of Rapamycin (MTOR) Kinase Inhibitor (GDC-0980) for the Treatment of Cancer. *J. Med. Chem.* **2011**, *54* (21), 7579–7587.

(52) Heffron, T. P.; Berry, M.; Castanedo, G.; Chang, C.; Chuckowree, I.; Dotson, J.; Folkes, A.; Gunzner, J.; Lesnick, J. D.; Lewis, C.; Mathieu, S.; Nonomiya, J.; Olivero, A.; Pang, J.; Peterson, D.; Salphati, L.; Sampath, D.; Sideris, S.; Sutherlin, D. P.; Tsui, V.; Wan, N. C.; Wang, S.; Wong, S.; Zhu, B. Identification of GNE-477, a Potent and Efficacious Dual PI3K/MTOR Inhibitor. *Bioorg. Med. Chem. Lett.* **2010**, *20* (8), 2408–2411.

(53) Safina, B. S.; Baker, S.; Baumgardner, M.; Blaney, P. M.; Chan, B. K.; Chen, Y.-H.; Cartwright, M. W.; Castanedo, G.; Chabot, C.; Cheguillaume, A. J.; Goldsmith, P.; Goldstein, D. M.; Goyal, B.; Hancox, T.; Handa, R. K.; Iyer, P. S.; Kaur, J.; Kondru, R.; Kenny, J. R.; Krintel, S. L.; Li, J.; Lesnick, J.; Lucas, M. C.; Lewis, C.; Mukadam, S.; Murray, J.; Nadin, A. J.; Nonomiya, J.; Padilla, F.; Palmer, W. S.; Pang, J.; Pegg, N.; Price, S.; Reif, K.; Salphati, L.; Savy, P. A.; Seward, E. M.; Shuttleworth, S.; Sohal, S.; Sweeney, Z. K.; Tay, S.; Tivitmahaisoon, P.; Waszkowycz, B.; Wei, B.; Yue, Q.; Zhang, C.; Sutherlin, D. P. Discovery of Novel PI3-Kinase δ Specific Inhibitors for the Treatment of Rheumatoid Arthritis: Taming CYP3A4 Time-Dependent Inhibition. *J. Med. Chem.* **2012**, *55* (12), 5887–5900.

(54) Heffron, T. P.; Salphati, L.; Alicke, B.; Cheong, J.; Dotson, J.; Edgar, K.; Goldsmith, R.; Gould, S. E.; Lee, L. B.; Lesnick, J. D.; Lewis, C.; Ndubaku, C.; Nonomiya, J.; Olivero, A. G.; Pang, J.; Plise, E. G.; Sideris, S.; Trapp, S.; Wallin, J.; Wang, L.; Zhang, X. The Design and Identification of Brain Penetrant Inhibitors of Phosphoinositide 3-Kinase α. *J. Med. Chem.* **2012**, *55* (18), 8007–8020.

(55) Sutherlin, D. P.; Baker, S.; Bisconte, A.; Blaney, P. M.; Brown, A.; Chan, B. K.; Chantry, D.; Castanedo, G.; DePledge, P.; Goldsmith, P.; Goldstein, D. M.; Hancox, T.; Kaur, J.; Knowles, D.; Kondru, R.; Lesnick, J.; Lucas, M. C.; Lewis, C.; Murray, J.; Nadin, A. J.; Nonomiya, J.; Pang, J.; Pegg, N.; Price, S.; Reif, K.; Safina, B. S.; Salphati, L.; Staben, S.; Seward, E. M.; Shuttleworth, S.; Sohal, S.; Sweeney, Z. K.; Ultsch, M.; Waszkowycz, B.; Wei, B. Potent and Selective Inhibitors of PI3Kδ: Obtaining Isoform Selectivity from the Affinity Pocket and Tryptophan Shelf. *Bioorg. Med. Chem. Lett.* **2012**, *22* (13), 4296–4302.

(56) Murray, J. M.; Sweeney, Z. K.; Chan, B. K.; Balazs, M.; Bradley, E.; Castanedo, G.; Chabot, C.; Chantry, D.; Flagella, M.; Goldstein, D. M.; Kondru, R.; Lesnick, J.; Li, J.; Lucas, M. C.; Nonomiya, J.; Pang, J.; Price, S.; Salphati, L.; Safina, B.; Savy, P. P. A.; Seward, E. M.; Ultsch, M.; Sutherlin, D. P. Potent and Highly Selective Benzimidazole Inhibitors of PI3-Kinase Delta. *J. Med. Chem.* **2012**, *55* (17), 7686–7695.

(57) Safina, B. S.; Sweeney, Z. K.; Li, J.; Chan, B. K.; Bisconte, A.; Carrera, D.; Castanedo, G.; Flagella, M.; Heald, R.; Lewis, C.; Murray, J. M.; Nonomiya, J.; Pang, J.; Price, S.; Reif, K.; Salphati, L.; Seward, E. M.; Wei, B.; Sutherlin, D. P. Identification of GNE-293, a Potent and Selective PI3Kδ Inhibitor: Navigating in Vitro Genotoxicity While Improving Potency and Selectivity. *Bioorg. Med. Chem. Lett.* **2013**, *23* (17), 4953–4959.

(58) Yaguchi, S.; Fukui, Y.; Koshimizu, I.; Yoshimi, H.; Matsuno, T.; Gouda, H.; Hirono, S.; Yamazaki, K.; Yamori, T. Antitumor Activity of ZSTK474, a New Phosphatidylinositol 3-Kinase Inhibitor. *JNCI J. Natl. Cancer Inst.* **2006**, *98* (8), 545–556.

(59) Burger, M. T.; Pecchi, S.; Wagman, A.; Ni, Z.-J.; Knapp, M.; Hendrickson, T.; Atallah, G.; Pfister, K.; Zhang, Y.; Bartulis, S.; Frazier, K.; Ng, S.; Smith, A.; Verhagen, J.; Haznedar, J.; Huh, K.; Iwanowicz, E.; Xin, X.; Menezes, D.; Merritt, H.; Lee, I.; Wiesmann, M.; Kaufman, S.; Crawford, K.; Chin, M.; Bussiere, D.; Shoemaker, K.; Zaror, I.; Maira, S.-M.; Voliva, C. F. Identification of NVP-BKM120 as a Potent, Selective, Orally Bioavailable Class I PI3 Kinase Inhibitor for Treating Cancer. *ACS Med. Chem. Lett.* **2011**, *2* (10), 774–779.

(60) Pecchi, S.; Renhowe, P. A.; Taylor, C.; Kaufman, S.; Merritt, H.; Wiesmann, M.; Shoemaker, K. R.; Knapp, M. S.; Ornelas, E.; Hendrickson, T. F.; Fantl, W.; Voliva, C. F. Identification and Structure–activity Relationship of 2-Morpholino 6-(3-Hydroxyphenyl) Pyrimidines, a Class of Potent and Selective PI3 Kinase Inhibitors. *Bioorg. Med. Chem. Lett.* **2010**, *20* (23), 6895–6898.

(61) Brachmann, S. M.; Kleylein-Sohn, J.; Gaulis, S.; Kauffmann, A.; Blommers, M. J. J.; Kazic-Legueux, M.; Laborde, L.; Hattenberger, M.; Stauffer, F.; Vaxelaire, J.; Romanet, V.; Henry, C.; Murakami, M.; Guthy, D. A.; Sterker, D.; Bergling, S.; Wilson, C.; Brummendorf, T.; Fritsch, C.; Garcia-Echeverria, C.; Sellers, W. R.; Hofmann, F.; Maira, S.-M. Characterization of the Mechanism of Action of the Pan Class I PI3K Inhibitor NVP-BKM120 across a Broad Range of Concentrations. *Mol. Cancer Ther.* **2012**, *11* (8), 1747–1757.

(62) Bohnacker, T.; Prota, A. E.; Beaufils, F.; Burke, J. E.; Melone, A.; Inglis, A. J.; Rageot, D.; Sele, A. M.; Cmiljanovic, V.; Cmiljanovic, N.; Bargsten, K.; Aher, A.; Akhmanova, A.; Díaz, J. F.; Fabbro, D.; Zvelebil, M.; Williams, R. L.; Steinmetz, M. O.; Wymann, M. P. Deconvolution of Buparlisib's Mechanism of Action Defines Specific PI3K and Tubulin Inhibitors for Therapeutic Intervention. *Nat. Commun.* **2017**, *8*, 14683.

(63) Zhang, J.-Q.; Luo, Y.-J.; Xiong, Y.-S.; Yu, Y.; Tu, Z.-C.; Long, Z.-J.; Lai, X.-J.; Chen, H.-X.; Luo, Y.; Weng, J.; Lu, G. Design, Synthesis, and Biological Evaluation of Substituted Pyrimidines as Potential Phosphatidylinositol 3-Kinase (PI3K) Inhibitors. *J. Med. Chem.* **2016**, *59* (15), 7268–7274.

(64) Venkatesan, A. M.; Dehnhardt, C. M.; Delos Santos, E.; Chen, Z.; Dos Santos, O.; Ayral-Kaloustian, S.; Khafizova, G.; Brooijmans, N.; Mallon, R.; Hollander, I.; Feldberg, L.; Lucas, J.; Yu, K.; Gibbons, J.; Abraham, R. T.; Chaudhary, I.; Mansour, T. S. Bis(Morpholino-1,3,5-Triazine) Derivatives: Potent Adenosine 5′-Triphosphate Competitive Phosphatidylinositol-3-Kinase/Mammalian Target of Rapamycin Inhibitors: Discovery of Compound 26 (PKI-587), a Highly Efficacious Dual Inhibitor. *J. Med. Chem.* **2010**, *53* (6), 2636–2645.

(65) Dehnhardt, C. M.; Venkatesan, A. M.; Delos Santos, E.; Chen, Z.; Santos, O.; Ayral-Kaloustian, S.; Brooijmans, N.; Mallon, R.; Hollander, I.; Feldberg, L.; Lucas, J.; Chaudhary, I.; Yu, K.; Gibbons, J.; Abraham, R.; Mansour, T. S. Lead Optimization of N-3-Substituted 7-Morpholinotriazolopyrimidines as Dual Phosphoinositide 3-Kinase/Mammalian Target of Rapamycin Inhibitors: Discovery of PKI-402. *J. Med. Chem.* **2010**, *53* (2), 798–810.

(66) Miller, M. S.; Pinson, J.-A.; Zheng, Z.; Jennings, I. G.; Thompson, P. E. Regioselective Synthesis of 5- and 6-Methoxybenzimidazole-1,3,5-Triazines as Inhibitors of Phosphoinositide 3-Kinase. *Bioorg. Med. Chem. Lett.* **2013**, *23* (3), 802–805.

(67) Miller, M. S.; Mountford, S. J.; Pinson, J.-A.; Zheng, Z.; Künzli, M.; Patel, V.; Hogg, S. J.; Shortt, J.; Jennings, I. G.; Thompson, P. E. Development of Single and Mixed Isoform Selectivity PI3Kδ Inhibitors by Targeting Asn836 of PI3Kδ. *Bioorg. Med. Chem. Lett.* **2016**, *26* (19), 4790–4794.

(68) Pinson, J.-A.; Zheng, Z.; Miller, M. S.; Chalmers, D. K.; Jennings, I. G.; Thompson, P. E. L-Aminoacyl-Triazine Derivatives Are Isoform-Selective PI3Kβ Inhibitors That Target Nonconserved Asp862 of PI3Kβ. *ACS Med. Chem. Lett.* **2013**, *4* (2), 206–210.

(69) Dugar, S.; Hollinger, F. P.; Mahajan, D.; Sen, S.; Kuila, B.; Arora, R.; Pawar, Y.; Shinde, V.; Rahinj, M.; Kapoor, K. K.; Bhumkar, R.; Rai, S.; Kulkarni, R. Discovery of Novel and Orally Bioavailable Inhibitors of PI3 Kinase Based on Indazole Substituted Morpholino-Triazines. *ACS Med. Chem. Lett.* **2015**, *6* (12), 1190–1194.

(70) Gamage, S. A.; Giddens, A. C.; Tsang, K. Y.; Flanagan, J. U.; Kendall, J. D.; Lee, W.-J.; Baguley, B. C.; Buchanan, C. M.; Jamieson, S. M. F.; Shepherd, P. R.; Denny, W. A.; Rewcastle, G. W. Synthesis and Biological Evaluation of Sulfonamide Analogues of the Phosphatidylinositol 3-Kinase Inhibitor ZSTK474. *Bioorg. Med. Chem.* **2017**, *25* (20), 5859–5874.

(71) Ohwada, J.; Ebiike, H.; Kawada, H.; Tsukazaki, M.; Nakamura, M.; Miyazaki, T.; Morikami, K.; Yoshinari, K.; Yoshida, M.; Kondoh, O.; Kuramoto, S.; Ogawa, K.; Aoki, Y.; Shimma, N. Discovery and Biological Activity of a Novel Class I PI3K Inhibitor,

CH5132799. *Bioorg. Med. Chem. Lett.* **2011**, *21* (6), 1767–1772.

(72) Kawada, H.; Ebiike, H.; Tsukazaki, M.; Nakamura, M.; Morikami, K.; Yoshinari, K.; Yoshida, M.; Ogawa, K.; Shimma, N.; Tsukuda, T.; Ohwada, J. Lead Optimization of a Dihydropyrrolopyrimidine Inhibitor against Phosphoinositide 3-Kinase (PI3K) to Improve the Phenol Glucuronic Acid Conjugation. *Bioorg. Med. Chem. Lett.* **2013**, *23* (3), 673–678.

(73) Kawada, H.; Ebiike, H.; Tsukazaki, M.; Yamamoto, S.; Koyama, K.; Nakamura, M.; Morikami, K.; Yoshinari, K.; Yoshida, M.; Ogawa, K.; Shinma, N.; Tsukuda, T.; Ohwada, J. Modification of a Dihydropyrrolopyrimidine Phosphoinositide 3-Kinase (PI3K) Inhibitor to Improve Oral Bioavailability. *Bioorg. Med. Chem.* **2015**, *23* (24), 7650–7660.

(74) Kawada, H.; Ebiike, H.; Tsukazaki, M.; Yamamoto, S.; Koyama, K.; Nakamura, M.; Morikami, K.; Yoshinari, K.; Yoshida, M.; Ogawa, K.; Shimma, N.; Tsukuda, T.; Ohwada, J. Optimization of the Phenylurea Moiety in a Phosphoinositide 3-Kinase (PI3K) Inhibitor to Improve Water Solubility and the PK Profile by Introducing a Solubilizing Group and Ortho Substituents. *Bioorg. Med. Chem.* **2016**, *24* (13), 2897–2906.

(75) Wang, J.; Wang, X.; Chen, Y.; Chen, S.; Chen, G.; Tong, L.; Meng, L.; Xie, Y.; Ding, J.; Yang, C. Discovery and Bioactivity of 4-(2-Arylpyrido[3′,2′:3,4]Pyrrolo[1,2-f][1,2,4]Triazin-4-Yl) Morpholine Derivatives as Novel PI3K Inhibitors. *Bioorg. Med. Chem. Lett.* **2012**, *22* (1), 339–342.

(76) Martínez González, S.; Rodríguez-Arístegui, S.; Hernández, A. I.; Varela, C.; González Cantalapiedra, E.; Álvarez, R. M.; Rodríguez Hergueta, A.; Bischoff, J. R.; Albarrán, M. I.; Cebriá, A.; Cendón, E.; Cebrián, D.; Alfonso, P.; Pastor, J. Generation of Tricyclic Imidazo[1,2- a]Pyrazines as Novel PI3K Inhibitors by Application of a Conformational

Restriction Strategy. *Bioorg. Med. Chem. Lett.* **2017**, *27* (11), 2536–2543.

(77) Martínez González, S.; Hernández, A. I.; Álvarez, R. M.; Rodríguez, A.; Ramos-Lima, F.; Bischoff, J. R.; Albarrán, M. I.; Cebriá, A.; Hernández-Encinas, E.; García-Arocha, J.; Cebrián, D.; Blanco-Aparicio, C.; Pastor, J. Identification of Novel PI3K Inhibitors through a Scaffold Hopping Strategy. *Bioorg. Med. Chem. Lett.* **2017**, *27* (21), 4794–4799.

(78) Nacht, M.; Qiao, L.; Sheets, M. P.; St. Martin, T.; Labenski, M.; Mazdiyasni, H.; Karp, R.; Zhu, Z.; Chaturvedi, P.; Bhavsar, D.; Niu, D.; Westlin, W.; Petter, R. C.; Medikonda, A. P.; Singh, J. Discovery of a Potent and Isoform-Selective Targeted Covalent Inhibitor of the Lipid Kinase PI3Kα. *J. Med. Chem.* **2013**, *56* (3), 712–721.

(79) Saurat, T.; Buron, F.; Rodrigues, N.; de Tauzia, M.-L.; Colliandre, L.; Bourg, S.; Bonnet, P.; Guillaumet, G.; Akssira, M.; Corlu, A.; Guillouzo, C.; Berthier, P.; Rio, P.; Jourdan, M.-L.; Bénédetti, H.; Routier, S. Design, Synthesis, and Biological Activity of Pyridopyrimidine Scaffolds as Novel PI3K/MTOR Dual Inhibitors. *J. Med. Chem.* **2014**, *57* (3), 613–631.

(80) Dugar, S.; Hollinger, F. P.; Kuila, B.; Arora, R.; Sen, S.; Mahajan, D. Synthesis and Evaluation of Pyrrolotriazine Based Molecules as PI3 Kinase Inhibitors. *Bioorg. Med. Chem. Lett.* **2015**, *25* (16), 3142–3146.

(81) Wang, X.-M.; Xin, M.-H.; Xu, J.; Kang, B.-R.; Li, Y.; Lu, S.-M.; Zhang, S.-Q. Synthesis and Antitumor Activities Evaluation of M-(4-Morpholinoquinazolin-2-Yl)Benzamides in Vitro and in Vivo. *Eur. J. Med. Chem.* **2015**, *96*, 382–395.

(82) Wang, Q.; Li, X.; Sun, C.; Zhang, B.; Zheng, P.; Zhu, W.; Xu, S. Synthesis and Structure–

Activity Relationships of 4-Morpholino-7,8-Dihydro-5H-Thiopyrano[4,3-d]Pyrimidine Derivatives Bearing Pyrazoline Scaffold. *Molecules* **2017**, *22* (11), 1870.

(83) Xu, S.; Sun, C.; Chen, C.; Zheng, P.; Zhou, Y.; Zhou, H.; Zhu, W. Synthesis and Biological Evaluation of Novel 8-Morpholinoimidazo[1,2-a]Pyrazine Derivatives Bearing Phenylpyridine/Phenylpyrimidine-Carboxamides. *Molecules* **2017**, *22* (2), 310.

(84) Schwehm, C.; Kellam, B.; Garces, A. E.; Hill, S. J.; Kindon, N. D.; Bradshaw, T. D.; Li, J.; Macdonald, S. J. F.; Rowedder, J. E.; Stoddart, L. A.; Stocks, M. J. Design and Elaboration of a Tractable Tricyclic Scaffold To Synthesize Druglike Inhibitors of Dipeptidyl Peptidase-4 (DPP-4), Antagonists of the C–C Chemokine Receptor Type 5 (CCR5), and Highly Potent and Selective Phosphoinositol-3 Kinase δ (PI3Kδ) Inhib. *J. Med. Chem.* **2017**, *60* (4), 1534–1554.

(85) Ritchie, T. J.; Luscombe, C. N.; Macdonald, S. J. F. Analysis of the Calculated Physicochemical Properties of Respiratory Drugs: Can We Design for Inhaled Drugs Yet? *J. Chem. Inf. Model.* **2009**, *49* (4), 1025–1032.

(86) Bhide, R. S.; Neels, J.; Qin, L.-Y.; Ruan, Z.; Stachura, S.; Weigelt, C.; Sack, J. S.; Stefanski, K.; Gu, X.; Xie, J. H.; Goldstine, C. B.; Skala, S.; Pedicord, D. L.; Ruepp, S.; Dhar, T. G. M.; Carter, P. H.; Salter-Cid, L. M.; Poss, M. A.; Davies, P. Discovery and SAR of Pyrrolo[2,1-f][1,2,4]Triazin-4-Amines as Potent and Selective PI3Kδ Inhibitors. *Bioorg. Med. Chem. Lett.* **2016**, *26* (17), 4256–4260.

(87) Qin, L.-Y.; Ruan, Z.; Cherney, R. J.; Dhar, T. G. M.; Neels, J.; Weigelt, C. A.; Sack, J. S.; Srivastava, A. S.; Cornelius, L. A. M.; Tino, J. A.; Stefanski, K.; Gu, X.; Xie, J.; Susulic, V.; Yang, X.; Yarde-Chinn, M.; Skala, S.; Bosnius, R.; Goldstein, C.; Davies, P.; Ruepp,

S.; Salter-Cid, L.; Bhide, R. S.; Poss, M. A. Discovery of 7-(3-(Piperazin-1-Yl)Phenyl)Pyrrolo[2,1-f][1,2,4]Triazin-4-Amine Derivatives as Highly Potent and Selective PI3Kδ Inhibitors. *Bioorg. Med. Chem. Lett.* **2017**, *27* (4), 855–861.

(88) Marcoux, D.; Qin, L.-Y.; Ruan, Z.; Shi, Q.; Ruan, Q.; Weigelt, C.; Qiu, H.; Schieven, G.; Hynes, J.; Bhide, R.; Poss, M.; Tino, J. Identification of Highly Potent and Selective PI3Kδ Inhibitors. *Bioorg. Med. Chem. Lett.* **2017**, *27* (13), 2849–2853.

(89) Liu, Q.; Shi, Q.; Marcoux, D.; Batt, D. G.; Cornelius, L.; Qin, L.-Y.; Ruan, Z.; Neels, J.; Beaudoin-Bertrand, M.; Srivastava, A. S.; Li, L.; Cherney, R. J.; Gong, H.; Watterson, S. H.; Weigelt, C.; Gillooly, K. M.; McIntyre, K. W.; Xie, J. H.; Obermeier, M. T.; Fura, A.; Sleczka, B.; Stefanski, K.; Fancher, R. M.; Padmanabhan, S.; RP, T.; Kundu, I.; Rajareddy, K.; Smith, R.; Hennan, J. K.; Xing, D.; Fan, J.; Levesque, P. C.; Ruan, Q.; Pitt, S.; Zhang, R.; Pedicord, D.; Pan, J.; Yarde, M.; Lu, H.; Lippy, J.; Goldstine, C.; Skala, S.; Rampulla, R. A.; Mathur, A.; Gupta, A.; Arunachalam, P. N.; Sack, J. S.; Muckelbauer, J. K.; Cvijic, M. E.; Salter-Cid, L. M.; Bhide, R. S.; Poss, M. A.; Hynes, J.; Carter, P. H.; Macor, J. E.; Ruepp, S.; Schieven, G. L.; Tino, J. A. Identification of a Potent, Selective, and Efficacious Phosphatidylinositol 3-Kinase δ (PI3Kδ) Inhibitor for the Treatment of Immunological Disorders. *J. Med. Chem.* **2017**, *60* (12), 5193–5208.

(90) Peterson, E. A.; Andrews, P. S.; Be, X.; Boezio, A. A.; Bush, T. L.; Cheng, A. C.; Coats, J. R.; Colletti, A. E.; Copeland, K. W.; DuPont, M.; Graceffa, R.; Grubinska, B.; Harmange, J.-C.; Kim, J. L.; Mullady, E. L.; Olivieri, P.; Schenkel, L. B.; Stanton, M. K.; Teffera, Y.; Whittington, D. A.; Cai, T.; La, D. S. Discovery of Triazine-Benzimidazoles as Selective Inhibitors of MTOR. *Bioorg. Med. Chem. Lett.* **2011**, *21* (7), 2064–2070.

(91) Smith, A. L.; D'Angelo, N. D.; Bo, Y. Y.; Booker, S. K.; Cee, V. J.; Herberich, B.; Hong, F.-T.; Jackson, C. L. M.; Lanman, B. A.; Liu, L.; Nishimura, N.; Pettus, L. H.; Reed, A. B.; Tadesse, S.; Tamayo, N. A.; Wurz, R. P.; Yang, K.; Andrews, K. L.; Whittington, D. A.; McCarter, J. D.; Miguel, T. S.; Zalameda, L.; Jiang, J.; Subramanian, R.; Mullady, E. L.; Caenepeel, S.; Freeman, D. J.; Wang, L.; Zhang, N.; Wu, T.; Hughes, P. E.; Norman, M. H. Structure-Based Design of a Novel Series of Potent, Selective Inhibitors of the Class I Phosphatidylinositol 3-Kinases. *J. Med. Chem.* **2012**, *55* (11), 5188–5219.

(92) D'Angelo, N. D.; Kim, T.-S.; Andrews, K.; Booker, S. K.; Caenepeel, S.; Chen, K.; D'Amico, D.; Freeman, D.; Jiang, J.; Liu, L.; McCarter, J. D.; San Miguel, T.; Mullady, E. L.; Schrag, M.; Subramanian, R.; Tang, J.; Wahl, R. C.; Wang, L.; Whittington, D. A.; Wu, T.; Xi, N.; Xu, Y.; Yakowec, P.; Yang, K.; Zalameda, L. P.; Zhang, N.; Hughes, P.; Norman, M. H. Discovery and Optimization of a Series of Benzothiazole Phosphoinositide 3-Kinase (PI3K)/Mammalian Target of Rapamycin (MTOR) Dual Inhibitors. *J. Med. Chem.* **2011**, *54* (6), 1789–1811.

(93) Wurz, R. P.; Liu, L.; Yang, K.; Nishimura, N.; Bo, Y.; Pettus, L. H.; Caenepeel, S.; Freeman, D. J.; McCarter, J. D.; Mullady, E. L.; San Miguel, T.; Wang, L.; Zhang, N.; Andrews, K. L.; Whittington, D. A.; Jiang, J.; Subramanian, R.; Hughes, P. E.; Norman, M. H. Synthesis and Structure-Activity Relationships of Dual PI3K/MTOR Inhibitors Based on a 4-Amino-6-Methyl-1,3,5-Triazine Sulfonamide Scaffold. *Bioorg. Med. Chem. Lett.* **2012**, *22* (17), 5714–5720.

(94) Norman, M. H.; Andrews, K. L.; Bo, Y. Y.; Booker, S. K.; Caenepeel, S.; Cee, V. J.; D'Angelo, N. D.; Freeman, D. J.; Herberich, B. J.; Hong, F.-T.; Jackson, C. L. M.; Jiang,

J.; Lanman, B. A.; Liu, L.; McCarter, J. D.; Mullady, E. L.; Nishimura, N.; Pettus, L. H.; Reed, A. B.; San Miguel, T.; Smith, A. L.; Stec, M. M.; Tadesse, S.; Tasker, A.; Aidasani, D.; Zhu, X.; Subramanian, R.; Tamayo, N. A.; Wang, L.; Whittington, D. A.; Wu, B.; Wu, T.; Wurz, R. P.; Yang, K.; Zalameda, L.; Zhang, N.; Hughes, P. E. Selective Class I Phosphoinositide 3-Kinase Inhibitors: Optimization of a Series of Pyridyltriazines Leading to the Identification of a Clinical Candidate, AMG 511 [Erratum to Document Cited in CA157:426662]. *J. Med. Chem.* **2012**, *55* (20), 8975.

(95) Lanman, B. A.; Reed, A. B.; Cee, V. J.; Hong, F.-T.; Pettus, L. H.; Wurz, R. P.; Andrews, K. L.; Jiang, J.; McCarter, J. D.; Mullady, E. L.; San Miguel, T.; Subramanian, R.; Wang, L.; Whittington, D. A.; Wu, T.; Zalameda, L.; Zhang, N.; Tasker, A. S.; Hughes, P. E.; Norman, M. H. Phosphoinositide-3-Kinase Inhibitors: Evaluation of Substituted Alcohols as Replacements for the Piperazine Sulfonamide Portion of AMG 511. *Bioorg. Med. Chem. Lett.* **2014**, *24* (24), 5630–5634.

(96) Stec, M. M.; Andrews, K. L.; Bo, Y.; Liao, H.; Tamayo, N.; Norman, M. H.; Caenepeel, S.; Wang, L.; Zhang, N.; Hughes, P. E.; McCarter, J.; San, M. T.; Zalameda, L. P.; Mullady, E. L.; Subramanian, R.; Whittington, D. A.; Wu, T. The Imidazo[1,2-a]Pyridine Ring System as a Scaffold for Potent Dual Phosphoinositide-3-Kinase (PI3K)/Mammalian Target of Rapamycin (MTOR) Inhibitors. *Bioorg. Med. Chem. Lett.* **2015**, *25* (19), 4136–4142.

(97) Scott, W. J.; Hentemann, M. F.; Rowley, R. B.; Bull, C. O.; Jenkins, S.; Bullion, A. M.; Johnson, J.; Redman, A.; Robbins, A. H.; Esler, W.; Fracasso, R. P.; Garrison, T.; Hamilton, M.; Michels, M.; Wood, J. E.; Wilkie, D. P.; Xiao, H.; Levy, J.; Stasik, E.; Liu, N.; Schaefer, M.; Brands, M.; Lefranc, J. Discovery and SAR of Novel 2,3-Dihydroimidazo[1,2-

c]Quinazoline PI3K Inhibitors: Identification of Copanlisib (BAY 80-6946). *ChemMedChem* **2016**, 1517–1530.

(98) Markham, A. Copanlisib: First Global Approval. *Drugs* **2017**, *77* (18), 2057–2062.

(99) Patnaik, A.; Appleman, L. J.; Tolcher, A. W.; Papadopoulos, K. P.; Beeram, M.; Rasco, D. W.; Weiss, G. J.; Sachdev, J. C.; Chadha, M.; Fulk, M.; Ejadi, S.; Mountz, J. M.; Lotze, M. T.; Toledo, F. G. S.; Chu, E.; Jeffers, M.; Peña, C.; Xia, C.; Reif, S.; Genvresse, I.; Ramanathan, R. K. First-in-Human Phase I Study of Copanlisib (BAY 80-6946), an Intravenous Pan-Class I Phosphatidylinositol 3-Kinase Inhibitor, in Patients with Advanced Solid Tumors and Non-Hodgkin's Lymphomas. *Ann. Oncol.* **2016**, *27* (10), 1928–1940.

(100) Down, K.; Amour, A.; Baldwin, I. R.; Cooper, A. W. J.; Deakin, A. M.; Felton, L. M.; Guntrip, S. B.; Hardy, C.; Harrison, Z. A.; Jones, K. L.; Jones, P.; Keeling, S. E.; Le, J.; Livia, S.; Lucas, F.; Lunniss, C. J.; Parr, N. J.; Robinson, E.; Rowland, P.; Smith, S.; Thomas, D. A.; Vitulli, G.; Washio, Y.; Hamblin, J. N. Optimization of Novel Indazoles as Highly Potent and Selective Inhibitors of Phosphoinositide 3-Kinase δ for the Treatment of Respiratory Disease. *J. Med. Chem.* **2015**, *58* (18), 7381–7399.

(101) Cahn, A.; Hamblin, J. N.; Begg, M.; Wilson, R.; Dunsire, L.; Sriskantharajah, S.; Montembault, M.; Leemereise, C. N.; Galinanes-Garcia, L.; Watz, H.; Kirsten, A. M.; Fuhr, R.; Hessel, E. M. Safety, Pharmacokinetics and Dose-Response Characteristics of GSK2269557, an Inhaled PI3Kδ Inhibitor under Development for the Treatment of COPD. *Pulm. Pharmacol. Ther.* **2017**, *46*, 69–77.

(102) Cheng, H.; Li, C.; Bailey, S.; Baxi, S. M.; Goulet, L.; Guo, L.; Hoffman, J.; Jiang, Y.; Johnson, T. O.; Johnson, T. W.; Knighton, D. R.; Li, J.; Liu, K. K.-C.; Liu, Z.; Marx, M.

A.; Walls, M.; Wells, P. A.; Yin, M.-J.; Zhu, J.; Zientek, M. Discovery of the Highly Potent PI3K/MTOR Dual Inhibitor PF-04979064 through Structure-Based Drug Design. *ACS Med. Chem. Lett.* **2013**, *4* (1), 91–97.

(103) Hoegenauer, K.; Soldermann, N.; Zecri, F.; Strang, R. S.; Graveleau, N.; Wolf, R. M.; Cooke, N. G.; Smith, A. B.; Hollingworth, G. J.; Blanz, J.; Gutmann, S.; Rummel, G.; Littlewood-Evans, A.; Burkhart, C. Discovery of CDZ173 (Leniolisib), Representing a Structurally Novel Class of PI3K Delta-Selective Inhibitors. *ACS Med. Chem. Lett.* **2017**, *8* (9), 975–980.

(104) Hoegenauer, K.; Soldermann, N.; Stauffer, F.; Furet, P.; Graveleau, N.; Smith, A. B.; Hebach, C.; Hollingworth, G. J.; Lewis, I.; Gutmann, S.; Rummel, G.; Knapp, M.; Wolf, R. M.; Blanz, J.; Feifel, R.; Burkhart, C.; Zecri, F. Discovery and Pharmacological Characterization of Novel Quinazoline-Based PI3K Delta-Selective Inhibitors. *ACS Med. Chem. Lett.* **2016**, *7* (8), 762–767.

(105) Hoegenauer, K.; Soldermann, N.; Hebach, C.; Hollingworth, G. J.; Lewis, I.; von, M. A.; Smith, A. B.; Wolf, R. M.; Wilcken, R.; Zecri, F.; Haasen, D.; Burkhart, C. Discovery of Novel Pyrrolidineoxy-Substituted Heteroaromatics as Potent and Selective PI3K Delta Inhibitors with Improved Physicochemical Properties. *Bioorg. Med. Chem. Lett.* **2016**, *26* (23), 5657–5662.

(106) Rao, V. K.; Webster, S.; Dalm, V. A. S. H.; Šedivá, A.; van Hagen, P. M.; Holland, S.; Rosenzweig, S. D.; Christ, A. D.; Sloth, B.; Cabanski, M.; Joshi, A. D.; de Buck, S.; Doucet, J.; Guerini, D.; Kalis, C.; Pylvaenaeinen, I.; Soldermann, N.; Kashyap, A.; Uzel, G.; Lenardo, M. J.; Patel, D. D.; Lucas, C. L.; Burkhart, C. Effective "Activated PI3Kδ

Syndrome"–targeted Therapy with the PI3Kδ Inhibitor Leniolisib. *Blood* **2017**, *130* (21), 2307–2316.

(107) Xin, M.; Hei, Y.-Y.; Zhang, H.; Shen, Y.; Zhang, S.-Q. Design and Synthesis of Novel 6-Aryl Substituted 4-Anilinequinazoline Derivatives as Potential PI3Kδ Inhibitors. *Bioorg. Med. Chem. Lett.* **2017**, *27* (9), 1972–1977.

(108) Xin, M.; Duan, W.; Feng, Y.; Hei, Y.-Y.; Zhang, H.; Shen, Y.; Zhao, H.-Y.; Mao, S.; Zhang, S.-Q. Novel 6-Aryl Substituted 4-Pyrrolidineaminoquinazoline Derivatives as Potent Phosphoinositide 3-Kinase Delta (PI3Kδ) Inhibitors. *Bioorg. Med. Chem.* **2018**, *26* (8), 2028–2040.

(109) Hei, Y.-Y.; Xin, M.; Zhang, H.; Xie, X.-X.; Mao, S.; Zhang, S.-Q. Synthesis and Antitumor Activity Evaluation of 4,6-Disubstituted Quinazoline Derivatives as Novel PI3K Inhibitors. *Bioorg. Med. Chem. Lett.* **2016**, *26* (18), 4408–4413.

(110) Xin, M.; Hei, Y.-Y.; Zhang, H.; Shen, Y.; Zhang, S.-Q. Design and Synthesis of Novel 6-Aryl Substituted 4-Anilinequinazoline Derivatives as Potential PI3Kδ Inhibitors. *Bioorg. Med. Chem. Lett.* **2017**, *27* (9), 1972–1977.

(111) Zhang, J.; Lv, X.; Ma, X.; Hu, Y. Discovery of a Series of N-(5-(Quinolin-6-Yl)Pyridin-3-Yl)Benzenesulfonamides as PI3K/MTOR Dual Inhibitors. *Eur. J. Med. Chem.* **2017**, *127*, 509–520.

(112) Mah, S.; Park, J. H.; Jung, H.-Y.; Ahn, K.; Choi, S.; Tae, H. S.; Jung, K. H.; Rho, J. K.; Lee, J. C.; Hong, S.-S.; Hong, S. Identification of 4-Phenoxyquinoline Based Inhibitors for L1196M Mutant of Anaplastic Lymphoma Kinase by Structure-Based Design. *J. Med.*

Chem. **2017**, *60* (22), 9205–9221.

(113) Fan, Y.-H.; Ding, H.-W.; Liu, D.-D.; Song, H.-R.; Xu, Y.-N.; Wang, J. Novel 4-Aminoquinazoline Derivatives Induce Growth Inhibition, Cell Cycle Arrest and Apoptosis via PI3Kα Inhibition. *Bioorg. Med. Chem.* **2018**, *26* (8), 1675–1685.

(114) Lin, H.; Erhard, K.; Hardwicke, M. A.; Luengo, J. I.; Mack, J. F.; McSurdy-Freed, J.; Plant, R.; Raha, K.; Rominger, C. M.; Sanchez, R. M.; Schaber, M. D.; Schulz, M. J.; Spengler, M. D.; Tedesco, R.; Xie, R.; Zeng, J. J.; Rivero, R. A. Synthesis and Structure–activity Relationships of Imidazo[1,2-a]Pyrimidin-5(1H)-Ones as a Novel Series of Beta Isoform Selective Phosphatidylinositol 3-Kinase Inhibitors. *Bioorg. Med. Chem. Lett.* **2012**, *22* (6), 2230–2234.

(115) Sanchez, R. M.; Erhard, K.; Hardwicke, M. A.; Lin, H.; McSurdy-Freed, J.; Plant, R.; Raha, K.; Rominger, C. M.; Schaber, M. D.; Spengler, M. D.; Moore, M. L.; Yu, H.; Luengo, J. I.; Tedesco, R.; Rivero, R. A. Synthesis and Structure–activity Relationships of 1,2,4-Triazolo[1,5-a]Pyrimidin-7(3H)-Ones as Novel Series of Potent β Isoform Selective Phosphatidylinositol 3-Kinase Inhibitors. *Bioorg. Med. Chem. Lett.* **2012**, *22* (9), 3198–3202.

(116) Barlaam, B.; Cosulich, S.; Degorce, S.; Fitzek, M.; Giordanetto, F.; Green, S.; Inghardt, T.; Hennequin, L.; Hancox, U.; Lambert-van der Brempt, C.; Morgentin, R.; Pass, S.; Ple, P.; Saleh, T.; Ward, L. Discovery of 9-(1-Anilinoethyl)-2-Morpholino-4-Oxo-Pyrido[1,2-a]Pyrimidine-7-Carboxamides as PI3Kβ/δ Inhibitors for the Treatment of PTEN-Deficient Tumours. *Bioorg. Med. Chem. Lett.* **2014**, *24* (16), 3928–3935.

(117) Barlaam, B.; Cosulich, S.; Degorce, S.; Fitzek, M.; Green, S.; Hancox, U.; Lambert-van der

Brempt, C.; Lohmann, J.-J.; Maudet, M.; Morgentin, R.; Pasquet, M.-J.; Péru, A.; Plé, P.; Saleh, T.; Vautier, M.; Walker, M.; Ward, L.; Warin, N. Discovery of (R)-8-(1-(3,5-Difluorophenylamino)Ethyl)- N , N -Dimethyl-2-Morpholino-4-Oxo-4 H -Chromene-6-Carboxamide (AZD8186): A Potent and Selective Inhibitor of PI3Kβ and PI3Kδ for the Treatment of PTEN-Deficient Cancers. *J. Med. Chem.* **2015**, *58* (2), 943–962.

(118) Marshall, A. J.; Lill, C. L.; Chao, M.; Kolekar, S. V.; Lee, W.-J.; Marshall, E. S.; Baguley, B. C.; Shepherd, P. R.; Denny, W. A.; Flanagan, J. U.; Rewcastle, G. W. Exploring the Isoform Selectivity of TGX-221 Related Pyrido[1,2- a]Pyrimidinone-Based Class IA PI 3-Kinase Inhibitors: Synthesis, Biological Evaluation and Molecular Modelling. *Bioorg. Med. Chem.* **2015**, *23* (13), 3796–3808.

(119) Giordanetto, F.; Wållberg, A.; Cassel, J.; Ghosal, S.; Kossenjans, M.; Yuan, Z.-Q.; Wang, X.; Liang, L. Discovery of 4-Morpholino-Pyrimidin-6-One and 4-Morpholino-Pyrimidin-2-One-Containing Phosphoinositide 3-Kinase (PI3K) P110β Isoform Inhibitors through Structure-Based Fragment Optimisation. *Bioorg. Med. Chem. Lett.* **2012**, *22* (21), 6665–6670.

(120) Giordanetto, F.; Wållberg, A.; Ghosal, S.; Iliefski, T.; Cassel, J.; Yuan, Z.-Q.; von Wachenfeldt, H.; Andersen, S. M.; Inghardt, T.; Tunek, A.; Nylander, S. Discovery of Phosphoinositide 3-Kinases (PI3K) P110β Isoform Inhibitor 4-[2-Hydroxyethyl(1-Naphthylmethyl)Amino]-6-[(2S)-2-Methylmorpholin-4-Yl]-1H-Pyrimidin-2-One, an Effective Antithrombotic Agent without Associated Bleeding and Insulin Resistance. *Bioorg. Med. Chem. Lett.* **2012**, *22* (21), 6671–6676.

(121) Giordanetto, F.; Barlaam, B.; Berglund, S.; Edman, K.; Karlsson, O.; Lindberg, J.;

Nylander, S.; Inghardt, T. Discovery of 9-(1-Phenoxyethyl)-2-Morpholino-4-Oxo-Pyrido[1,2-a]Pyrimidine-7-Carboxamides as Oral PI3Kβ Inhibitors, Useful as Antiplatelet Agents. *Bioorg. Med. Chem. Lett.* **2014**, *24* (16), 3936–3943.

(122) Certal, V.; Halley, F.; Virone-Oddos, A.; Delorme, C.; Karlsson, A.; Rak, A.; Thompson, F.; Filoche-Romme, B.; El-Ahmad, Y.; Carry, J.-C.; Abecassis, P.-Y.; Lejeune, P.; Vincent, L.; Bonnevaux, H.; Nicolas, J.-P.; Bertrand, T.; Marquette, J.-P.; Michot, N.; Benard, T.; Below, P.; Vade, I.; Chatreaux, F.; Lebourg, G.; Pilorge, F.; Angouillant-Boniface, O.; Louboutin, A.; Lengauer, C.; Schio, L. Discovery and Optimization of New Benzimidazole- and Benzoxazole-Pyrimidone Selective PI3Kβ Inhibitors for the Treatment of Phosphatase and TENsin Homologue (PTEN)-Deficient Cancers. *J. Med. Chem.* **2012**, *55* (10), 4788–4805.

(123) Certal, V.; Carry, J.-C.; Halley, F.; Virone-Oddos, A.; Thompson, F.; Filoche-Rommé, B.; El-Ahmad, Y.; Karlsson, A.; Charrier, V.; Delorme, C.; Rak, A.; Abecassis, P.-Y.; Amara, C.; Vincent, L.; Bonnevaux, H.; Nicolas, J.-P.; Mathieu, M.; Bertrand, T.; Marquette, J.-P.; Michot, N.; Benard, T.; Perrin, M.-A.; Lemaitre, O.; Guerif, S.; Perron, S.; Monget, S.; Gruss-Leleu, F.; Doerflinger, G.; Guizani, H.; Brollo, M.; Delbarre, L.; Bertin, L.; Richepin, P.; Loyau, V.; Garcia-Echeverria, C.; Lengauer, C.; Schio, L. Discovery and Optimization of Pyrimidone Indoline Amide PI3Kβ Inhibitors for the Treatment of Phosphatase and Tensin Homologue (PTEN)-Deficient Cancers. *J. Med. Chem.* **2014**, *57* (3), 903–920.

(124) Bédard, P. L.; Davies, M. A.; Kopetz, S.; Juric, D.; Shapiro, G. I.; Luke, J. J.; Spreafico, A.; Wu, B.; Castell, C.; Gomez, C.; Cartot-Cotton, S.; Mazuir, F.; Dubar, M.; Micallef, S.; Demers, B.; Flaherty, K. T. First-in-Human Trial of the PI3Kβ-Selective Inhibitor

SAR260301 in Patients with Advanced Solid Tumors. *Cancer* **2018**, *124* (2), 315–324.

(125) Staben, S. T.; Siu, M.; Goldsmith, R.; Olivero, A. G.; Do, S.; Burdick, D. J.; Heffron, T. P.; Dotson, J.; Sutherlin, D. P.; Zhu, B.-Y.; Tsui, V.; Le, H.; Lee, L.; Lesnick, J.; Lewis, C.; Murray, J. M.; Nonomiya, J.; Pang, J.; Prior, W. W.; Salphati, L.; Rouge, L.; Sampath, D.; Sideris, S.; Wiesmann, C.; Wu, P. Structure-Based Design of Thienobenzoxepin Inhibitors of PI3-Kinase. *Bioorg. Med. Chem. Lett.* **2011**, *21* (13), 4054–4058.

(126) Staben, S. T.; Blaquiere, N.; Tsui, V.; Kolesnikov, A.; Do, S.; Bradley, E. K.; Dotson, J.; Goldsmith, R.; Heffron, T. P.; Lesnick, J.; Lewis, C.; Murray, J.; Nonomiya, J.; Olivero, A. G.; Pang, J.; Rouge, L.; Salphati, L.; Wei, B.; Wiesmann, C.; Wu, P. Cis-Amide Isosteric Replacement in Thienobenzoxepin Inhibitors of PI3-Kinase. *Bioorg. Med. Chem. Lett.* **2013**, *23* (3), 897–901.

(127) Staben, S. T.; Ndubaku, C.; Blaquiere, N.; Belvin, M.; Bull, R. J.; Dudley, D.; Edgar, K.; Gray, D.; Heald, R.; Heffron, T. P.; Jones, G. E.; Jones, M.; Kolesnikov, A.; Lee, L.; Lesnick, J.; Lewis, C.; Murray, J.; McLean, N. J.; Nonomiya, J.; Olivero, A. G.; Ord, R.; Pang, J.; Price, S.; Prior, W. W.; Rouge, L.; Salphati, L.; Sampath, D.; Wallin, J.; Wang, L.; Wei, B.; Weismann, C.; Wu, P. Discovery of Thiazolobenzoxepin PI3-Kinase Inhibitors That Spare the PI3-Kinase β Isoform. *Bioorg. Med. Chem. Lett.* **2013**, *23* (9), 2606–2613.

(128) Ndubaku, C. O.; Heffron, T. P.; Staben, S. T.; Baumgardner, M.; Blaquiere, N.; Bradley, E.; Bull, R.; Do, S.; Dotson, J.; Dudley, D.; Edgar, K. A.; Friedman, L. S.; Goldsmith, R.; Heald, R. A.; Kolesnikov, A.; Lee, L.; Lewis, C.; Nannini, M.; Nonomiya, J.; Pang, J.; Price, S.; Prior, W. W.; Salphati, L.; Sideris, S.; Wallin, J. J.; Wang, L.; Wei, B.; Sampath, D.; Olivero, A. G. Discovery of 2-{3-[2-(1-Isopropyl-3-Methyl-1 H -1,2–4-Triazol-5-Yl)-5,6-

Dihydrobenzo[f]Imidazo[1,2- d][1,4]Oxazepin-9-Yl]-1 H -Pyrazol-1-Yl}-2-Methylpropanamide (GDC-0032): A β-Sparing Phosphoinositide 3-Kinase Inhibitor with High Unbound Exposure and Ro. *J. Med. Chem.* **2013**, *56* (11), 4597–4610.

(129) Heffron, T. P.; Heald, R. A.; Ndubaku, C.; Wei, B.; Augistin, M.; Do, S.; Edgar, K.; Eigenbrot, C.; Friedman, L.; Gancia, E.; Jackson, P. S.; Jones, G.; Kolesnikov, A.; Lee, L. B.; Lesnick, J. D.; Lewis, C.; McLean, N.; Mörtl, M.; Nonomiya, J.; Pang, J.; Price, S.; Prior, W. W.; Salphati, L.; Sideris, S.; Staben, S. T.; Steinbacher, S.; Tsui, V.; Wallin, J.; Sampath, D.; Olivero, A. G. The Rational Design of Selective Benzoxazepin Inhibitors of the α-Isoform of Phosphoinositide 3-Kinase Culminating in the Identification of (S)-2-((2-(1-Isopropyl-1 H -1,2,4-Triazol-5-Yl)-5,6-Dihydrobenzo[f]Imidazo[1,2- d][1,4]Oxazepin-9-Yl)Oxy)Propa. *J. Med. Chem.* **2016**, *59* (3), 985–1002.

(130) Safina, B. S.; Elliott, R. L.; Forrest, A. K.; Heald, R. A.; Murray, J. M.; Nonomiya, J.; Pang, J.; Salphati, L.; Seward, E. M.; Staben, S. T.; Ultsch, M.; Wei, B.; Yang, W.; Sutherlin, D. P. Design of Selective Benzoxazepin PI3Kδ Inhibitors Through Control of Dihedral Angles. *ACS Med. Chem. Lett.* **2017**, *8* (9), 936–940.

(131) Bergamini, G.; Bell, K.; Shimamura, S.; Werner, T.; Cansfield, A.; Müller, K.; Perrin, J.; Rau, C.; Ellard, K.; Hopf, C.; Doce, C.; Leggate, D.; Mangano, R.; Mathieson, T.; O'Mahony, A.; Plavec, I.; Rharbaoui, F.; Reinhard, F.; Savitski, M. M.; Ramsden, N.; Hirsch, E.; Drewes, G.; Rausch, O.; Bantscheff, M.; Neubauer, G. A Selective Inhibitor Reveals PI3Kγ Dependence of TH17 Cell Differentiation. *Nat. Chem. Biol.* **2012**, *8* (6), 576–582.

(132) Sunose, M.; Bell, K.; Ellard, K.; Bergamini, G.; Neubauer, G.; Werner, T.; Ramsden, N.

Discovery of 5-(2-Amino-[1,2,4]Triazolo[1,5-a]Pyridin-7-Yl)-N-(Tert-Butyl)Pyridine-3-Sulfonamide (CZC24758), as a Potent, Orally Bioavailable and Selective Inhibitor of PI3K for the Treatment of Inflammatory Disease. *Bioorg. Med. Chem. Lett.* **2012**, *22* (14), 4613–4618.

(133) Bell, K.; Sunose, M.; Ellard, K.; Cansfield, A.; Taylor, J.; Miller, W.; Ramsden, N.; Bergamini, G.; Neubauer, G. SAR Studies around a Series of Triazolopyridines as Potent and Selective PI3Kγ Inhibitors. *Bioorg. Med. Chem. Lett.* **2012**, *22* (16), 5257–5263.

(134) Ellard, K.; Sunose, M.; Bell, K.; Ramsden, N.; Bergamini, G.; Neubauer, G. Discovery of Novel PI3Kγ/δ Inhibitors as Potential Agents for Inflammation. *Bioorg. Med. Chem. Lett.* **2012**, *22* (14), 4546–4549.

(135) Oka, Y.; Yabuuchi, T.; Fujii, Y.; Ohtake, H.; Wakahara, S.; Matsumoto, K.; Endo, M.; Tamura, Y.; Sekiguchi, Y. Discovery and Optimization of a Series of 2-Aminothiazole-Oxazoles as Potent Phosphoinositide 3-Kinase γ Inhibitors. *Bioorg. Med. Chem. Lett.* **2012**, *22* (24), 7534–7538.

(136) Oka, Y.; Yabuuchi, T.; Oi, T.; Kuroda, S.; Fujii, Y.; Ohtake, H.; Inoue, T.; Wakahara, S.; Kimura, K.; Fujita, K.; Endo, M.; Taguchi, K.; Sekiguchi, Y. Discovery of N-{5-[3-(3-Hydroxypiperidin-1-Yl)-1,2,4-Oxadiazol-5-Yl]-4-Methyl-1,3-Thiazol-2-Yl}acetamide (TASP0415914) as an Orally Potent Phosphoinositide 3-Kinase γ Inhibitor for the Treatment of Inflammatory Diseases. *Bioorg. Med. Chem.* **2013**, *21* (24), 7578–7583.

(137) Bruce, I.; Akhlaq, M.; Bloomfield, G. C.; Budd, E.; Cox, B.; Cuenoud, B.; Finan, P.; Gedeck, P.; Hatto, J.; Hayler, J. F.; Head, D.; Keller, T.; Kirman, L.; Leblanc, C.; Grand, D. Le; McCarthy, C.; O'Connor, D.; Owen, C.; Oza, M. S.; Pilgrim, G.; Press, N. E.;

Sviridenko, L.; Whitehead, L. Development of Isoform Selective PI3-Kinase Inhibitors as Pharmacological Tools for Elucidating the PI3K Pathway. *Bioorg. Med. Chem. Lett.* **2012**, *22* (17), 5445–5450.

(138) Furet, P.; Guagnano, V.; Fairhurst, R. A.; Imbach-Weese, P.; Bruce, I.; Knapp, M.; Fritsch, C.; Blasco, F.; Blanz, J.; Aichholz, R.; Hamon, J.; Fabbro, D.; Caravatti, G. Discovery of NVP-BYL719 a Potent and Selective Phosphatidylinositol-3 Kinase Alpha Inhibitor Selected for Clinical Evaluation. *Bioorg. Med. Chem. Lett.* **2013**, *23* (13), 3741–3748.

(139) Collier, P. N.; Martinez-Botella, G.; Cornebise, M.; Cottrell, K. M.; Doran, J. D.; Griffith, J. P.; Mahajan, S.; Maltais, F.; Moody, C. S.; Huck, E. P.; Wang, T.; Aronov, A. M. Structural Basis for Isoform Selectivity in a Class of Benzothiazole Inhibitors of Phosphoinositide 3-Kinase γ. *J. Med. Chem.* **2015**, *58* (1), 517–521.

(140) Collier, P. N.; Messersmith, D.; Le Tiran, A.; Bandarage, U. K.; Boucher, C.; Come, J.; Cottrell, K. M.; Damagnez, V.; Doran, J. D.; Griffith, J. P.; Khare-Pandit, S.; Krueger, E. B.; Ledeboer, M. W.; Ledford, B.; Liao, Y.; Mahajan, S.; Moody, C. S.; Roday, S.; Wang, T.; Xu, J.; Aronov, A. M. Discovery of Highly Isoform Selective Thiazolopiperidine Inhibitors of Phosphoinositide 3-Kinase γ. *J. Med. Chem.* **2015**, *58* (14), 5684–5688.

(141) Come, J. H.; Collier, P. N.; Henderson, J. A.; Pierce, A. C.; Davies, R. J.; Le Tiran, A.; O'Dowd, H.; Bandarage, U. K.; Cao, J.; Deininger, D.; Grey, R.; Krueger, E. B.; Lowe, D. B.; Liang, J.; Liao, Y.; Messersmith, D.; Nanthakumar, S.; Sizensky, E.; Wang, J.; Xu, J.; Chin, E. Y.; Damagnez, V.; Doran, J. D.; Dworakowski, W.; Griffith, J. P.; Jacobs, M. D.; Khare-Pandit, S.; Mahajan, S.; Moody, C. S.; Aronov, A. M. Design and Synthesis of a Novel Series of Orally Bioavailable, CNS-Penetrant, Isoform Selective Phosphoinositide 3-

Kinase γ (PI3Kγ) Inhibitors with Potential for the Treatment of Multiple Sclerosis (MS). *J. Med. Chem.* **2018**, *61* (12), 5245–5256.

(142) Pemberton, N.; Mogemark, M.; Arlbrandt, S.; Bold, P.; Cox, R. J.; Gardelli, C.; Holden, N. S.; Karabelas, K.; Karlsson, J.; Lever, S.; Li, X.; Lindmark, H.; Norberg, M.; Perry, M. W. D.; Petersen, J.; Rodrigo Blomqvist, S.; Thomas, M.; Tyrchan, C.; Westin Eriksson, A.; Zlatoidsky, P.; Öster, L. Discovery of Highly Isoform Selective Orally Bioavailable Phosphoinositide 3-Kinase (PI3K)-γ Inhibitors. *J. Med. Chem.* **2018**, *61* (12), 5435–5441.

(143) Qian, C.; Lai, C.-J.; Bao, R.; Wang, D.-G.; Wang, J.; Xu, G.-X.; Atoyan, R.; Qu, H.; Yin, L.; Samson, M.; Zifcak, B.; Ma, A. W. S.; DellaRocca, S.; Borek, M.; Zhai, H.-X.; Cai, X.; Voi, M. Cancer Network Disruption by a Single Molecule Inhibitor Targeting Both Histone Deacetylase Activity and Phosphatidylinositol 3-Kinase Signaling. *Clin. Cancer Res.* **2012**, *18* (15), 4104–4113.

(144) Younes, A.; Berdeja, J. G.; Patel, M. R.; Flinn, I.; Gerecitano, J. F.; Neelapu, S. S.; Kelly, K. R.; Copeland, A. R.; Akins, A.; Clancy, M. S.; Gong, L.; Wang, J.; Ma, A.; Viner, J. L.; Oki, Y. Safety, Tolerability, and Preliminary Activity of CUDC-907, a First-in-Class, Oral, Dual Inhibitor of HDAC and PI3K, in Patients with Relapsed or Refractory Lymphoma or Multiple Myeloma: An Open-Label, Dose-Escalation, Phase 1 Trial. *Lancet. Oncol.* **2016**, *17* (5), 622–631.

(145) Sun, K.; Atoyan, R.; Borek, M. A.; Dellarocca, S.; Samson, M. E. S.; Ma, A. W.; Xu, G.-X.; Patterson, T.; Tuck, D. P.; Viner, J. L.; Fattaey, A.; Wang, J. Dual HDAC and PI3K Inhibitor CUDC-907 Downregulates MYC and Suppresses Growth of MYC-Dependent Cancers. *Mol. Cancer Ther.* **2017**, *16* (2), 285–299.

(146) Chen, D.; Soh, C. K.; Goh, W. H.; Wang, H. Design, Synthesis, and Preclinical Evaluation of Fused Pyrimidine-Based Hydroxamates for the Treatment of Hepatocellular Carcinoma. *J. Med. Chem.* **2018**, *61* (4), 1552–1575.

(147) Ding, H.-W.; Deng, C.-L.; Li, D.-D.; Liu, D.-D.; Chai, S.-M.; Wang, W.; Zhang, Y.; Chen, K.; Li, X.; Wang, J.; Song, S.-J.; Song, H.-R. Design, Synthesis and Biological Evaluation of Novel 4-Aminoquinazolines as Dual Target Inhibitors of EGFR-PI3Kα. *Eur. J. Med. Chem.* **2018**, *146*, 460–470.

(148) Pujala, B.; Agarwal, A. K.; Middya, S.; Banerjee, M.; Surya, A.; Nayak, A. K.; Gupta, A.; Khare, S.; Guguloth, R.; Randive, N. A.; Shinde, B. U.; Thakur, A.; Patel, D. I.; Raja, M.; Green, M. J.; Alfaro, J.; Avila, P.; Perez de Arce, F.; Almirez, R. G.; Kanno, S.; Bernales, S.; Hung, D. T.; Chakravarty, S.; McCullagh, E.; Quinn, K. P.; Rai, R.; Pham, S. M. Discovery of Pyrazolopyrimidine Derivatives as Novel Dual Inhibitors of BTK and PI3Kδ. *ACS Med. Chem. Lett.* **2016**, *7* (12), 1161–1166.

(149) Furman, R. R.; Sharman, J. P.; Coutre, S. E.; Cheson, B. D.; Pagel, J. M.; Hillmen, P.; Barrientos, J. C.; Zelenetz, A. D.; Kipps, T. J.; Flinn, I.; Ghia, P.; Eradat, H.; Ervin, T.; Lamanna, N.; Coiffier, B.; Pettitt, A. R.; Ma, S.; Stilgenbauer, S.; Cramer, P.; Aiello, M.; Johnson, D. M.; Miller, L. L.; Li, D.; Jahn, T. M.; Dansey, R. D.; Hallek, M.; O'Brien, S. M. Idelalisib and Rituximab in Relapsed Chronic Lymphocytic Leukemia. *N. Engl. J. Med.* **2014**, *370* (11), 997–1007.

(150) de Weerdt, I.; Koopmans, S. M.; Kater, A. P.; van Gelder, M. Incidence and Management of Toxicity Associated with Ibrutinib and Idelalisib: A Practical Approach. *Haematologica* **2017**, *102* (10), 1629–1639.

(151) Coutré, S. E.; Barrientos, J. C.; Brown, J. R.; de Vos, S.; Furman, R. R.; Keating, M. J.; Li, D.; O'Brien, S. M.; Pagel, J. M.; Poleski, M. H.; Sharman, J. P.; Yao, N.-S.; Zelenetz, A. D. Management of Adverse Events Associated with Idelalisib Treatment: Expert Panel Opinion. *Leuk. Lymphoma* **2015**, *56* (10), 2779–2786.

(152) Patnaik, A.; Appleman, L. J.; Tolcher, A. W.; Papadopoulos, K. P.; Beeram, M.; Rasco, D. W.; Weiss, G. J.; Sachdev, J. C.; Chadha, M.; Fulk, M.; Ejadi, S.; Mountz, J. M.; Lotze, M. T.; Toledo, F. G. S.; Chu, E.; Jeffers, M.; Peña, C.; Xia, C.; Reif, S.; Genvresse, I.; Ramanathan, R. K. First-in-Human Phase I Study of Copanlisib (BAY 80-6946), an Intravenous Pan-Class I Phosphatidylinositol 3-Kinase Inhibitor, in Patients with Advanced Solid Tumors and Non-Hodgkin's Lymphomas. *Ann. Oncol. Off. J. Eur. Soc. Med. Oncol.* **2016**, *27* (10), 1928–1940.

(153) Ritchie, T. J.; Macdonald, S. J. F. Physicochemical Descriptors of Aromatic Character and Their Use in Drug Discovery. *J. Med. Chem.* **2014**, *57* (17), 7206–7215.

(154) Lovering, F.; Bikker, J.; Humblet, C. Escape from Flatland: Increasing Saturation as an Approach to Improving Clinical Success. *J. Med. Chem.* **2009**, *52* (21), 6752–6756.

Table of contents graphic